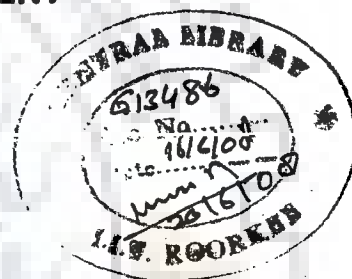# PERFORMANCE ASSESSMENT
OF
A RADIAL COLLECTOR WELL NEAR A STREAM

A THESIS

Submitted in partial fulfilment of the
requirements for the award of the degree
of

DOCTOR OF PHILOSOPHY

in

WATER RESOURCES DEVELOPMENT

by

MOHD. FAHIMUDDIN

DEPARTMENT OF WATER RESOURCES DEVELOPMENT & MANAGEMENT
INDIAN INSTITUTE OF TECHNOLOGY ROORKEE
ROORKEE-247 667 (INDIA)

MARCH, 2007

INDIAN INSTITUTE OF TECHNOLOGY ROORKEE
ROORKEE

CANDIDATE'S DECLARATION

I hereby certify that the work which is being presented in the thesis entitled **PERFORMANCE ASSESSMENT OF A RADIAL COLLECTOR WELL NEAR A STREAM** in the partial fulfilment of the requirements for the award of the Degree of Doctor of Philosophy and submitted in the Department of Water Resources Development and Management of Indian Institute of Technology Roorkee, Roorkee is an authentic record of my own work carried out during a period of January 2004 to February 2007 under the supervision of Dr. M. L. Kansal, Associate Professor, and Dr. G. C. Mishra, Emeritus Fellow, Water Resources Development and Management, Indian Institute of Technology Roorkee, Roorkee.

The matter presented in this thesis has not been submitted by me for the award of any other degree of this or any other institute.

(MOHD. FAHIMUDDIN)

This is to certify that the above statement made by the candidate is correct to the best of our knowledge

Dr. G. C. Mishra
Emeritus Fellow
WRD&M
I.I.T.Roorkee-247667
Date- 05/3/2007

Dr. M. L. Kansal 5/3/07
Associate Professor
WRD&M
I.I.T.Roorkee-247667

The Ph.D Viva-Voce Examination of Mr. Mohd. Fahimuddin, Research Scholar, has been held on ...26th April, 2007

Signature of Supervisor(s)   26/4/07

Signature of External Examiner   26/04/07

ABSTRACT

Traditionally, water supplies for drinking or industrial uses have been drawn from rivers, streams, and from natural or artificial collections of water. The systems of tapping under-ground water have been tube wells (vertical well), infiltration galleries, and radial collector wells. Vertical wells are generally suitable in a thick aquifer and it can tap water from an aquifer lying at greater depth. An infiltration gallery is a horizontal perforated pipe or conduit suitable for tapping water from a shallow aquifer. Infiltration galleries are generally laid near a stream or river to intercept infiltration water from the river. Infiltration galleries may be laid in different alignment, such as parallel or perpendicular to the stream or a river.

A radial collector well (RCW) consists of a number of horizontal perforated pipes laid in an aquifer and connected to a vertical cylindrical caisson, plugged at the bottom end. These wells are particularly suitable for shallow highly permeable thin aquifers in which vertical wells have low yields due to the limited drawdown. RCWs have significantly longer well screen, which is exposed to the aquifer, and produce large quantities of water under the moderate drawdown conditions. A radial collector well with one or two collinear laterals can be treated as a horizontal collector pipe or an infiltration gallery. However, in case of multiple laterals in a radial collector well, the laterals interfere with each other, and hence it is important to provide non-perfortaed portion of pipes near the caisson.

Riverbank filtration (RBF) (Ray, 2002) describes the process of extracting groundwater through horizontal collector wells or vertical wells installed along the riverbank which induces infiltration from the river. RBF provides passive exposure to

various processes such as adsorption, physiochemical filtration, and biodegradation. It produces water that is relatively consistent in quality and is easier to treat to achieve higher levels of finished quality. Radial collector wells are generally installed near rivers as a part of *riverbank filtration system* to increase the potential yield and to improve the quality of the withdrawn water.

Estimation of flow to a radial collector well is a complex problem. Even under simplified conditions, estimation of safe yield is complex than in case of a vertical well. Since, the water enters through a number of horizontal screened pipes (laterals), analytical solutions of flow to the RCW are based on the theory of flow to a horizontal pipe. Estimation of flow to a lateral can be based on two fundamental assumptions, i.e., (i) the total discharge through a lateral is uniformly distributed along its entire length, i.e., the uniform flux boundary condition exist along the lateral, and (ii) that the head along the lateral is uniform, i.e., Dirichelt type boundary condition exists along the lateral.

In this study, before going into detail analysis of groundwater flow to multiple laterals of a radial collector well, an attempt has been made to ascertain the flow characteristics(i.e., laminar or turbulent), and the appropriate boundary condition in a horizontal collector pipe (i.e., constant head or constant flux) along the lateral. It is found that barring for a small length near the tip (free end) of a horizontal collector pipe, the flow condition in the pipe is turbulent. Collector pipe of diameter 0.3m-0.4 is generally adopted and for collector pipe with diameter 0.2m and above, the total head loss is very marginal. Therefore, for steady state flow condition, either Dirichlet boundary condition or uniform flux condition can be applied without introducing appreciable error. Dirichelt boundary condition is to be applied for solving Laplace

equation for steady state flow condition. For unsteady state flow condition, the uniform flux boundary condition can be adopted conveniently.

The groundwater flow near a radial collector well or a horizontal collector pipe (infiltration gallery) is distinctly three-dimensional in nature. However, if the objective is to estimate the production rate of a radial collector well installed in a thin aquifer, flow field can be considered to be two-dimensional (in x-y horizontal plane) only neglecting the resistance to vertical flow. If the well is located near to a surface water body, the flow to the well can be treated as steady state flow during later stage of long pumping. At late pumping stage, horizontal pseudoradial flow takes place towards a horizontal collector pipe (Park and Cao, 2000). This postulate supports the assumption of sheet flow condition in a thin aquifer and horizontal collector well system and the flow can be estimated by solving well known Laplace equation for 2D flow field under steady state conditions and, thereafter, a correction factor can be applied on account of resistance to vertical flow. Conformal mapping technique is one of the methods available to solve the 2D groundwater flow.

In the present study, Schwartz Christoffel conformal mapping technique has been applied assuming steady state flow condition and implementing a constant head distribution along the infiltration galleries and laterals of a radial collector well. Before analyzing flow to a radial collector well with multiple laterals, flow to single horizontal collector pipe or infiltration gallery near river (meandering or straight reach) has been analyzed.

In case of an infiltration gallery near a meandering river reach or at the centre of an island, flow increase and travel time reduces with the increase in the length of infiltration gallery. For a given size of island, the length of the infiltration gallery has

to be fixed on the basis of permissible minimum travel time. The minimum travel time should be greater than the survival life of bacteria in concern. Infiltration gallery near a straight reach of a river may be laid in different orientations. In case of a gallery perpendicular and aligned towards the river from the caisson, the flow increases and travel time decreases sharply with the increase in the length of gallery for a given distance from the river. Whereas, in case of a gallery perpendicular and towards landside, the flow increases monotonically and minimum travel time reduces and becomes constant.

Most of the studies on radial collector wells have been carried out by assuming that the laterals are fully screened. However, in practice, the laterals are kept non-perforated (blind) near the caisson as no flow zone is created near the caisson due to the interference of laterals. Hence, it is desirable to investigate the effect of partially screened laterals on the potential yield of the well and corresponding entrance velocity to the laterals.

The performance assessment of a radial collector well near straight reach of a river or near meandering river has been carried out in terms of specific capacity and minimum travel time for river water to reach the well screens. Sensitivity analysis has been carried out for various parameters such as, laterals arrangement around the caisson, their number, radius, length of screened and blind portion, and the distance of caisson from the river for the given hydro-geologic conditions.

The average entrance velocity mainly depends on the length of screen portion of laterals. It increases sharply with the increase in blind portion. The minimum travel time depends on storage coefficient, drawdown, and distance of screens from the river.
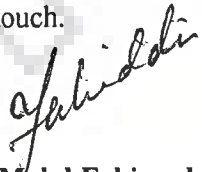
AKNOWLEDGEMENTS

CONTENTS

NOTATIONS

b	=	thickness of aquifer;
d	=	diameter of horizontal collector pipe or lateral;
f	=	friction factor;
g	=	acceleration due to gravity;
H_0	=	maximum rise in stream stage during flood;
h_r	=	water level in stream;
h_w	=	water level in caisson;
h	=	h_r-h_w =drawdown in caisson;
i	=	imaginary number = $\pm\sqrt{-1}$;
k	=	hydraulic conductivity;
L_a	=	thickness of aquiclude layer;
L	=	length of horizontal collector pipe;
l	=	length of lateral;
l_1	=	length of laminar flow zone in a collector pipe;
l_2	=	length of turbulent flow zone in a collector pipe;
l_b	=	length of blind(non-perforated) section of a lateral;
l_s	=	length of screened(perforated) part of lateral;
L_1, L_2, L_3	=	length of laterals;
L_{1b}, L_{2b}, L_{3b}	=	length of non perforated sections of laterals, 1, 2, 3, respectively
n, m	=	time step, integer;
n	=	number of lateral,

$Q(n)$	=	volume of water passing through shaft during n^{th} time step;
R	=	distance of caisson /vertical shaft from stream;
r_w	=	radius of vertical shaft and horizontal lateral;
S	=	storage coefficient of aquifer;
S_1	=	storage coefficient of upper aquifer;
S_2	=	storage coefficient of lower aquifer;
T	=	transmissivity of aquifer and thickness;
T_1	=	transmissivity of upper aquifer;
T_2	=	transmissivity of lower aquifer;
t	=	time parameter;
t_c	=	time to the flood peak;
t_d	=	duration of flood wave;
α	=	real number;
β	=	hydraulic diffusivity of aquifer$= T/S$;
Δt	=	time step size;
γ	=	time step, integer;
$\delta_1\left(r_w, n-\gamma+1, \Delta t\right)$	=	coefficients of discrete kernel for drawdown at shaft face due to passing of water from upper aquifer to lower aquifer;
$\delta_2\left(r_w, n-\gamma+1, \Delta t\right)$	=	coefficients of discrete kernel for rise in piezometric level at shaft face owing to recharge from upper aquifer;

$\delta_1(2R, n - \gamma + 1, \Delta t)$ = coefficients of discrete kernel for water- level rise at shaft face due to image recharge well;

$\delta_h(R, n - \gamma + 1, \Delta t)$ = coefficients of discrete kernel for water-level rise at shaft face due to stream stage rise; and

σ_γ = rise in stream stage at $t = \gamma \Delta t$.

Other notations are locally defined wherever these appear

LIST OF FIGURES

LIST OF TABLES

INTRODUCTION

1.1 GENERAL

Providing safe and adequate drinking water to the masses is one of the most vital services to the society. Traditionally, water supplies for drinking or industrial uses have been drawn from rivers, streams, and from natural or artificial collection of water. As the surface water sources are becoming more and more inadequate and unsafe due to contamination, the decision-makers are looking towards ground water as a sustainable and safe source of drinking water. The traditional systems of tapping under-ground water have been tube wells (deep vertical wells), infiltration galleries or horizontal collector wells (screened pipes or conduits, trenches), and radial collector wells (RCW) which consist of multiple horizontal screened pipes (called laterals or radials) connected to a central caisson plugged at the bottom end.

In some sedimentary groundwater basins, even though the aquifer is hydraulically connected to a nearby surface water body, the aquifer may not be thick enough to supply the required volume of water to a vertical well. The hydraulic conductivity of the sediment deposit may be excellent but transmissivity may be limited as the deposits are thin. For example, in a typical river valley, there may be a thin alluvial deposit that may be sandwiched between clay deposits. In other situation, a thin layer of fresh water may overlie saline or brackish water. Vertical well at such sites would cause upconing of the saltwater, thereby degrading the

quality of water withdrawn. Under these hydro-geologic conditions, RCWs can produce large quantity of freshwater under the moderate draw-down conditions as there are significant longer well screens exposed to the aquifer.

The first RCW, commonly known as Ranney well (after the name of Leo Ranney), was installed at London, England, in 1933. Since then, many municipalities throughout the world have successfully operated this type of groundwater collection system to obtain part of their water supply. The advantages of the RCW over traditional vertical well are (Spiridonoff, 1964): (1) the horizontal perforated collector pipe (the configuration and length of which may vary) enable a large area of an aquifer to be exploited; (2) the removal of fine sand and gravel in the path of the projected collector pipe establishes an artificial aquifer of much higher permeability than the virgin soil; (3) after construction, the collector pipe simply serves as a sub drain in a filter surrounded by a circle of course gravels several feet in diameter; (4) the unrestricted access and independent control of each collector pipe permit easy regulation of flow into a caisson and inspection and backwash of the collector pipe; (5) the large area of exposed perforations in the collector well causes low inflow velocities, which minimizes incrustation, clogging, and sand transport.

RCWs are often used to induce recharge from surface water bodies and installed close to major streams/ rivers. In some cases, laterals of the RCW are extended below the rivers. The laterals intercept and collect groundwater derived principally from surface water infiltration. Such supplies usually pass through the underlying sand and gravel deposits and hydraulically connected with surface sources, such as river, lake, or ocean. Water withdrawn from RCW is comparatively of better quality than river water as the water goes through various physiochemical and

2

biological processes in the porous medium between the river and the well (Ray et al 2002). The laterals can be arranged in different pattern around the caisson to optimize the yield and quality of water. The RCWs are generally installed near a river as a part of *Riverbank Filtration (RBF) system* to increase the potential yield and the quality of the water.

RBF is generally performed when the quality of water in the river is not suitable for water supplies due to intermittent or chronic pollution. The riverbed sediments and aquifer materials provide 'slow-rate filtration' and the recovered water is of higher and more consistent quality than water drawn directly from the river. RBF provides passive exposure to various processes such as adsorption, reduction, physiochemical filtration, and biodegradation. It produces water that is relatively consistent in quality and easier to treat to higher levels of finished quality.

Under flood conditions, contaminant could reach the RBF wells from the combined effect of pumping stresses and enhanced hydraulic gradient between the river and the aquifer. The portion of riverbank filtrate in the pumped raw water would depend on source water quality, geo-hydrologic conditions of the aquifer, river-aquifer interface, hydraulic gradient, infiltration rates, hydraulic conductivity, and the distance between the riverbank and the pumping well. The early emphasis of RBF was on the enhancement of well yields, whereas the later emphasis has been on the improvement of water quality as the surface water sources are getting polluted day after day due to increasing population and industrialization. During the time of flood in river, the collector pipes that are oriented towards the river can be closed to minimize the contamination of the collected water and water will enter the caisson only through those collector pipes that are oriented away from the river. In this way,

water will flow through a longer distance, maintaining larger residence time in porous medium, and hence the chances of contamination will be less.

Through riverbank filtration, many communities located along riverbanks have developed the water supplies by pumping water from alluvial aquifers using RCWs and vertical wells along the riverbank. In Europe, RBF has been the primary mode of drinking water production for many cities located along major rivers such as the Danube in Central Europe (from Austria to Black sea), Rhine and Elbe in Germany, Lot and Seine in France, Rhine in the Netherlands, as well as along rivers in Austria, Switzerland, Slovenia, and Spain. Lake Bank filtration is also common in many European countries, including Finland, where wells are placed close to natural lakes or artificial reservoirs for drinking water production.

A typical RCW having multiple laterals located near a straight reach of a fully penetrating river is shown in Fig. 1.1 below:
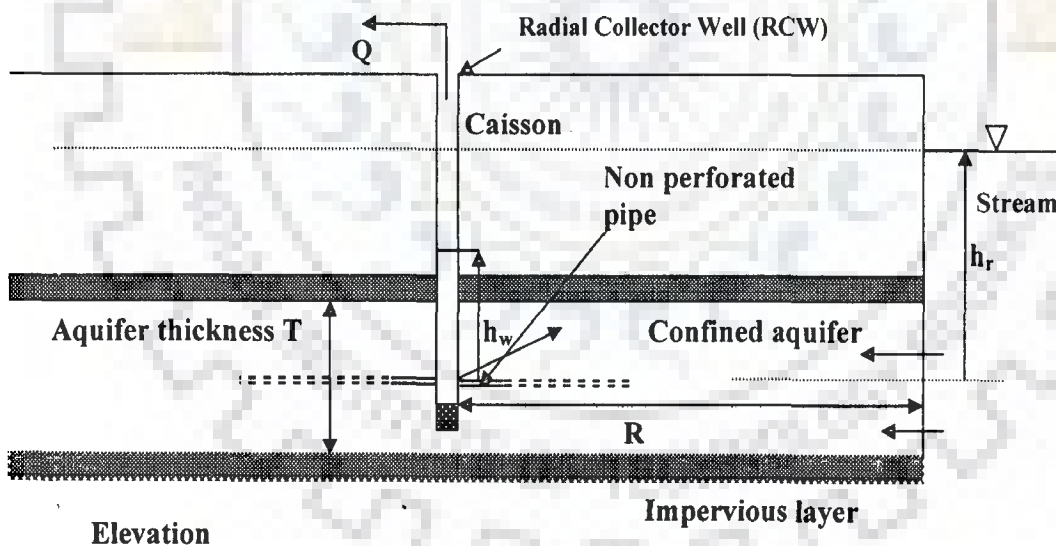
Fig.1.1. Line diagram of a typical radial collector well near a stream.

1.2 THEORY OF FLOW TO A RADIAL COLLECTOR WELL

Estimation of flow to a radial collector well is a complex problem. Even under simplified conditions, its estimation is complex than in case of a vertical well. Since, the water enters through a number of horizontal screened pipes (laterals), analytical solutions of flow to a RCW are based on the theory of flow to a horizontal pipe. Estimations of flow to a lateral can be based on two fundamental assumptions, i.e., (i) the total discharge through a lateral is uniformly distributed along its entire length, i.e., the uniform flux boundary condition exist along the laterals, and (ii) that the head along the lateral is uniform, i.e., Dirichelt type boundary condition exists along the laterals.

Hantush and Papadopulos (1962) have derived analytical solutions for drawdown distribution around a collector well with several horizontally laid laterals in confined and unconfined aquifer located near or under a stream channel satisfying uniform-flux boundary condition along the laterals. Hantush (1964) has suggested that instead of assuming each of the laterals to be line sink of uniform strength, Dirichelt type of boundary condition (uniform head condition) needs to be imposed along the laterals. Milojevic (1963) has conducted an experimental study using electro-dynamic analog model to analyse the yield of a radial collector well for the constant head boundary condition along the pipes. Debrine (1970) has conducted an experiment on electrolytic model to test the validity of the condition if the flux or the head should be uniform along the laterals. The results of his model study agreed with the solutions of Hantush and Papadopulos (1962) with relative deviation of about 2.2%. He concluded that the flow to a collector well could be estimated using the assumptions of either uniform flux or uniform head along the laterals. Zhan and Park (2003) have

5

assumed uniform flux distribution along the lateral axis for solving unsteady flow to the well under various aquifer conditions. They have mentioned that if a horizontal well is pumped with a large pumping rate, different flow states such as laminar, transitional, and turbulent flows can co-exist inside the lateral and the problem must be treated as a coupled well-aquifer hydraulics problem. Chen et al. (2003) using simplified numerical model of a horizontal well underneath a river have shown that the use of either a uniform flux or uniform boundary condition on the well screen misrepresents the realistic flux or head distribution along the laterals. The finding of Chen et al. pertains to a collector well, which has laterals of very small diameter (0.05m) and large length (116m). The Zhan and Cao (2000) put forward that at late pumping stage, horizontal pseudo-radial flow takes place towards a horizontal collector pipe. This postulate supports the assumption of sheet flow condition in a thin aquifer and horizontal collector well system. Mishra and Kansal (2007) have analysed the flow to a RCW having four coplanar fully screened laterals in a thin confined aquifer nearby a stream by applying conformal mapping technique. They have found that a constant head boundary condition along the lateral is applicable for laterals of diameter more than 0.2 m.

Generally, a RCW system has many laterals ranging from 2 to 23 per well and in such case, due to interference of laterals, the flux distribution along any lateral will not be uniform. The flux per unit length will be more near the tips of the pipes than that near the caisson. The flux per unit length at any section depends on entry gradient, pipe diameter, perforation percentage, hydraulic conductivity, and the hydraulic head difference across the flow boundaries. The entry gradient, hence the flux distribution, is governed by the geometry of flow domain. Thus, in case of a

6

collector well with several laterals, an assumption of uniform flux distribution along the laterals would misrepresent the true situation.

The groundwater flow problem near a horizontal or radial collector well can be described as a three-dimensional flow problem. The safe yield of a radial collector well can be estimated by solving Boussinesq's equation for 3-D flow with appropriate initial and boundary conditions. The flow to the radial collector well can be estimated using a numerical modelling approach by assuming the hydraulic head along the laterals as the same as that in the caisson. Though, the numerical methods are versatile for analyzing both steady and unsteady flow in non-homogeneous flow domain, they need more effort to discretise the flow domain for any parametric study. For example, a study on flow to radial collector well with several laterals would require fine grid size to compute the hydraulic gradient near the laterals with precision. Further, numerical models have their own limitations due to truncation error, convergence and stability problems.

Alternately, the design of the collector well can be based on steady state flow condition satisfying Laplace equation and the pertinent boundary condition (Harr (1962)). For a given layout of radials, and for a prescribed draw down in the well caisson, the unsteady flow to the collector radials can be computed. While estimating the flow, the entrance velocity to the radials is computed and compared with the limiting entrance velocity (3 cm/sec) for the prescribed draw down. Further, the axial velocity inside the screen should be less than 0.9 m/sec (Ray (2002), Driscoll (1987)). Varying the draw down and simultaneously computing the entrance velocity and comparing with the permissible velocity, the maximum flow rate for a given layout

7

and length of radials is computed, which is the capacity supply rate of the collector well.

The flow domain of a collector well in a thin aquifer near a stream can be considered as homogeneous as the radius of influence would not progress with time due to presence of the surface water body. The effective flow domain of a collector well will be a small part of the aquifer. The advantage of homogeneity can be taken for solving the well hydraulics problem analytically. If the objective is to estimate the production rate of a radial collector well, flow field can be considered as two-dimensional (x-y horizontal plane) neglecting the resistance to vertical flow. If the well is located near to a surface water body, the flow to the well could be treated as steady state flow during the later stage of long pumping. Thus, the flow can be estimated by solving well-known Laplace equation for 2D flow field $\left(d^2h/dx^2 + d^2h/dy^2 \right)$ under steady state conditions and, thereafter, a correction factor can be applied on account of resistance to vertical flow.

Yield of a collector well is influenced by length, orientation, number and diameter of laterals, etc. and can be studied through analytical technique such as the conformal mapping technique. Conformal mapping technique is one of the methods available to solve the 2D groundwater flow. Hunt (1983), applying Schwarz Christoffel conformal mapping, has analyzed steady flow to a single collector pipe, which is located near a stream, for different orientation of the collector pipe implementing constant head boundary condition along the pipe. Assumption of two-dimensional flow in a horizontal plane implies that the lateral as well as the river penetrates the entire thickness of aquifer. Applications of the classical Schwartz Christoffel conformal mapping technique in solving two-dimensional saturated steady

8

flow in homogeneous flow domain are well documented in several text books (Polubarinova-Kochina, 1962; Harr, 1962; Bear, 1972; Halek and Svec, 1979; Hunt, 1983). The Schwarz-Christoffel conformal mapping technique is applicable to a simply connected polygon with straight-line boundaries having a finite number of vertices one or more of which may be at infinity.

Most of the studies on radial collector wells have been carried out by assuming that the laterals are fully screened and meet at the centre of the collector well, whereas, in practical application, screen part of the laterals start at a certain distance from the circumference of the well. Hence, it is desirable to see the effect of partially screened laterals on the potential yield of the well and corresponding entrance velocity to the laterals.

In this study, the performance assessment of a RCW near a stream has been carried out, in terms of the estimation of maximum safe yield for various arrangements and parameters (like the numbers, radius, length of screened and blind portion, and distance of caisson from the river) of the laterals for various hydro-geologic conditions. By closing the valves of laterals, a RCW having multiple laterals can be made as a RCW with single or two collinear horizontal laterals only and can be treated and termed as an infiltration gallery.

Further, in an alluvial part of a river basin, the river meanders. In such situation it is advantageous to locate a RCW at the center of the meandering reach. By locating RCW on the concave side, higher specific capacity would be achieved. Also, if the river and aquifer system is in hydrostatic state, the flow to a RCW near a meandering reach can be conceptualized as a well at the center of a circular island.

Also, RCW may be used in a small island to withdraw fresh groundwater lying over saline water or from thin aquifer.

The basic concept of locating a RCW or vertical wells near a stream-bank is to take the advantage of induced infiltration from the stream and increase the water supply capacity of the aquifer under limiting drawdown condition. Several research works on the flow to a vertical pumped well near a stream have been carried out in which the estimations of stream depletion (combination of base flow reduction and induced infiltration) have been the primary objective. All these works have been carried out for the well tapping from upper unconfined aquifer only considering stream stage as constant. The stream stage rises during time of flood and water infiltrate from stream to the hydraulically connected unconfined aquifer; consequently, water level in the unconfined aquifer also rises. If the unconfined aquifer is connected to a confined aquifer through a vertical screened shaft nearby a river, unsteady flow will take place from the unconfined aquifer to the lower confined aquifer till its piezometric level is below the water level of the unconfined aquifer. Consequently, the lower confined aquifer will get recharged. In other terms the water supply capacity (i.e., specific capacity) of the confined aquifer will increase. This situation can be considered in context of groundwater recharge of lower confined aquifers. The practical application of this study is that these vertical shafts could be installed in series along the riverbank and water supply well (RCW or vertical well) could then be installed at some distance from these shafts on landside. Under these circumstances, specific capacity of water supply well would increase.

Generally, the RCWs and vertical wells are being used for drinking water supply as a part of riverbank filtration system. Thus, the quality of water produced by

the well in terms of presence of pathogenic bacteria needs to be assessed. Hence, it is important to estimate the travel time (or retention time) of the water particle from river to the well so that it is more than the survival life of the bacteria. Gerba and Melnick (1975) have presented the survival lives of pathogenic bacteria in porous medium in different conditions. Lesser bacterial concentration in produced water will require lesser dose of chlorination and hence lesser quantity of Disinfection-by-Product (DBP) production in the treated water and lesser risk of carcinogenic disease.

The minimum travel time will be the time taken by a water particle to reach the nearest part of the well screen moving along *critical shortest path (stream line)* which should be more than the survival time of particular pathogenic bacteria in concern. The distance of the well should be sufficiently large so that no bacteria can survive till it reaches the well.

1.3 OBJECTIVES OF THE PRESENT STUDY

In the light of the status of the studies on the flow to radial collector well or horizontal well with special reference to its application as part of riverbank filtration systems, objectives of the present study are:

1. Analysis to ascertain the flow characteristics such as the type of flow (laminar or turbulent) in a horizontal well (i.e., collector pipe, infiltration gallery, lateral, or drain) and the appropriate boundary condition (i.e., constant head or constant flux) along the lateral.

2. Analysis of flow to an infiltration gallery (or single horizontal collector well) for its different orientations with respect to the river.

11

3. Analysis of flow to a radial collector well with multiple partly screened laterals near a meandering reach of a river.

4. Analysis of flow to a radial collector well with partly screened laterals near straight reach of a stream.

5. Estimation of minimum travel time (retention time) taken by a water particle from the river to the nearest part of an infiltration gallery or laterals of a radial collector well to assess the possibility of survival of pathogenic bacteria in the produced water.

6. Estimation of groundwater recharge through a multi-aquifer shaft located near a stream during time of flood.

1.4   ORGANIZATION OF THE THESIS

The thesis has been organized as follows:

Chapter 1 describes the general importance of the radial collector well and the basic concepts of flow to horizontal well. It highlights the basic assumptions and the performance parameters of a RCW. It emphasis on the use of RCW and vertical well as a part of riverbank filtration system. The scope and objectives of the present study have been summarized and the organization of thesis has been described.

In Chapter 2, the existing literature review is presented. It briefly discuss the highlights of the important studies on the flow, design and construction of radial collector well, riverbank filtration, stream-aquifer interaction, stream-aquifer-well-interaction, multi-aquifers system, and natural attenuation of contaminant in the porous medium.

In Chapter 3, analytical studies have been carried out to ascertain the flow characteristics such as the type of flow (laminar or turbulent) inside a lateral/pipe and the appropriate boundary condition (i.e., constant head or constant flux) along the lateral.

In Chapter 4, flow to an infiltration gallery (i.e., a single horizontal collector pipe) has been analyzed by applying conformal mapping. Flow has been estimated for (i) an infiltration gallery laid near a meandering reach of a river, and (ii) an infiltration gallery laid in different position(s) with respect to the straight reach of a river such as (a) infiltration gallery oriented perpendicularly towards the river side, (b) an infiltration gallery oriented perpendicularly away from the river, i.e. towards the land side, (c) an infiltration gallery running parallel to the river. The minimum travel time taken by river water to reach the infiltration gallery has been estimated for all the mentioned above cases.

In Chapter 5, yield of a radial collector well having multiple partly screened laterals around the caisson and located in a meandering reach of a river has been estimated. Assuming the river and the aquifer system in hydrostatic state, the flow to a well near meandering reach of a river has been conceptualized as a well at the centre of a circular island. The flow is estimated using the conformal mapping technique. The laterals are considered as partly screened and partly blind (non-perforated). Further, the minimum travel time for river water to reach gallery has been estimated.

In Chapter 6, the performance of a radial collector well (horizontal well) having four co-planner laterals which are partly screened (perforated) and partly blind (non-perforated) by the side of a straight reach of a river has been studied. The performance has been evaluated in terms of yield and quality of water with respect to

13

the length of laterals, lengths of perforated and blind portions, orientation of laterals with respect to the river, and the distance of the well (i.e., central caisson) from the river. Further, the minimum travel time for river water to reach the nearest lateral has been estimated.

In Chapter 7, groundwater recharge through a shaft situated near a stream is estimated during passage of a flood wave. Recharge volume and the flow rate have been estimated for (i) a shaft, which is fully penetrating the lower confined aquifer, and (ii) a shaft, which has penetrated marginally into the confined aquifer, i.e., partially penetrating shaft. In this study, a discrete kernel approach based on Duhamel' superposition principle for linear systems, and image well theory are applied to quantify the recharge.

In Chapter 8, the important conclusions of the study have been summarized.

LITERATURE REVIEW

2.1 INTRODUCTION

It has been known for many years that the productivity of well fields located near a river can be improved by way of induced infiltration (Thies, 1935; Kazmann, 1947, 1948). Several studies have been carried out to estimate the proportion of water withdrawn from rivers by pumping from vertical wells located near a river for different hydro geologic conditions (Thies, 1941; Glover and Balmer, 1954; Todd, 1959; Hantush, 1959, 1964, 1965; Wilson, 1993; etc). Horizontal wells recently generated great interest among hydrologists and environmental engineers because of numerous advantages over vertical wells in many hydrological and environmental applications. A Radial collector well consists of a number of horizontal wells (i.e., laterals or radials) connected to a central caisson. Despite of this, very limited studies have been carried out to estimate the flow to a radial collector well nearby a river for different arrangement of laterals and its parameters. In the present chapter, some of the important works on flow to a radial collector well, its construction, use of a radial collector well, and infiltration gallery (i.e., single horizontal well) are briefly discussed.

2.2 STUDIES ON RADIAL COLLECTOR WELL

2.2.1 Field Studies

Kazmann (1948) provides a brief outline of the design and construction aspects and described at length the methods of horizontal collector well field testing to determine

the firm yields of the well under different conditions of the stream.

Kazmann (1949) has cited a typical and interesting example of the use of radial collector well for dual- purpose (i.e., aquifer storage and water supply) at Canton, Ohio. Three units dual-purpose horizontal wells were to be installed. One of these units was designed to built deep enough to act as the supply unit and was equipped with suitable pumps. The other two were designed to replenish the lower aquifer as it became depleted and have no pumps installed in them.

Gildley (1952) has presented details of the installation and performance of 13 radial collector wells in Ohio River valley, West Virginia. The initial yield of the wells varied from 1.75 mgd to more than 4.5 mgd. The wells output was substantially increased during high stage of the Ohio River. He also presented the data of water quality (alkalinity and hardness) and compared with Ohio river water quality.

Yale (1957) has presented a case study on the use of Radial collector well by Public District No.1 of Skagit County, Washington (USA). He explained the situation when the radial collector well faced the problem of higher iron content in produced water after a period of high rainfall in the lowlands, thereby raising the groundwater table by several feet. The river level did not rise appreciably as it originates primarily from higher snowfield. Further, the river water was very cold with higher viscosity and thereby reduced its transmissibility to the well. To make the river water gradient steeper than the groundwater gradient, a pump was installed in an old abandoned well located about 300 ft from the collector towards landside. Within 7 days after starting this pump the iron content dropped from high of 1.5 ppm to 0.7 ppm, while all other conditions remained constant.

Gidley and Miller (1960) have studied the performance records of 24 radial

collector wells in West Virginia and found that the initial yield of a radial collector wells adjacent to a river ranged from 1.5 to 4.5 MGD. This initial yield was found to be sustained with continuous pumping and was forecasted to decline by 30 to 50% over a period of 6 to 12 years.

Spiridonoff (1964) has discussed the outstanding features of the radial collector wells, design details, construction methods, yield, limitations, comparison with surface water treatment and problems in operation of radial collector well. He also presented a comprehensive list of radial collector wells with users and year of installation in North America and Europe. He concluded that there is a paucity of basic engineering information in the literature concerning radial collector wells due to the existence of patents and franchise rights connected with the apparatus and methods leading to a relative reluctance of the developers to use radial collector wells.

Hunt (2002) presents a timeline showing notable dates regarding the use of radial collector wells worldwide. He presented three types of laterals methods, such as perforated pipe screen, wire wrapped continuous slot screen, and gravel packed screen. He presented construction technique of well and lateral installation.

2.2.2 Experimental Studies

Mikel and Klair (1956) have given the first empirical solution for computing the drawdown in the centre (caisson) of a radial collector well. They introduced *equivalent well radius* r_e for a radial collector well, which is the radius of a vertical large diameter well having the same specific capacity as the collector well. They computed the value of the equivalent radius r_e of vertical large diameter well which simulates a collector well, and found to be 75-85 percent of the average lateral for

17

collectors of equal lengths, placed symmetrically and in the same horizontal plane all along the perimeter of the shaft.

Milojevic (1963) has conducted experiment using electro dynamic analog model to analyze steady flow to a radial collector well near a river and far from any recharge boundary. Results have been presented by means of four formulas for capacity of RCWs in a free water-table and in a confined aquifer of limited thickness and unconfined side expansion. Out of four formulae given by him, two formulae were for the radial collector well located far from any recharge boundaries and two formulae were for the well located nearby a riverbank. He studied the yield distribution along the drains and along the individual drains. He assumed the constant head along the drains.

Debrine (1970) has conducted an experiment on electrolytic model to test the validity of the condition that if the flux or the head should be uniform along the laterals. He conducted the experiment to estimate the flow to a well with a single lateral, located under riverbed and along which the head is maintained uniform. The results of his model study agreed with the solutions of Hantush and Papadopulos (1962) with relative deviation of about 2.2%. He concluded that the flow to a collector well could be estimated using the assumptions of either uniform flux or uniform head along the laterals.

2.2.3 Analytical Solutions

Hantush and Papadopulos (1962) have derived analytical solutions for drawdown distribution around a collector well with several horizontally laid laterals in confined and unconfined aquifer located near or under a stream channel satisfying uniform-flux boundary condition along the laterals. The three-dimensional unsteady flow problem

18

has been solved treating an element of the collector pipe as a partially penetrating vertical well. Hantush (1964) has suggested that instead of assuming each of the laterals to be the line sink of uniform strength, Dirichelt type of boundary condition (uniform head condition) needs to be imposed along the laterals.

Mishra et al. (1999), satisfying Dirichelt type boundary condition at the laterals as suggested by Hantush (1964), have analysed the unsteady three dimensional flow to a collector well system located under a streambed for prescribed draw-down at the well face using a finite difference numerical method. For the prescribed draw-down the entrance velocity to the radials is computed and compared with the limiting entrance velocity (3 cm/sec) (Driscoll, 1987). Varying the draw-down and simultaneously computing the entrance velocity and comparing with the permissible velocity, the maximum flow rate for a given layout and length of radials is computed, which is the capacity supply rate of the collector well.

Baker et al. (2005) have applied multi-layer analytic element modelling to estimate flow to a two-tier radial collector well with several radials under steady state condition. The three dimensional nature of flow and non-homogeneity in aquifer properties have been considered by them. Horizontal flow inside a layer is computed analytically while vertical flow is approximated with a standard finite-difference scheme.

Mishra and Kansal (2005) have studied the specific capacity of a radial collector well having 2-tiers of 12 numbers of laterals in each tier. The flow domain has been conceptualised as an island with the collector well at the centre of the island. The study indicates that the specific capacity increases marginally with increase in number of radials of equal length.

2.3   STUDIES ON A SINGLE HORIZONTAL WELL (INFILTRATION GALLERY)

Stone (1954) has presented the details of many infiltration galleries in the United States along the various rivers such as Ohio, Mississipi, etc. He concluded that infiltration galleries may supply 1 mgd per 1000 ft of length. He has also discussed the details of gallery construction and operation.

Ground water manual (1981) of U.S. department of Interior includes a separate chapter on infiltration galleries. According to the manual, the design should provide for an average entrance velocity of 0.1 ft per second or less. Manual provides some applicable equations to estimate the yield of a gallery for different types of construction or setting in the subsurface.

Huisman and Olsthoorn (1983) have analyzed steady flow to a drainage gallery of finite length that runs parallel to a river by drawing flow nets. Both the gallery and river are assumed to be fully penetrating.

Hunt (1983) has applied Schwarz Christoffel conformal mapping technique to analyze steady flow to a single collector pipe, which is located near a stream, for different orientation of the collector pipe implementing constant head boundary condition along the pipe. Hunt has treated the problem as two-dimensional in horizontal plane and has modified the velocity potential function suitably. Assumption of two-dimensional flow in a horizontal plane implies that the lateral as well as the river penetrates the entire thickness of aquifer.

Zhan and Cao (2000) states that flow to a finite horizontal well includes three stages: an early pumping stage, nearly radial flow, intermediate flow, and a late horizontal pseudoradial flow. At the early stage of pumping, the influences of the top

20

and bottom boundaries are not perceptible, thus the flow is radial in a plane perpendicular to the well axis. After the intermediate period, the flow enters the pseudoradial flow stage during which the equipotential surfaces are similar to vertical cylinders in the far field. This situation is similar to a fully penetrating large diameter vertical pumping well. This postulation supports the assumption of sheet flow condition in a thin aquifer and horizontal collector well system.

Zhan and Park (2003) have assumed uniform flux distribution along the horizontal well axis for solving unsteady flow to the well under various aquifer conditions. They state that, if a horizontal well is pumped with a large pumping rate, different flow states such as laminar, transitional, and turbulent flows can co-exist inside the well bore and the problem must be treated as a coupled well-aquifer hydraulics problem. However, a couple well-aquifer hydraulics problems need a numerical solution because a closed form analytical solution in this case is not possible.

Chen et al. (2003) has conducted theoretical and experimental studies of couple-seepage flow (i.e., well-aquifer hydraulics) to a horizontal well. They have used simplified numerical model of a horizontal well underneath a river and have shown that the use of either a uniform flux or uniform boundary condition on the well screen misrepresents the realistic flux or head distribution along the horizontal well bore. The finding of Chen et al. pertains to a collector well, which has a very small diameter (0.05m) and a large length (116m).

Mohammed and Rushton (2006) have carried out field experiment and numerical model to analyse the flow in a shallow aquifer before entering into a horizontal well, the flow from the aquifer into the horizontal well and flow inside the

21

efficiency of riverbank filtration to remove microorganism from the infiltrating surface water depends on (1) attachment of the microorganism to the soil or sand and inactivation, (2) the climate and hydrological conditions (temperatures, heterogeneity, flood), (3) the geometry of production well (horizontal well or vertical well) and surface water body (lake, river, island), (4) the character of the bank materials and streambed, and (5) groundwater flow field. Aquifer materials with significant fracturing are capable of transmitting groundwater at high velocity in a direct flow path with less travel time, i.e., less opportunity for inactivation or removal of microbial pathogens.

Dillon et.al. (2002) have considered two basic factors which are most important for the assessment of quality of recovered water from a well pumping nearby a river as a part of RBF for drinking water supplies from brackish aquifers. These two factors are (i) minimum travel time from the river to the well, t_{min}, and (ii) the proportion of the recovered water which is derived from the river (q/Q), where q is the rate of induced infiltration from the river and Q is the discharge rate of the pumping well. The first factor allows an estimate of contamination attenuation through adsorption and biodegradation and the second factor contribute to the further reduction in contaminant concentration through dilution. For well close to the river, t_{min} is small and q/Q is large, and with increasing distance from the river t_{min} increase and q/Q may decline. They have considered only vertical well for the study and used MODFLOW for simulation. There results show that a well located 50m from the bank would pump 94% water from the closest reach at steady state and will have a t_{min} of about 84 days for initially horizontal water table taking adsorption and biodegradation into consideration. Further, to minimize the risk of bacterial contamination of

produced water, the t_{min} should be more than the survival time of pathogenic bacteria in concern.

Schubert (2002) reported the field studies conducted in the lower Rhine region to know the flow and transport phenomena of riverbank filtration and to develop numerical models for dynamic simulation of flow and transport. In this study, the important finding was about the age stratification of the bank filtrate between the river and the wells. Age stratification means that water enters a well near a river at widely different times. This difference in time is the reason for equalization of the fluctuating concentrations between the river and the wells. From 3D modeling under steady state condition, results of the flow path, flow time and mean flow velocity were reported and are reproduced as

Flow path (m)	Flow time (days)	Mean flow velocity (m/day)
290	157	0.25
162	120	1.35
108	33	3.27
68	20	3.40

Wiess (2003) discusses the significance of RBF in removing natural organic matter (NOM) present in surface water. NOM present in water reacts with chlorine used for disinfection and halogenated DBPs such as trihalomethanes (THMs) and haloacetic acid (HAAs) are formed, many of which are suspected or known human carcinogens (Singer, 1999). Possible approaches for controlling DBP formation include (1) use of alternative disinfectants, such as ultraviolet radiation or monochloramines which do not react readily with NOM, (2) removal of DBPs from finished water through such process as granular activated carbon adsorption or stripping, and (3) better control of source water quality through removal of precursor NOM to prevent DBP formation. RBF's value for controlling DBPs lies in its ability

to achieve this last benefit, namely removal of NOM through ground passage. In this study, they estimated travel time using USGS's MODFLOW for groundwater flow and MODPATH for particle tracking. Travel time of 13 to 19 days estimated to reach the vertical well (1.5 mgd) located about 177m from the river, whereas 3 to 5 days estimated to reach the vertical well (7.6 mgd) located at a distance of 30m from the stream. The travel time varies with the variation in pumping rates, porosity, and hydraulic conductivity.

Weiss (2005) reported a study conducted for microbial monitoring over a period of more than one year at three full scale RBF facilities, located in US along the Ohio, Missouri, and Wabash Rivers. Results of this study demonstrated the potential for RBF to provide substantial reductions in microorganism concentration relative to the raw water sources. The travel times are highly uncertain, and the purpose of this study was to characterize the average concentrations over time particularly for the river.

2.5 STREAM AQUIFER INTERACTION

The basic concept for locating a radial collector well or vertical well near a stream-bank is to increase the water supply capacity of an aquifer under limiting drawdown condition. The unconfined aquifer gets recharged from stream during passage of flood wave. If a vertical screened shaft is located near the stream, water will pass from the unconfined aquifer to the lower aquifer through the shaft due the rise in stream stage during time of flood. The lower confined aquifers will receive water from the upper unconfined aquifer through the shaft under gravity till the peizometric level of the confined aquifer is lower than the water level in the unconfined aquifer.

Consequently, the lower aquifers will get recharged. In other terms the water supply capacity (i.e., specific capacity) of the confined aquifers will increase. This situation can be considered in context of groundwater recharge of lower confined aquifers.

In this study, it has been attempted to estimate the quantity of water that would pass from the water table aquifer to the lower confined aquifer through a screened shaft, which is located near a stream, during time of flood. The shaft penetrates multi-aquifers system. Since a well-aquifer-stream system is a linear system. Hence, to estimate the quantity of recharge through the well, a better understanding of works on the stream-aquifer interaction without a pumped well and in presence of a pumped well nearby the stream is required.

Several investigators have worked on stream-aquifer interactions with their different objectives, such as, aquifer's response to stream stage changes; estimation of hydraulic diffusivity and estimations of aquifer recharge. Some investigators have applied the equation developed for stream-aquifer relationship to estimate the hydraulic diffusivity of the aquifer (Ferris, 1952; Rowe, 1960; Pinder et at. 1969; Mishra and Jain, 1999; Singh, et al., 2002; Singh, 2003, etc). To compute the rise in piezometric level in the adjoining aquifer due to the stream stage rise, solutions have been developed by several investigators (Todd, 1955; Rowe, 1960; Cooper and Rorabough, 1963; Hornberger, et al., 1970; Moench and Kisiel, 1970; Hall and Moench, 1972; Lin, 1972; Morel-Seytoux and Daly, 1975; Singh, 2004, etc).

2.5.1 Stream Aquifer Well Interactions: Induced Infiltration

The estimations of induced infiltration due to abstraction of water from a well nearby a river, has been the main objectives in various theoretical and field studies which are presented subsequently.

Theis (1941) have computed analytically the proportion of pumped water taken from stream flow. He has used Thies (1935)'s basic solution for drawdown around a infinitesimally small diameter pumped well and the *theory of image well*. He concluded that the proportion of water taken from stream flow varies widely depending on the transmissibility of the aquifer and the distance of the well from the stream.

Kazmann (1948) have proposed two methods based on pumping test data for determining whether water from a surface water body will infiltrate to an adjacent aquifer if wells are pumped at the site tested. The maximum rate of infiltration from a surface water body is not involved in either of these methods. The only answer sought is whether infiltration will occur after pumping begins. Further, he has given a method for determining the effective distance to the line of recharge.

Hantush (1959) has proposed methods, on the basis of analysis of data from pumping wells near a stream, for determining the hydrologic characteristics of an aquifer adjacent to the stream and the effective distance from a pumped well to a line in the stream bed where the water is entering or leaving the aquifer. He has applied the basic equation for drawdown due to unsteady flow towards a well steadily discharging from an infinite aquifer and the theory of image well for the analysis.

Hantush (1965) has presented analytical solution for rate and volume of stream depletion due to pumping of a well near stream with semi pervious bed. He replaced the resistance of flow due to the semi-perviousness of the bed of the stream by an equivalent resistance due to horizontal flow through a semi-pervious layer. The semi-pervious layer has insignificant storage capacity which is lying between the aquifer and the stream. He has presented a procedure for obtaining the transmissibility

28

of the aquifer, the effective distance from the stream and the retardation coefficient of the streambed.

Moore and Jenkins (1966) have conducted a field study on the Arkansas River in Colarado to evaluate the effect of groundwater pumpage on the infiltration rate of a semipervious streambed. The studies shown that groundwater pumping can easily lower the water table below the level of the streambed, thereby breaking the hydraulic connections between the stream and the water table. Once this connection is broken, change in depth to water table has no measurable effect on the rate of stream flow depletion.

Newson and Wilson (1988) have developed an analytical model to evaluate steady state flow of groundwater towards a well near a gaining stream. In this model they have taken the ambient groundwater flow (i.e., regional groundwater flow) into consideration. They have given solution to determine the minimum rate of pumping that will induce infiltration from a stream to a well, and the components of pumping that are derived from the stream and the aquifer. The model is based on *image well theory* and stream is fully penetrating.

Wilson (1993) has developed a two-dimensional vertical integrated analytical model to compute the induced infiltration with ambient flow for various geometry and sources of recharge. Model shows that the propensity for discharge and rate of induced infiltration are enhanced by higher pumping rates, proximity of the well to the stream, and the presence of nearby barrier boundaries. He concluded that the induced infiltration to wells located near a gaining stream is essentially independent of the source of ambient discharge to the stream, whether it is composed of local recharge, lateral inflow, or some combination of the two. Infiltration also appears to

be indifferent to the assumption of constant transmissivity or transmissivity is allowed to vary with the saturated thickness.

Sophocleous, et al. (1988) have conducted field experiments to study the stream-aquifer interaction in presence of a pumping well along the Arkansas River. They have conducted eight days comprehensive pumping test followed by recovery monitoring. Drawdown and recharge boundary effects were observed in all observation wells completed within the aquifer, including the ones on the opposite side of the Arkansas River. Actual stream flow depletion due to groundwater pumping was appreciably less than the computed depletion based on analytical solutions. They concluded that pumping tests are the most reliable way of obtaining aquifer properties for use in developing groundwater supplies, in predictive numerical simulations and management of water resources. However, they are expensive tests because of both the required equipment and manpower.

Wallace et al. (1990) have derived equations to compute the stream depletion caused by non-uniform, cyclic pumping from a well located in a hydraulically connected aquifer. Equations were developed applying the principle of superposition and existing analytical solutions for steady, continuous pumping. Analysis shows that the volume of stream depletion over a cycle ending at time t, is the same as the volume depletion between the start of pumping and time t by a single period of pumping. However, they conclude that in some circumstances, approximating the effect of cyclic pumping by a steady, continuous pumping at the equivalent cycle average rate is not adequate.

Hunt (1999) has given an analytical solution for stream depletion created by pumping from a well beside a semi-pervious stream. He assumed the streambed

penetration of the aquifer and dimension of streambed cross section, all are relatively small. He assumed streambed is clogged and that a linear relationship exists between the outflow seepage through the streambed and the change in peizometric head across the semi-pervious layer.

Analysis of stream aquifer interaction in presence of a pumped well nearby a stream has traditionally focused on the determination of the amount of water in the stream depleted due to induced infiltration and base flow reduction. When a well is placed nearby a stream for the purpose of drinking water supply as part of riverbank filtration system, then quality of pumped water becomes a concern. Estimation of induced infiltration determines the proportion of dilution of surface water with native groundwater in context of RBF process. In this case attention has to be paid to the movement of infiltrated stream water inside the aquifer.

Chen (2001) has studied the migration of induced-infiltrated stream water towards a pumped well using *particle tracking techniques* He has determined the travel times, pathlines and influence zones between a stream and nearby pumping well. Analysis were conducted for transient conditions, both pumping and non pumping periods. He has also determined the percentage of stream water entering the well using path lines of stream water. Knowing these path lines help in wellhead protection.

Chen (2003) has computed critical time which is the earliest time of reversal of hydraulic gradient occurring along the stream aquifer interface, infiltration reach which is the stream segment where stream water recharges the aquifer and *the shortest travel time for the stream particle to get into a pumping well along the meridian line.* He concluded that when a steady state condition is assumed for a

transient flow, the rate and volume of stream infiltration is overestimated and this overestimation can be very significant in early stage of pumping.

2.6 CONCLUSIONS

From the literature review on the subject, it is observed that very little analytical works have been carried out on the flow to a radial collector well located near a river are reported. However, several works on the flow to a vertical well located near a river have been carried out to estimate the induced infiltration, stream depletion or base flow reduction due to pumping. A radial collector well consists of group of horizontal wells, hence from the theory of flow to a horizontal pipe, total flow to a radial collector well can be estimated. From the literature review, it is clear that there are two basic approaches to find the solutions of flow to a horizontal well. These two approaches are: either constant flux or constant head boundary condition persists along the horizontal well. Hence, it is desirable to investigate the characteristic of flow inside a horizontal well. Analytic works on the flow to a single horizontal wells are also reported but analytical solution to the flow to a multi- laterals radial collector well a near a stream are very rare. Most of the radial collector wells are used as a part of riverbank filtration systems. The total travel time taken by a water particle to reach the nearest well screen from the stream needs to be estimated to assess the risk of bacterial contamination and organic contamination. Only a few works on the travel time of water particle from river to production well are reported.

GRADUALLY VARIED FLOW
IN A HORIZONTAL COLLECTOR PIPE

3.1 INTRODUCTION

Flow to a lateral of radial collector well is a case of gradually varied flow. Several

investigators have presented analytical solutions for flow to a horizontal collector pipe

under different hydro-geological conditions (Zhan, and Cao, 2000; Chen et al., 2003).

Zhan and Park (2003) have assumed uniform flux distribution along the lateral axis

for solving unsteady flow to the well under various aquifer conditions. They postulate

that, if a horizontal well is pumped with a large pumping rate, different flow states

such as laminar, transitional, and turbulent flows can co-exist inside the lateral and the

problem must be treated as a coupled well-aquifer hydraulics problem. Chen et al.

(2003) using simplified numerical model of a horizontal well underneath a river have

shown that the use of either a uniform flux or uniform boundary condition on the well

screen misrepresents the realistic flux or head distribution along the lateral. The

finding of Chen et al. pertains to a collector well in which laterals have a very small

diameter (0.05m) and a large length (116m). Mishra and Kansal (2007) have analysed

steady flow in a collector pipe assuming exclusively laminar or turbulent flow

condition and found that Chen et al.'s finding is true for pipe having diameter of the

order of 0.05m. For pipe diameter of 0.2 and more, uniform head boundary as well as

uniform flux per unit length boundary condition is applicable as the friction loss is

negligible for pipe with radius more than 0.1m.

In this chapter, considering the co existence of laminar and turbulent flow in a collector pipe, an analytical solution has been derived for steady state flow condition and applicability of uniform head or uniform flux condition along the collector pipe has been investigated.

3.2 STATEMENT OF THE PROBLEM

Gradually varied flow in a horizontal collector well (a perforated horizontal pipe) is to be analysed to ascertain whether uniform head distribution or uniform water flux per unit length exist along the horizontal collector pipe. It is desired to predict magnitude of the axial velocity along the collector pipe and entrance velocity at the periphery of the collector pipe for radius adopted in practice. The perforated pipe is assumed to be located along the axis of a conceptual horizontal cylindrical flow domain of radius R and length L as shown in Fig.3.1. It is closed at the left end and the right end is connected to a reservoir (caisson) where a hydraulic head h_w is maintained. The drawdown D_w in the well is h_R-h_w. The flow is laminar up to an unknown length l_1 at which the critical Reynold number is 3000. Beyond l_1 the flow is turbulent. The length of the turbulent flow zone is l_2 which is equal to ($L - l_1$). The transition zone has been merged with smooth turbulent flow zone. At the periphery of the flow domain the hydraulic head is h_R. The flow has reached a steady state condition.

3.3 ANALYTICAL SOLUTION

The axial frictional head loss in the pipe follows Darcy-Weisbach equation and can be expressed as

$$-\frac{\Delta h}{\Delta x} = \frac{f}{d}\frac{u^2}{2g}$$

(3.1)
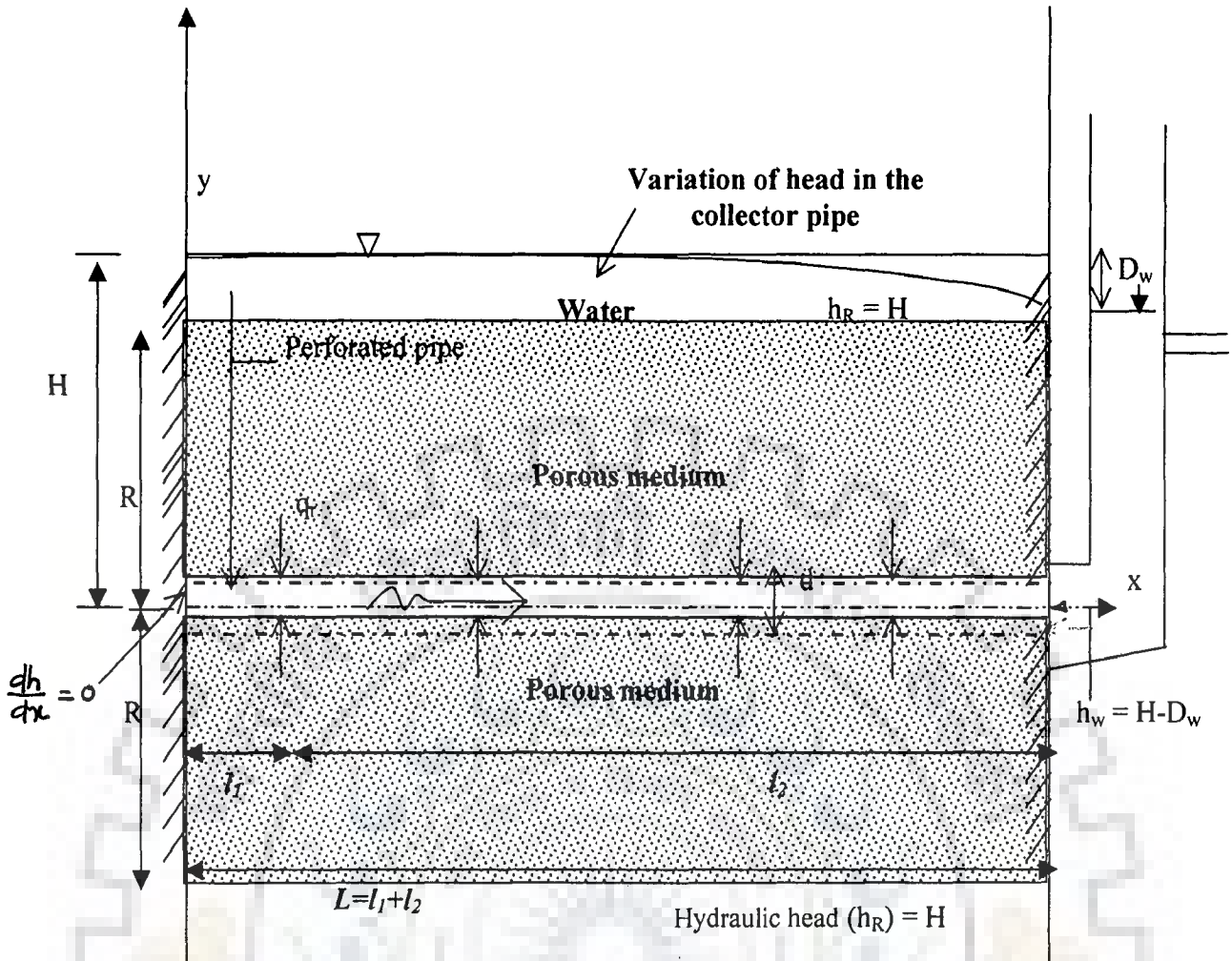
Fig.3.1: A conceptual cylindrical flow-domain around horizontal collector pipe.

where $\Delta h = h(x + \Delta x) - h(x)$; f is the friction factor which can be estimated using the

relation $f = 64 / R_e$ for laminar flow having Reynold's number $R_e (= u d \rho / \mu) < 2300$

(d=diameter of the perforated pipe, u=axial velocity at x; ρ = density and μ =

viscosity of water) or by using the Blasius equation $f = 0.316 / R_e^{0.25}$ for smooth

turbulent flow having Reynold's number between 3000 to 100, 000. In the zone where

the Reynolds number is less than 3000, the flow is considered as laminar, otherwise,

the flow is smooth turbulent.

The axial velocity and the corresponding Reynold's number and flow regimes are unknown a priori. The flow in the horizontal collector pipe near the left end is laminar and it may turn into turbulent with a transition condition in between as it approaches towards the caisson. Thus the flow may be a composite flow consisting of laminar, transition and turbulent flow zones. The head distribution is computed in the horizontal collector pipe assuming that the laminar flow at the left end changes to smooth turbulent flow condition.

3.3.1 Head Distribution for Laminar Flow Zone

In order to estimate the frictional head loss corresponding to laminar flow in a pipeline, Hagen-Poiseuille equation, which can be derived by substituting $f = 64/R_e$ in Darcy Weisbach equation, is used. Accordingly,

$$u = \frac{-\rho g d^2}{32\mu} \frac{dh}{dx} \tag{3.2}$$

Therefore, the axial flow, $q_{lx}(x)$, at x in laminar flow zone is:

$$q_{lx}(x) = \frac{\pi g \rho d^4}{128\mu} \left(-\frac{dh}{dx} \right) \tag{3.3}$$

The variation of axial flow with x is: $\dfrac{dq_{lx}(x)}{dx} = \dfrac{\pi g \rho d^4}{128\mu} \left(-\dfrac{d^2 h(x)}{dx^2} \right)$ (3.4)

The variation in axial flow in the pipe is equal to the radial flow into the pipe. Hence,

$$\frac{dq_{lx}(x)}{dx} = q_r(x) \tag{3.5}$$

Assuming the flow to be radial in a plane normal to the pipe axis and applying Darcy's law, the radial flux, $q_r(x)$, at any radial distance r, $d/2 \le r \le R$, from the pipe axis, for a steady state flow condition, is given by

$$-2\pi r k \frac{dh}{dr} = \text{a constant} = -q_r(x) \tag{3.6}$$

Integrating and applying the boundary condition $h(R, x) = h_R$ and $h(d/2, x) = h(x)$

$$q_r(x) = \frac{2\pi k}{\ln(2R/d)} \{h_R - h(x)\} \tag{3.7}$$

$q_r(x)$ = water flux per unit length along the collector pipe. The entrance velocity $v_r(x)$

at x at the periphery of the collector pipe with P % of perforation is given by:

$$v_r(x) = \frac{2\pi k}{\ln(2R/d)} [h_R - h(x)] / [P\pi d] \tag{3.8}$$

Incorporating (3.5) and (3.7) in (3.4), the differential equation reduces to

$$-\frac{g\rho d^4}{256 \mu k} \ln(2R/d) \frac{d^2 h}{dx^2} = \{h_R - h(x)\} \tag{3.9}$$

Let the laminar flow persist up to length l_I and let the head at the interface of laminar

and smooth turbulent flow be $h(l_1)$. Both l_I and h (l_I) are unknown a priori. At the left

end of the collector pipe, i.e. at $x=0$, $\dfrac{dh}{dx} = 0$. The solution to differential equation

(3.9) satisfying the above mentioned boundary conditions is

$$h(x) = h_R - \{h_R - h(l_1)\} \frac{\cosh(Cx)}{\cosh(Cl_1)} \tag{3.10}$$

where $C = \sqrt{\dfrac{256 \mu k}{g\rho d^4 \ln(2R/d)}}$

Differentiating $h(x)$ and incorporating the differential in (3.3), the flow at section x in

the laminar flow zone is

$$q_{lx}(x) = C \frac{\pi g\rho d^4}{128 \mu} \frac{\sinh(Cx)}{\cosh(Cl_1)} \{h_R - h(l_1)\} \tag{3.11}$$

At $x = l_1$, where laminar flow becomes turbulent, the axial flow is

$$q_{lx}(l_1) = C \frac{\pi g\rho d^4}{128 \mu} \tanh(Cl_1) \{h_R - h(l_1)\} \tag{3.12}$$

37

3.3.2 Head Distribution in Smooth Turbulent Flow Zone

For analyzing flow in the smooth turbulent flow zone, a separate origin is chosen at the incipient of turbulent flow. In order to estimate the frictional head loss in smooth turbulent flow zone, Blasius equation is incorporated in equation (3.1). Accordingly,

$$u = \left[\frac{gd^{5/4}\rho^{1/4}}{0.158\mu^{1/4}}\right]^{4/7}\left[-\frac{dh}{dx}\right]^{4/7} \tag{3.13}$$

and $q_{tx}(x) = \frac{\pi}{4}\left[\frac{g\rho^{1/4}}{0.158\mu^{1/4}}\right]^{4/7} d^{19/7}\left(-\frac{dh}{dx}\right)^{4/7}$ (3.14)

Differentiating $q_{tx}(x)$ with respect to x and equating $\frac{dq_{tx}(x)}{dx} = q_r(x)$ and

simplifying

$$\frac{dq_{tx}(x)}{dx} = \frac{\pi}{7}\left[\frac{g\rho^{1/4}}{0.158\mu^{1/4}}\right]^{4/7} d^{19/7}\left(-\frac{dh}{dx}\right)^{-3/7}\left(-\frac{d^2h}{dx^2}\right) = \frac{2\pi k}{\ln(2R/d)}[h_R - h(x)] \tag{3.15}$$

Substituting $H = h_R - h$; $-\frac{dh}{dx} = \frac{dH}{dx}$; and $-\frac{d^2h}{dx^2} = \frac{d^2H}{dx^2}$ in equation (3.15) and

simplifying

$$\frac{\ln(2R/d)}{14k}\left[\frac{g\rho^{1/4}}{0.158\mu^{1/4}}\right]^{4/7} d^{19/7}\frac{d^2H}{dx^2} = H\left(\frac{dH}{dx}\right)^{3/7} \tag{3.16}$$

The smooth turbulent zone is discretized into n number of grids of equal size Δx. Let the grid point at the origin be assigned the number 1 and the grid at the caisson be assigned number N. The finite difference forms of the first and second order derivatives for intermediate nodes $[2 \le i \le (N-1)]$ are

$$\frac{dH}{dx} = \frac{H(i+1) - H(i-1)}{2\Delta x} \tag{3.17}$$

38

$$\frac{d^2 H}{dx^2} = \frac{H(i+1) - 2H(i) + H(i-1)}{\Delta x^2}$$

(3.18)

Incorporating equations (3.17) and (3.18) in equation (3.16), the finite difference form of the differential equation (3.16) reduces to

$$F\{H(i-1), H(i), H(i+1)\} = C_1 \{H(i+1) - 2H(i) + H(i-1)\} - H(i)\{H(i+1) - H(i-1)\}^m = 0$$
$$i = 2, 3, \ldots N - 1$$

(3.19)

where $C_1 = \dfrac{(2\Delta x)^{3/7}}{(\Delta x)^2} \dfrac{\ln(2R/d)}{14k} \left[\dfrac{g\rho^{1/4}}{0.158\mu^{1/4}}\right]^{4/7} d^{19/7}$ and $m = 3/7$; $N - 1 = l_2 / \Delta x$.

Let $H^*(i-1), H^*(i), H^*(i+1)$ are close to the true solution. Applying Taylor series expansion to the function in equation (3.19)

$$F(H_{i-1}^*, H_i^*, H_{i+1}^*) + \left.\frac{\partial F(H_{i-1}, H_i, H_{i+1})}{\partial H_{i-1}}\right|_{H_{i-1}^*, H_i^*, H_{i+1}^*} \Delta H_{i-1} + \left.\frac{\partial F(H_{i-1}, H_i, H_{i+1})}{\partial H_i}\right|_{H_{i-1}^*, H_i^*, H_{i+1}^*} \Delta H_i$$

$$+ \left.\frac{\partial F(H_{i-1}, H_i, H_{i+1})}{\partial H_{i+1}}\right|_{H_{i-1}^*, H_i^*, H_{i+1}^*} \Delta H_{i+1} \cong 0$$

(3.20)

Substituting the partial differential of $F(H_{i-1}, H_i, H_{i+1})$ with respect to H_{i-1}, H_i, H_{i+1} in equation (3.20) and simplifying

$$\left\{C_1 + mH^*(i)[H^*(i+1) - H^*(i-1)]^{m-1}\right\}\Delta H(i-1) +$$
$$\left\{-2C_1 - [H^*(i+1) - H^*(i-1)]^m\right\}\Delta H(i)$$

$$+ \left\{C_1 - mH^*(i)[H^*(i+1) - H^*(i-1)]^{m-1}\right\}\Delta H(i+1)$$

$$\cong -C_1 [H^*(i+1) - 2H^*(i) + H^*(i-1)] + H^*(i)[H^*(i+1) - H^*(i-1)]^m$$

(3.21)

$$i = 2, 3, \ldots N - 1$$

39

For $i = N - 1, H(N) = h_R - h_w = H^*(N)$ and $\Delta H(N) = 0$. With these substitutions in equation (3.21), one obtains

$$\left\{C_1 + mH^*(N-1)\left[(h_R - h_w) - H^*(N-2)\right]^{m-1}\right\}\Delta H(N-2) +$$

$$\left\{2C_1 - \left[(h_R - h_w) - H^*(N-2)\right]^m\right\}\Delta H(N-1)$$

$$\cong -C_1\left[(h_R - h_w) - 2H^*(N-1) + H^*(N-2)\right] + H^*(N-1)\left[(h_R - h_w) - H^*(N-2)\right]^m$$

$$(3.22)$$

At the origin for grid 1, the finite difference form defined in equation (3.17) is not applicable as the head distribution is not differentiable at grid 1. The forward difference at grid 1 is given by:

$$\frac{dH}{dx} = \frac{H(2) - H(1)}{\Delta x} \qquad (3.23)$$

Incorporating equation (3.23) in equation(3.13)the following relation is obtained:

$$u = \left[\frac{gd^{5/4}\rho^{1/4}}{0.158\mu^{1/4}}\right]^{4/7}\left[\frac{H(2) - H(1)}{\Delta x}\right]^{4/7} \qquad (3.24)$$

Equating the Reynold's number $\dfrac{ud\rho}{\mu}$ equal to 3000, one gets

$$\left[\frac{gd^{5/4}\rho^{1/4}}{0.158\mu^{1/4}}\right]^{4/7}\left[\frac{H(2) - H(1)}{\Delta x}\right]^{4/7}\frac{d\rho}{\mu} = 3000 \qquad (3.25)$$

Further simplification leads to

$$H(2) - H(1) - \Delta x\, 3000^{7/4}\frac{0.158\mu^2}{gd^3\rho^2} = 0 \qquad (3.26)$$

Applying Taylor series expansion for the function in equation (3.26) one finds

$$-\Delta H(1) + \Delta H(2) = H^*(1) - H^*(2) + \Delta x\, 3000^{7/4}\frac{0.158\mu^2}{gd^3\rho^2} \qquad (3.27)$$

40

The required boundary conditions are incorporated through equations (3.22) and (3.27). Thus for an assumed value of smooth turbulent flow zone, the drawdown at $N-1$ grid locations are found using equations (3.21), (3.22) and (3.27). From equations (3.21), (3.22), (3.27), the elements of the Jacobian matrix are as follows:

$$A(1,1) = -1;$$

$$A(1,2) = 1;$$

$$A(1,3) = 0; \ldots, A(1, N-2) = 0; A(1, N-1) = 0 \tag{3.28}$$

$$A(2,1) = \left\{ C_1 + mH^*(2)\left[H^*(3) - H^*(1)\right]^{m-1} \right\}$$

$$A(2,2) = \left\{ -2C_1 - \left[H^*(3) - H^*(1)\right]^{m} \right\}$$

$$A(2,3) = \left\{ C_1 - mH^*(2)\left[H^*(3) - H^*(1)\right]^{m-1} \right\}$$

$$A(2,4), \ldots, A(2, N-2), A(2, N-1) = 0 \tag{3.29}$$

$$A(3,1) = 0;$$

$$A(3,2) = \left\{ C_1 + mH^*(3)\left[H^*(4) - H^*(2)\right]^{m-1} \right\};$$

$$A(3,3) = \left\{ -2C_1 - \left[H^*(4) - H^*(2)\right]^{m} \right\}$$

$$A(3,4) = \left\{ C_1 - mH^*(3)\left[H^*(4) - H^*(2)\right]^{m-1} \right\}$$

$$A(3,5) = A(3,6) = \ldots, A(3, N-1) = 0 \tag{3.30}$$

$$A(N-1,1) = A(N-1,2) = \ldots = A(N-1, N-3) = 0$$

$$A(N-1, N-2) = \left\{ C_1 + mH^*(N-1)\left[(h_R - h_w) - H^*(N-2)\right]^{m-1} \right\}$$

$$A(N-1, N-1) = \left\{ -2C_1 - \left[(h_R - h_w) - H^*(N-2)\right]^{m} \right\} \tag{3.31}$$

$$E(1) = H^*(1) - H^*(2) + \Delta x \, 3000^{7/4} \frac{0.158 \mu^2}{g d^3 \rho^2}$$

$$E(2) = -C_1 \left[H^*(3) - 2H^*(2) + H^*(1)\right] + H^*(2)\left[H^*(3) - H^*(1)\right]^{m}$$

$$E(3) = -C_1 \left[H^*(4) - 2H^*(3) + H^*(2)\right] + H^*(3)\left[H^*(4) - H^*(2)\right]^{m}$$

$$E(N-1) = -C_1 \left[(h_R - h_w) - 2H^*(N-1) + H^*(N-2)\right] + H^*(N-1)\left[(h_R - h_w) - H^*(N-2)\right]^{m}$$

$$\tag{3.32}$$

Let the column matrix $[B]$ be defined as:

$$[B] = \{\Delta H(1), \Delta H(2), \Delta H(3), ..., \Delta H(N-2), \Delta H(N-1)\}^{'} \qquad (3.33)$$

The set of $N-1$ equations including one at $x = 0$; and at $x = (N-1)\Delta x$ in matrix notation are expressed as:

$$[A][B] = [E] \qquad (3.34)$$

Hence,

$$[B] = [A]^{-1}[E] \qquad (3.35)$$

The initial guessed values $H^{*}(i), i = 1,2,....(N-1)$ are improved by adding $\Delta H(i)$ to them and the process is repeated till the desired accuracy is attained.

3.3.3 Determination of length of laminar flow zone

The Reynold's number at the end of laminar flow zone is equal to 3000. Thus, from equation (3.12), the axial velocity is

$$u = C\frac{g\rho d^2}{32\mu}\tanh(Cl_1)H(l_1) \qquad (3.36)$$

The corresponding Reynold number is

$$\frac{ud\rho}{\mu} = C\frac{g\rho^2 d^3}{32\mu^2}\tanh(Cl_1)H(l_1) = 3000 \qquad (3.37)$$

Replacing $H(l_1)$ by $H(1)$ in equation (3.37) one finds

$$C\frac{g\rho^2 d^3}{32\mu^2}\tanh(Cl_1)H(1) = 3000 \qquad (3.38)$$

or

$$\tanh(Cl_1) = \frac{\mu^2}{Cg\rho^2 d^3}\frac{96000}{H(1)} \qquad (3.39)$$

or

42

$$l_1 = \frac{1}{2C} \ln \left(\frac{1 + \dfrac{\mu^2}{Cg\rho^2 d^3} \dfrac{96000}{H(1)}}{1 - \dfrac{\mu^2}{Cg\rho^2 d^3} \dfrac{96000}{H(1)}} \right)$$

(3.40)

The length, L, of the collector well is:

$$L = l_1 + (N-1)\Delta x$$

(3.41)

3.4   RESULTS AND DISCUSSION

The variations of drawdown, axial flow, axial velocity, and entrance velocity along collector pipes having diameter ranging from 0.2m to 0.5m and lengths varying from 50 to 80m have been estimated using the following set of data.

$h_R - h_w = 10m$;   hydraulic   conductivity $k = 1m/day$;   density   of   water

$\rho = 998 kg/m^3$; viscosity of water $\mu = 10.1 \times 10^{-4} Ns/m^2$; radius of conceptual

cylindrical flow domain $R = 15m$.

The following procedure is adopted to obtain numerical result.

(1) A numerical value to length l_2 of the smooth turbulent flow zone is assigned.

(2) The turbulent flow zone is discretized into 20 equal size grids.

(3) The left end of smooth turbulent flow zone is assigned grid number 1. The right end grid of the turbulent flow zone is 21.

(4) An   initial   guess   of $H^*(i)$ is   made   using   a   relation

$H^*(i) = 0.9(h_r - h_w) + 0.9\, i/(i_{max}); i = 1,...20$

(5) The initial guess values are improved till $\Delta H(i) \rightarrow 0$. A sample result is presented in Table 3.1.

(6) For the assumed value of l_2, l_1 has been computed and corresponding L is found.

43

The variation of length of collector pipe, L $(=l_1+l_2)$ with the turbulent flow length, l_2, for different diameter of pipe is presented in Fig.(3.2). As seen from the figure for a collector of given diameter, the laminar flow zone varies very little with length of the collector. For example, for d=0.3m, l_2 = 20m, the length of laminar flow zone l_1 = 4.530m. For d= 0.3m, l_2 = 80m, the corresponding l_1 = 4.532m. The length of laminar flow zone varies with the diameter of the pipe. For example for d = 0.2m, l_2=80m, l_1=3.293m. For a given length of a collector pipe, as the diameter is increased, the laminar flow length is increased and turbulent flow length is decreased.

Variation of drawdown along the entire length of collector pipe for L=l_1+l_2=50m and diameter d=0.3m is presented in Fig.(3.3). The maximum head difference, i.e., difference of heads at x=0, and at x=50m, is 0.00085m only. For d=0.2m the corresponding head difference is 0.0050m. Thus the entire length of collector with diameter more than 0.2 m can be regarded as a constant head boundary.

Variation of flux per unit length along the length of the collector is presented in Fig.(3.4) for L=50 m and d=0.3 m. At x = 0, the flux per unit length is 13.643 $m^3/day/m$ and at x = 50m, the flux per unit length is 13.644 $m^3/day/m$. The difference in flux per unit length is 0.001 $m^3/day/m$. The corresponding values for d =0.2m are *12.533, 12.540,* and *0.007 $m^3/day/m$*. Thus for collector with diameter 0.2m and more both uniform head boundary condition or uniform flux per unit length is applicable.

Variation of axial flow, axial velocity, and Reynolds number along the collector pipe are presented in Fig.(3.5), Fig.(3.6), and Fig.(3.7) respectively for L = 50m and d = 0.3m. At the section where the flow changes from laminar to turbulent i.e. at x = l_1 = 4.53m, these graphs show kinks at the junction. This is due to

44

the fact that the graph of head with x is not differentiable at x=l_1. The kink is not visible in Fig.3.3 as the variation in head along the collector is insignificant. As seen in Fig3.7, at $x = l_1$, the Reynold Number=3000, which verifies that the boundary condition at $x = l_1$ been implemented.

The variation of maximum axial velocity, which occurs at $x = L$, i.e., near the caisson, with length of collector is presented in Fig (3.8) for different diameters of the collector. The maximum axial velocity increases with length of the collector and decreases with increase in diameter. Axial velocity increases more rapidly with decrease in diameter. The limiting maximum axial velocity is 0.9m/sec (Driscol, 1987). Thus with pipe diameter 0.2 and 0.3m and above, the axial velocity can be contained within permissible limit.

The entrance velocity has been computed assuming 20% perforation. The variation of maximum entrance velocity, which occurs at $x = L$, with diameter of the pipe is presented for various length of pipe in Fig.3.9. The limiting value of entrance velocity is 3cm/sec. Thus, with pipe diameter of 0.2 m and above, the entrance velocity can be contained within allowable limit for the normal length of collector pipe adopted in a collector well.

Variation of specific capacity of a collector well with diameter is presented in Fig. (3.10) for different lengths of pipe. Specific capacity increases with increase in length and diameter of collector pipe.
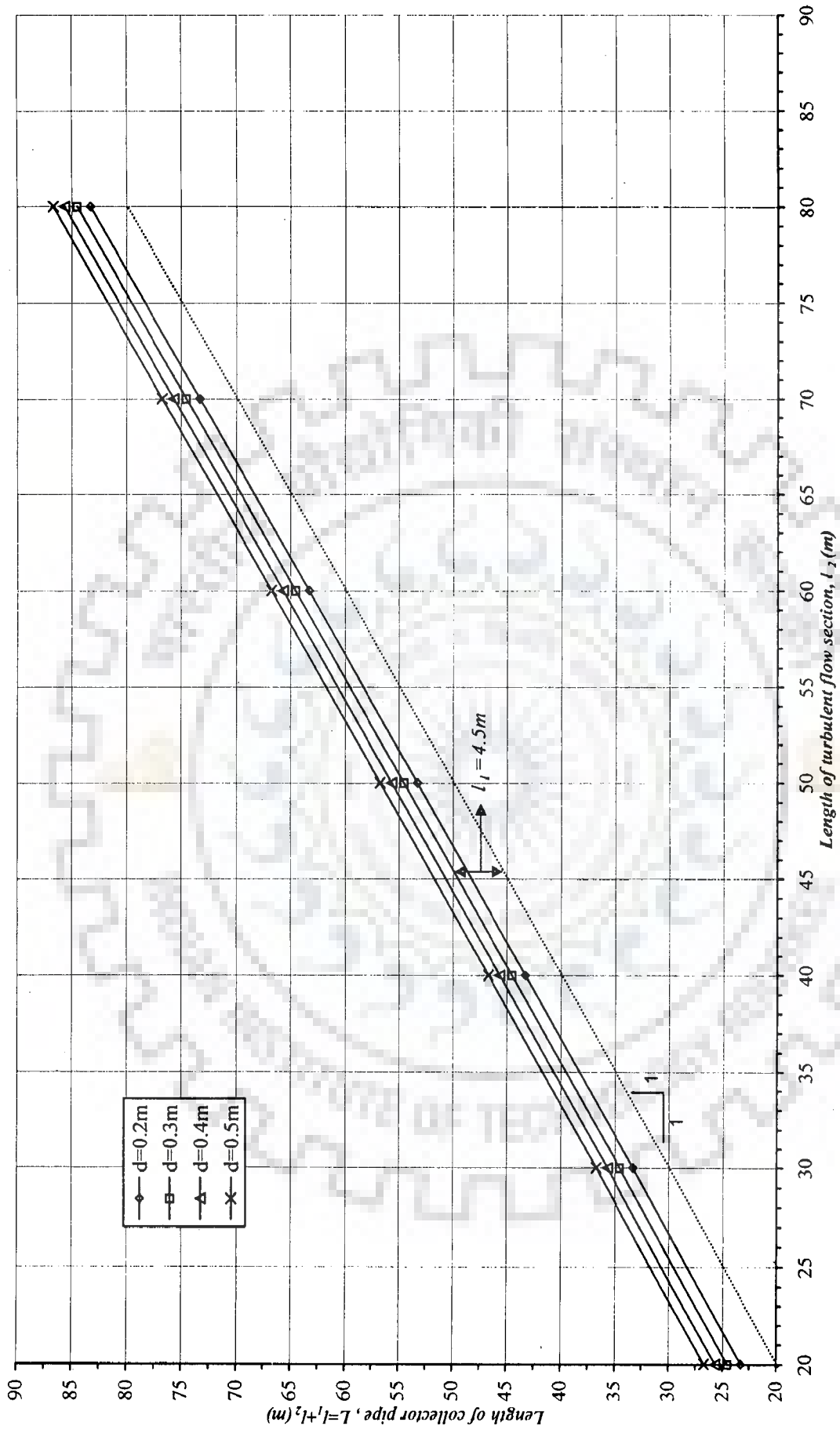
Fig.3.2 : Variation of total lateral length with turbulent flow length for different diameter of collector pipes

46
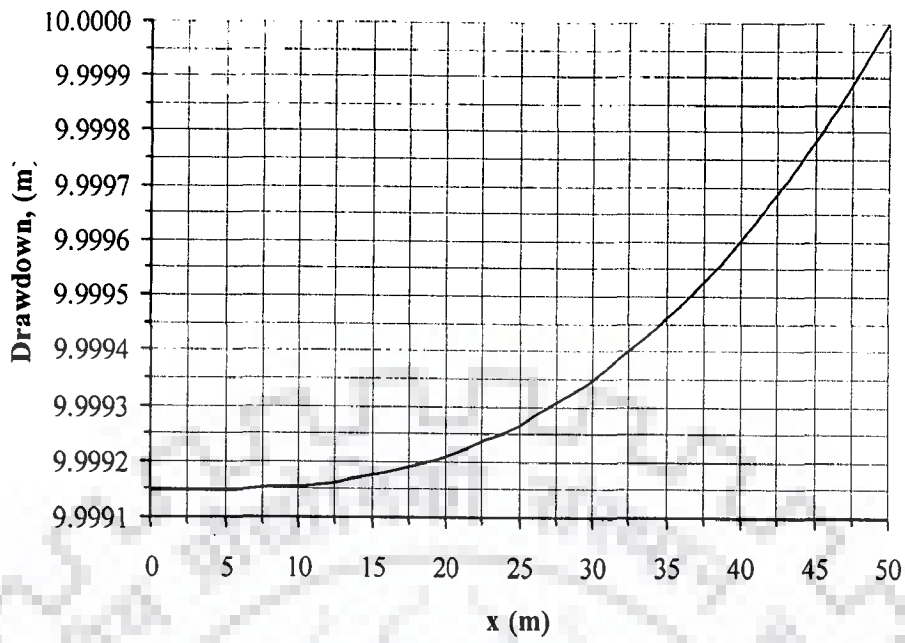
Fig.3.3: Variation of drawdown along a horizontal collector pipe of length *L=50m* and diameter *d=0.3m*
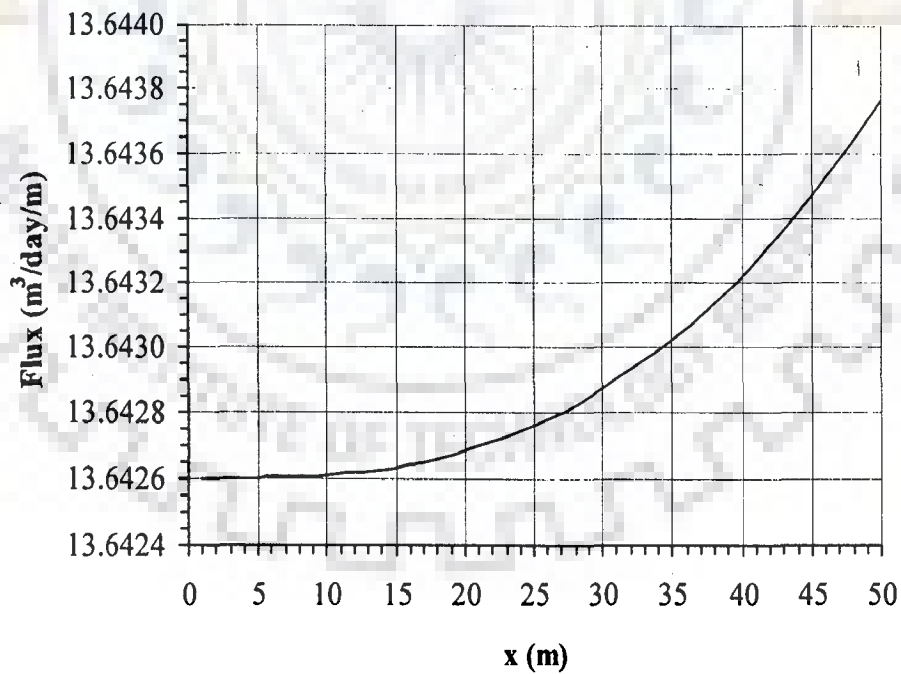
Fig.3.4: Variation of water flux per unit length along a horizontal collector pipe of length *L=50m* and diameter *d=0.3m*
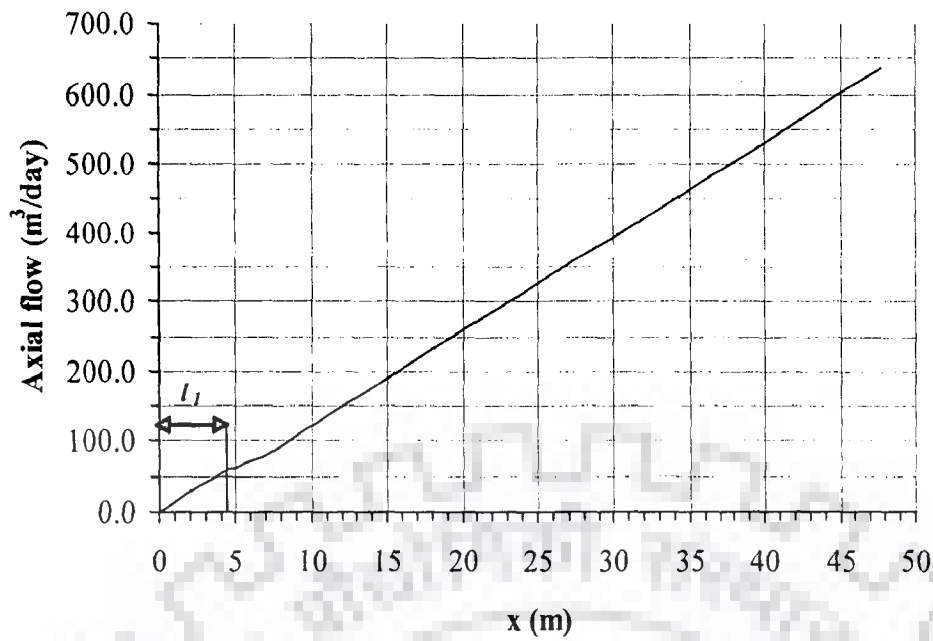
Fig.3.5: Variation of axial flow along a horizontal collector pipe of length *L=50m* and diameter *d=0.3m*
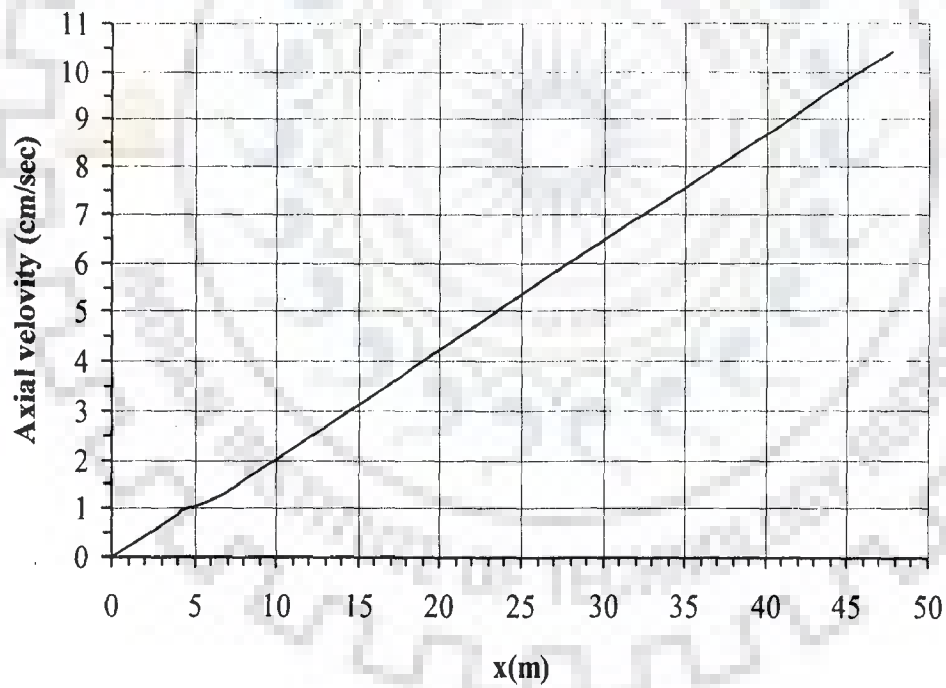
Fig.3.6: Variation of axial velocity along a horizontal collector pipe of length *L=50m* and diameter *d=0.3m*
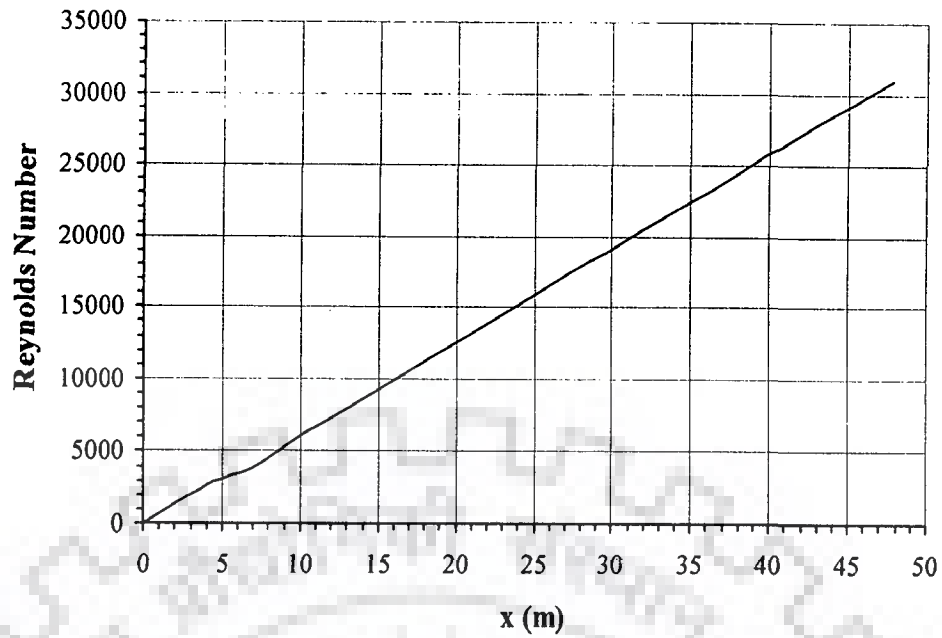
Fig.3.7: Variation of Reynolds number along a horizontal collector pipe of length
L=50m and diameter d=0.3m

(Turbulent flow section l_2=45.5m (corresponding laminar flow length x =4.5m), Reynold Number at transition section=3000)
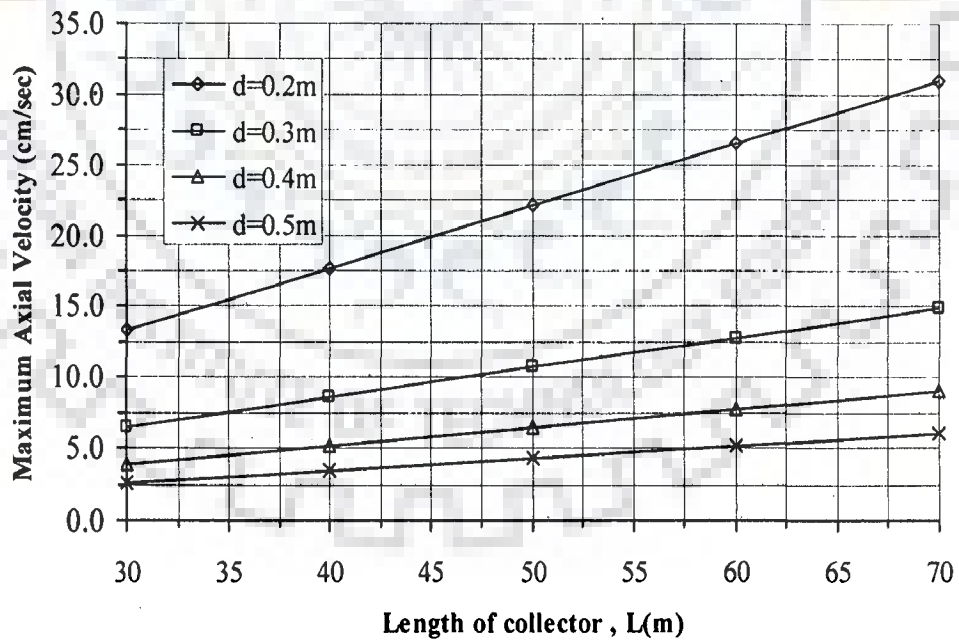
Fig.3.8: Variation of maximum axial velocity at the caisson with length of collector for different pipe diameter

49
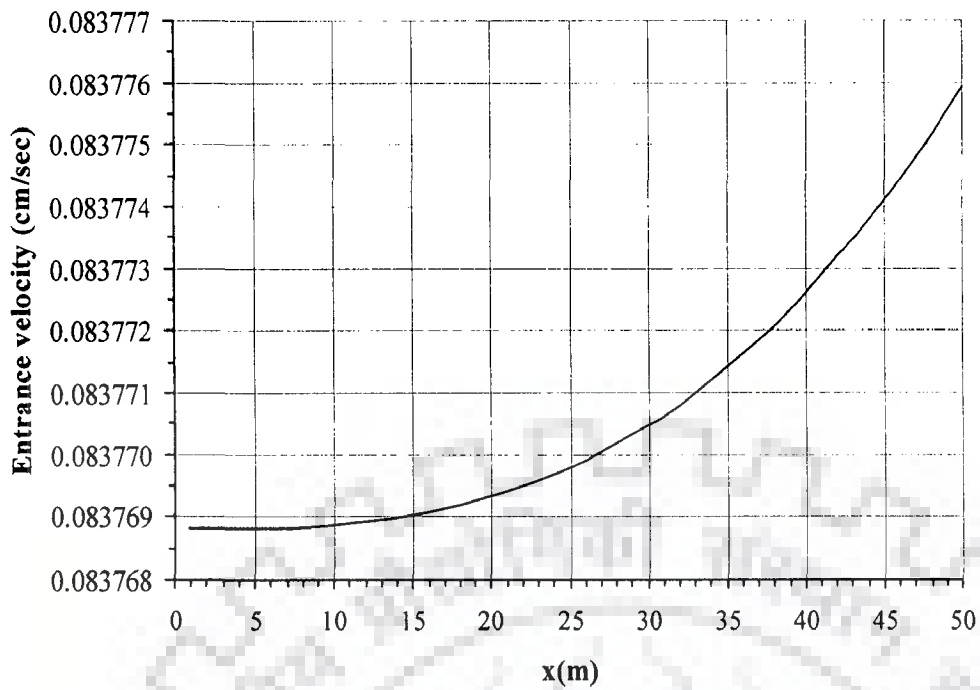
Fig.3.9: Variation of entrance velocity along a horizontal collector pipe of length *L=50m* and diameter *d=0.3m*
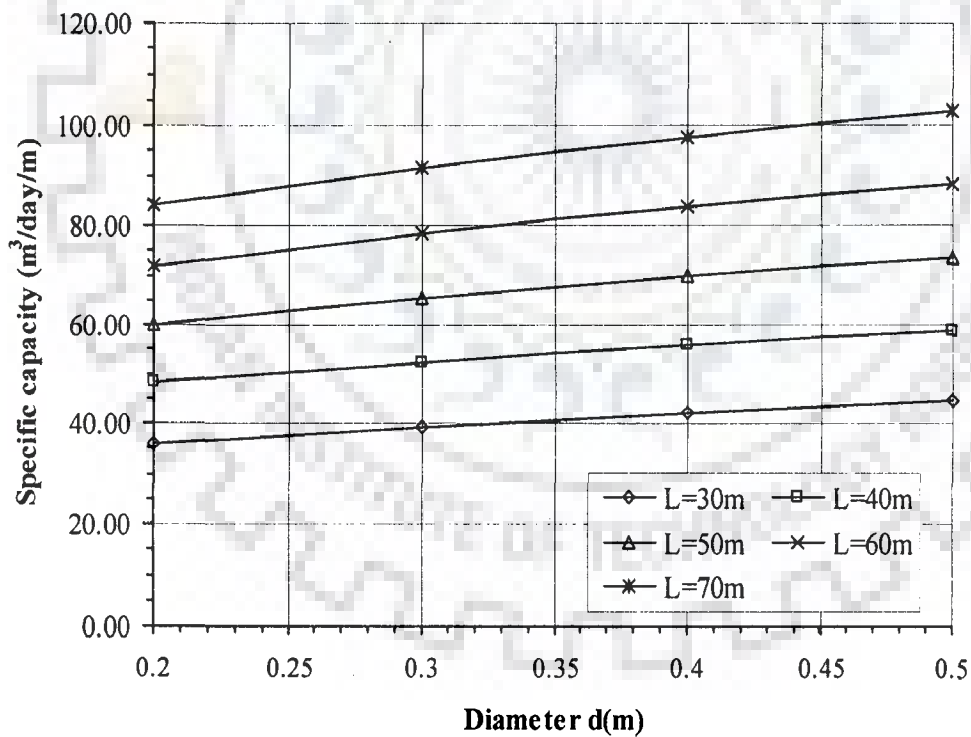
Fig.3.10: Variation of specific capacity of a horizontal collector pipe with diameter for different length of collector

50

Table3.1. Drawdown H*(i) in turbulent flow zone at different nodes, and corresponding function F(H*(i)) and ΔH(i) for d=0.3m, l_2=45.5m, and Δx=2.28m

Node (i)	x (m)	F(H$^\bullet$(i)	ΔH(i)	H*(i)
1	4.53	1.7600E-16	5.7300E-16	9.9991487
2	6.81	-3.9300E-11	7.4800E-16	9.9991504
3	9.08	5.4300E-11	-5.3200E-16	9.9991538
4	11.36	1.7900E-12	-1.1800E-16	9.9991596
5	13.63	-4.0600E-11	4.3500E-16	9.9991681
6	15.91	1.2500E-11	-3.6200E-16	9.9991798
7	18.18	4.0600E-11	-8.2100E-16	9.9991951
8	20.46	-9.2900E-12	7.6000E-17	9.9992145
9	22.73	-2.2100E-11	7.3700E-16	9.9992382
10	25.01	-1.0900E-11	6.9600E-16	9.9992668
11	27.28	1.0500E-13	2.8000E-16	9.9993006
12	29.56	7.6900E-12	-1.5900E-16	9.9993399
13	31.83	4.3200E-12	-3.6500E-16	9.9993851
14	34.11	3.2200E-11	-4.3600E-16	9.9994366
15	36.38	-3.9700E-11	5.7600E-16	9.9994946
16	38.66	-4.8900E-12	3.0200E-16	9.9995596
17	40.93	2.9300E-12	-1.4900E-16	9.9996319
18	43.21	4.0600E-11	-5.2000E-16	9.9997117
19	45.48	-6.1100E-11	4.5300E-16	9.9997995
20	47.76	4.9500E-11	-5.8200E-16	9.9998955

3.5 CONCLUSIONS

Barring for a small length near the tip of collector pipe (free end), the flow condition inside the pipe is turbulent. Collector pipe of diameter 0.3m-0.4 is generally adopted and for collector pipe with diameter 0.2m and above, the total head loss is very marginal. Therefore, for steady state flow condition, either Dirichlet boundary condition or uniform flux condition can be applied without introducing appreciable error. Dirichelt boundary condition is to be applied for solving Lalace equation for steady state flow condition. For unsteady state flow condition, the uniform flux boundary condition can be adopted conveniently.

For collector pipe with diameter ranging from 0.2 to 0.4m, the entrance velocity and axial velocity are contained within permissible limit for normal lengths of pipe laid in a radial collector well.

ANALYSIS OF FLOW TO
AN INFILTRATION GALLERY

4.1 INTRODUCTION

In some groundwater basins, the alluvial deposit in the vicinity of a river may contain boulders. Pushing horizontal radials into such deposits is very difficult. In such aquifers, infiltration galleries are laid at a shallow depth after making an open excavation. A gallery may be laid under the riverbed or in the vicinity of the riverbank. A significant quantity of water can be pumped from an infiltration gallery because the hydraulic conductivity of the natural material and the filter pack surrounding the screens is so high that recharge is sufficient to meet required pumping rate with permissible draw-down. A gallery laid under a riverbed is oriented perpendicular to the river flow direction whereas a gallery installed near the riverbank is placed parallel to the river i.e. perpendicular to the groundwater flow direction. The galleries located adjacent to a water body usually receive water that has lower turbidity and fewer bacteria than bed-mounted galleries, because the water gets filtered more extensively (Ray et. al, 2002). Moreover a gallery placed under a riverbed is to be safeguarded against scour problem.

In alluvial plain, rivers generally meander. In such situation, specific capacity of a well located near the concave side of the meandering reach will be more than that of the well located on the convex side. Conceptually, a well located in the concave side of a meandering river reach can be considered as a well at the center of an island.

An island provides a favorable setting for high groundwater yields as the well located in an island can potentially capture surface water from several directions.

In this chapter, the objective is to analyze flow to an infiltration gallery located (a) near a meandering river reach, and (b) near a straight river reach. For an infiltration gallery located near a straight river reach, three possible orientations of the gallery are considered. These are: (i) gallery perpendicular to and towards the river, (ii) gallery perpendicular to and towards landside, and (iii) gallery running parallel to the straight river reach. Further, it is desired to find the travel time of a tracer along the shortest ground water flow path from the surface water body to the infiltration galleries. The same has been found estimated for all the above mentioned orientation of the infiltration galleries.

4.2.   AN INFILTRATION GALLERY NEAR A MEANDERING RIVER

Statement of the Problem

An infiltration gallery of radius r_w and length $2l$ is located at a distance R from a meandering river reach or in the concave side (or located at the center of an island of radius R) in a thin aquifer of thickness T as shown in Fig.4.1(a). The caisson is located at the middle of the gallery to contain the axial velocity within the permissible limit. The water level in the river is at a height h_r measured from the middle of the thin aquifer which is assumed as the datum. The aquifer thickness being small, the flow is occurring in horizontal x-y plane. The collector well (caisson) is pumped at a constant rate Q. A steady state flow condition is attained. In the steady state condition, the water level in the caisson is at a height h_w above the datum. It is required to

quantify the specific capacity of the gallery and minimum travel time for river water

to reach the infiltration gallery for specified R, r_w, and l.

The following assumptions are made in the analysis:

(i) The aquifer is homogeneous and isotropic.

(ii) The aquifer thickness is small and the flow is taking place in a horizontal planes.

(iii) The flow is in steady state.

(iv) The gallery intercepts the entire thickness of the aquifer.

(v) The meandering river reach forms part of a circle.

(vi) Interference of the caisson on the flow characteristics is negligible.

Analytical Solution

An analytical solution is obtained by solving the Laplace equation using conformal

mapping technique. Under steady state flow condition, the governing equation for

two-dimensional flow is the Laplace equation which is written as

$$\frac{\partial^2 \phi}{\partial x^2} + \frac{\partial^2 \phi}{\partial y^2} = 0 \qquad (4.1)$$

where, $\phi =$ is a velocity potential function and is defined as for sheet flow (Hunt, 1983)

$$\phi = -kT(p/\gamma_w + Y) + C \qquad (4.2)$$

where, p=water pressure; γ_w =unit weight of water; Y=elevation head assumed as 0

for present case; C= a constant. ϕ = real part of the complex potential w which is

defined as $w = \phi + i\psi$, where, ψ is a stream function. The conceptualized flow

domain of the infiltration gallery is shown in Fig.4.1(b). The flow domain is

symmetrical about y-axis. Therefore, AB and DE are streamlines. Let $\psi = 0$ define

the streamline AB, and $\psi = +q$ define the streamline ED. q is the rate of flow entering

to the gallery from one side. Right half of the flow domain is considered to find the

solution to the Laplace equation. The component of velocity $\dfrac{\partial \phi}{\partial x}$ is in negative

Figure 4.1(a): An infiltration gallery near a meandering river

Figure 4.1(b): Flow Domain in z(=x+iy) plane (plan)

direction of x at $x = 0$ and $-l \le y \le l$. With the assumption of $\psi = +q$ along ED and

$\psi = 0$ along AB, $\dfrac{\partial \psi}{\partial y}$ is negative along the potential DB. The assumption is in

conformity with Cauchy- Reimann condition i.e. $\dfrac{\partial \phi}{\partial x} = \dfrac{\partial \psi}{\partial y}$. Assuming the constant

$C = -Tkh_w$ the complex potential plane for half of the flow domain is shown in Fig

4.2. For the present problem, the Laplace equation is to satisfy the following boundary

conditions:

$$\phi = -Tk(h_r - h_w) \text{ along } x^2 + y^2 = R^2 \tag{4.3}$$

and,

$$\phi = 0 \text{ along } (R - l) \le y \le (R + l), \text{ and } x = 0 \tag{4.4}$$

Inverse flow domain

The simple connected flow domain is comprised of a circular part EFA and a linear

part $ABCDE$ intersecting at points A and E. One of the points can be chosen as origin

to apply inverse mapping for converting the circular part and the straight line part

passing through origin into straight lines in inverse flow domain so that Schwarz-

Chirstoffel conformal mapping technique is applicable.

The inverse mapping is given by

$$\zeta = \xi + i\eta = \frac{1}{z} = \frac{1}{x + iy} = \frac{x - iy}{x^2 + y^2} = \frac{x}{x^2 + y^2} - i\frac{y}{x^2 + y^2} \tag{4.5}$$

Accordingly,the inverse flow domain is shown in Fig.4.3. As per equation (4.5) point

A ($z=i2R$) is mapped onto point $\zeta = \dfrac{-i}{2R}$; point B $(z = i(R + l))$ is mapped onto point

$\zeta = \dfrac{-i}{R + l}$; and point D $(z = i(R - l))$ is mapped onto $\zeta = \dfrac{-i}{R - l}$ .The inverse flow

domain has two vertices A and E, the latter one lying at infinity.

Mapping of ζ plane onto t plane

Conformal mapping of the inverse flow domain to the lower half an auxiliary $t(= r + is)$ plane (Fig.4.4) is given by

$$\frac{d\zeta}{dt} = \frac{M}{(0-t)^{1/2}} \tag{4.6}$$

The points E, D, B, A, F have been mapped onto $\pm\infty, -d, -1, 0, f$ respectively on real axis of $t(= r + is)$ plane. Integrating

$$\zeta = -2M(-t)^{1/2} + N \tag{4.7}$$

where M and N are complex constants. For vertex A, $t = 0$ and $\zeta = \dfrac{-i}{2R}$. Hence,

$$N = \frac{-i}{2R}.$$

For point B, $t = -1$, and $\zeta = \dfrac{-i}{R+l}$. Applying this condition in equation (4.5), and incorporating constant N, the constant M is found to be

$$M = i\frac{R-l}{4R(R+l)} \tag{4.8}$$

The mapping function reduces to

$$\zeta = i\frac{R-l}{2R(R+l)}(-t)^{1/2} - \frac{i}{2R} \tag{4.9}$$

Using equation (4.9), the parameter d and b are found to be

$$d = \left(\frac{R+l}{R-l}\right)^4 \tag{4.10}$$

$$b = 1 \tag{4.11}$$

Mapping of w Plane onto t Plane

The conformal mapping of the complex potential plane onto the 't' plane is given by:
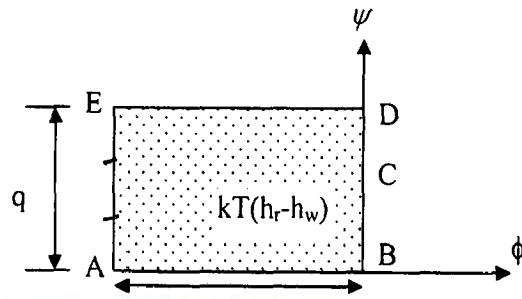
Figure 4.2: Complex potential w (=ϕ+iψ) plane
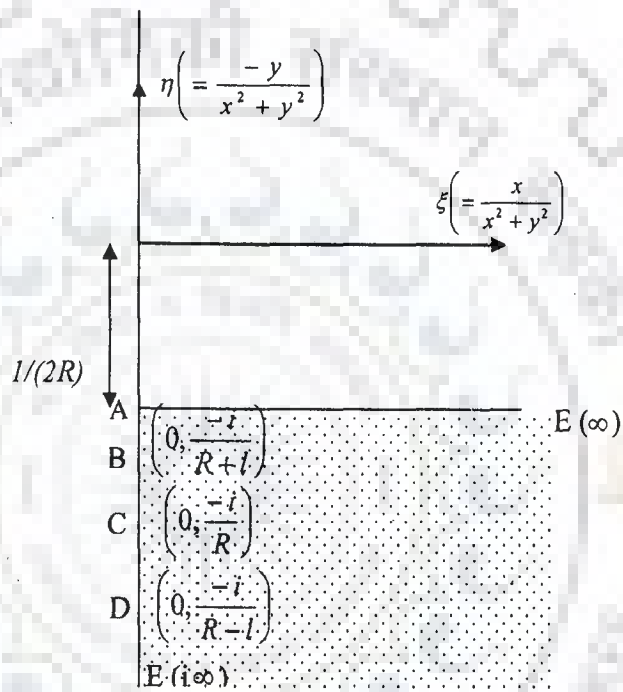
Fig. 4.3: Inverse flow domain in ξ (=ζ+i η) plane.
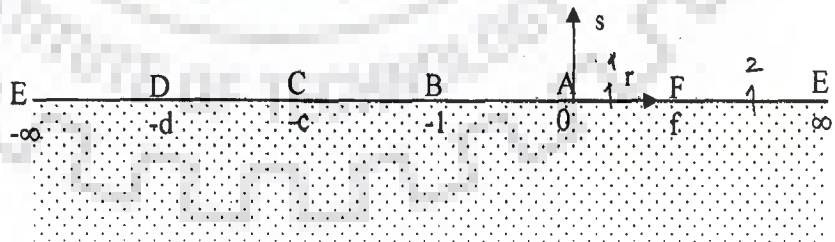
Figure 4.4: Auxiliary t (=r+is) plane

$$\frac{dw}{dt} = M_1 \frac{1}{(-d-t)^{1/2}(-1-t)^{1/2}(-t)^{1/2}}$$

(4.12a)

or

$$w = M_1 \int_{-\infty}^{\cdot} \frac{dt}{(-d-t)^{1/2}(-1-t)^{1/2}(-t)^{1/2}} - kT(h_r - h_w) + iq$$

(4.12b)

For point D, $t' = -d$ and $w = iq$. Hence,

$$iq = M_1 \int_{-\infty}^{-d} \frac{dt}{(-d-t)^{1/2}(-1-t)^{1/2}(-t)^{1/2}} - kT(h_r - h_w) + iq$$

(4.13)

Integrating (Byrd and Friedman, 1971) and simplifying, the constant M_1 is found to

be

$$M_1 = \frac{d^{1/2}kT(h_r - h_w)}{2F\left(\pi/2, 1/\sqrt{d}\right)}$$

(4.14)

where $F\left(\pi/2, 1/\sqrt{d}\right)$=Elliptical integral of the First kind with modulus $1/\sqrt{d}$. The

elliptical integral of the First kind with modulus k_1 is defined as

$$F\left(\pi/2, k_1\right) = \int_0^{\pi/2} \frac{d\theta}{\sqrt{1 - k_1^2 \sin^2 \theta}}.$$

For $-d \le t \le -1$, the relation between w and t plane is given by:

$$w = M_1 \int_{-d}^{t} \frac{dt}{(-d-t)^{1/2}(-1-t)^{1/2}(0-t)^{1/2}} + iq$$

(4.15)

For point B, $w=0$ and $t = -1$. Applying this condition in equation (4.15)

$$0 = M_1 \int_{-d}^{-1} \frac{dt}{(-1)^{1/2}(d+t)^{1/2}(-1-t)^{1/2}(0-t)^{1/2}} + iq$$

(4.16)

Integrating and simplifying

$$q = kT(h_r - h_w) \frac{F\left(\pi/2, \sqrt{(d-1)/d}\right)}{F\left(\pi/2, \sqrt{1/d}\right)}$$

(4.17)

The total flow to the gallery is given by:

$$Q = 2kT(h_r - h_w) \frac{F\left(\pi/2, \sqrt{(d-1)/d}\right)}{F\left(\pi/2, \sqrt{1/d}\right)} \qquad (4.18)$$

Substituting the value of parameter d, the relation between the dimensionless specific

capacity of drainage gallery and dimensionless length of gallery is found to be

$$\frac{Q}{kT(h_r - h_w)} = 2 \frac{F\left(\pi/2, \sqrt{1 - \left\{\frac{1-l/R}{1+l/R}\right\}^4}\right)}{F\left(\pi/2, \sqrt{\left\{\frac{1-l/R}{1+l/R}\right\}^4}\right)} \qquad (4.19)$$

Minimum Travel Time for a Tracer
The shortest distance between the river and the gallery is AB. Also, he velocity at

point B is infinite. Therefore, the travel time for path AB is derived as follows.

$$u - iv = \frac{1}{T}\frac{dw}{dz} = \frac{1}{T}\frac{dw}{dt}\frac{dt}{dz} \qquad (4.20)$$

From equation (4.5)

$$\frac{d\zeta}{dz} = -\frac{1}{z^2} \qquad (4.21)$$

Incorporating equations (4.12a), (4.6) and (4.21) in equation (4.20)

$$u - iv = \left\{ \frac{d^{1/2}k(h_r - h_w)}{2F\left(\pi/2, 1/\sqrt{d}\right)} \frac{1}{(-d-t)^{1/2}(-1-t)^{1/2}(-t)^{1/2}} \right\} \times$$
$$\left\{ \frac{4R(R+l)}{i(R-l)}(-t)^{1/2} \right\} \left\{ -\frac{1}{z^2} \right\} \qquad (4.22)$$

For $-1 \le t \le 0$, equating real parts and imaginary parts, the components of velocity

are found from equation (4.22) to be

$$u = 0 \qquad (4.23)$$

and

61

$$v = -\left\{\frac{d^{1/2}k(h_r - h_w)}{2F\left(\pi/2, 1/\sqrt{d}\right)} \frac{1}{(d+t)^{1/2}(1+t)^{1/2}}\right\}\left\{\frac{4R(R+l)}{(R-l)}\right\}\left\{\frac{1}{y^2}\right\} \tag{4.24}$$

The negative sign indicates that water is moving in the negative direction of y.

The total travel time τ is given by:

$$\tau = \int_{2R}^{R+l} \frac{dy}{v/S} = -S\int_{2R}^{R+l} \left\{\frac{2F\left(\pi/2, 1/\sqrt{d}\right)}{d^{1/2}k(h_r - h_w)}\right\}\left\{\frac{(R-l)}{4R(R+l)}\right\}(d+t)^{1/2}(1+t)^{1/2}y^2dy \tag{4.25}$$

where S = porosity of the aquifer medium.

Substituting $z = iy$ for flow path AB in equation (4.9)

$$\zeta = \frac{1}{z} = \frac{1}{iy} = i\frac{R-l}{2R(R+l)}(-t)^{1/2} - \frac{i}{2R} \tag{4.26}$$

Solving for t

$$t = -\left(1 - \frac{2R}{y}\right)^2\left(\frac{1+l/R}{1-l/R}\right)^2 \tag{4.27}$$

Incorporating the value of t from (4.27) in equation (4.25), and simplifying the equation, we get

$$\frac{k\tau(h_r - h_w)}{SR^2} = \int_{R+l}^{2R}\left\{\frac{2F\left(\pi/2, 1/\sqrt{d}\right)}{d^{1/2}}\right\}\left\{\frac{(1-l/R)}{4(1+l/R)}\right\}\left\{d - \left(1 - \frac{2R}{y}\right)^2\left(\frac{1+l/R}{1-l/R}\right)^2\right\}^{1/2} \times$$

$$\left\{1 - \left(1 - \frac{2R}{y}\right)^2\left(\frac{1+l/R}{1-l/R}\right)^2\right\}^{1/2}\left\{\frac{y}{R}\right\}^2\frac{dy}{R} \tag{4.28}$$

Let the variable y/R be replaced by another dummy variable χ and $\frac{dy}{R}$ by $d\chi$.

Incorporating these substitutions in Eq. (4.28) the dimensionless minimum time factor is found to be

$$\frac{k\tau(h_r - h_w)}{SR^2}$$

$$= \int_{1+l/R+\varepsilon}^{2} \left\{ \frac{2F\left(\pi/2, 1/\sqrt{d}\right)}{d^{1/2}} \right\} \left\{ \frac{(1-l/R)}{4(1+l/R)} \right\} \left\{ d - (1-2/\chi)^2 \left(\frac{1+l/R}{1-l/R}\right)^2 \right\}^{1/2} \times \quad (4.29)$$

$$\left\{ 1 - (1-2/\chi)^2 \left(\frac{1+l/R}{1-l/R}\right)^2 \right\}^{1/2} \chi^2 d\chi$$

$$\varepsilon \to 0$$

Results and Discussions

The variation of specific capacity with l/R is presented in Fig. 4.5. Specific capacity increases rapidly with the increase in the length of collector pipe. But for l/R ranging from 0.2 to 0.5, the specific capacity is linearly proportional to the length of collector pipe. Beyond $l/R=0.5$, the increase in yield is primarily due to closer proximity of the collector pipe to the river. However, the collector pipe is to be laid at a safe distance from the river. The safe distance is to be ascertained on the basis of the minimum time a tracer (a micro organism) would take to travel from water body to the collector pipe using Eq. (4.29). The minimum dimensionless travel time factor has been presented in Fig. 4.6. Travel time is inversely proportional to drawdown, hydraulic conductivity and directly proportional to porosity of the aquifer medium and square of the distance of the river from the caisson. Smaller the drawdown and conductivity longer the travel time and more the opportunity time for filtration. The travel time should be greater than the survival time of pathogenic bacteria in concern. A sample result is presented as below:

Illustrative Example:

Length of infiltration gallery, $l = 50$m;

Total length of infiltration gallery, $2l = 100$m;

Radius of island, R = 150m; $l/R=0.33$;

Aquifer thickness, T =7.5 m;

Diameter of gallery=0.32m; Drawdown, h_r-h_w= 6m;

Hydraulic conductivity, k= 10m/day; ⁻⁻ ⁻ ⁻⁻⁻ ⁻ S=0.2

For l/R=0.333, the non dimensional flow (Fig.4.5), $\dfrac{Q}{kT(h_r - h_w)} = 3.5$

or

$Q=3.5 \times kT(h_r - h_w)$ =1574m³/day. A correction factor needs to be applied to Q as the infiltration gallery (collector pipe) system partly intercepts the thickness of the aquifer. The correction factor, C1, has been derived (given in appendix D) for the case where the infiltration gallery is running parallel to the river. The same correction factor has been applied here. Hence , the modified flow is

$Q = C_1 \times 1574 = 1023m^3 / day$, where C_1=0.65

The corresponding non dimensional time factor from Fig.(4.6) is $\dfrac{k\tau(h_r - h_w)}{SR^2} = 0.66$.

For the above set of data, the minimum travel time, τ is 49.5 days. Thus, Bacteria will take 49.5 days to reach from point A to point B, i.e., 100m. The average travel time of pathogenic bacteria is 30-40 days. Hence, the infiltration gallery is located at a safe distance from the river.
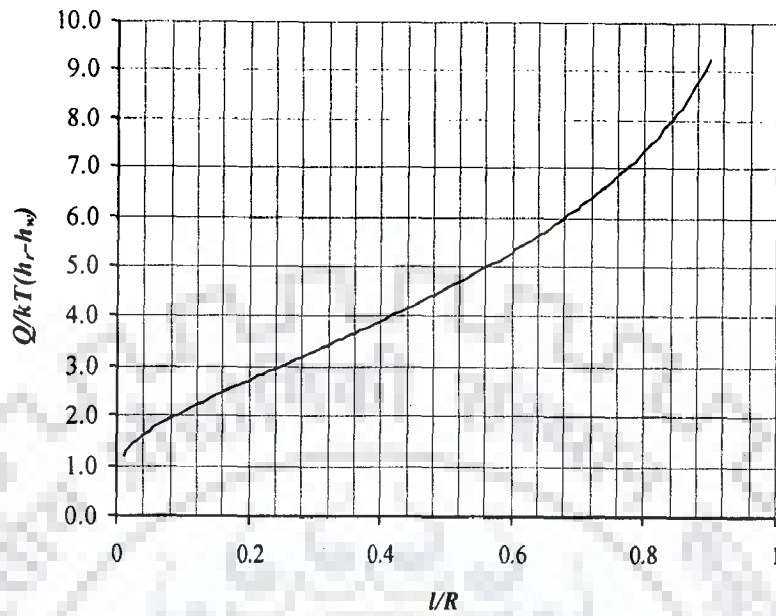
Fig. 4.5: Variation of non dimensional flow, $\dfrac{Q}{kT(h_r - h_w)}$ vs l/R for an infiltration gallery near meandering river
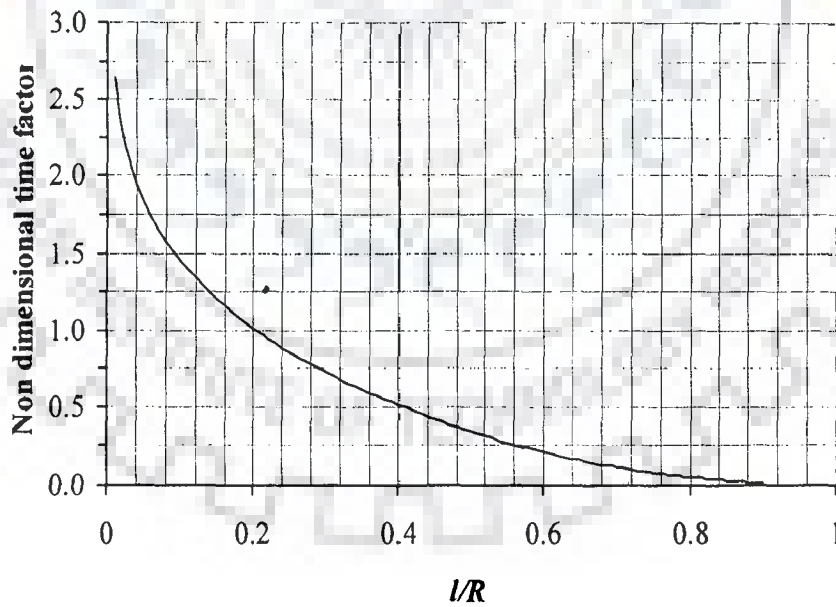
Fig. 4.6: Variation of non dimensional time factor, $k\tau \dfrac{(h_r - h_w)}{SR^2}$ vs l/R an infiltration gallery near meandering river

65

4.3 AN INFILTRATION GALLERY NEAR STRAIGHT REACH OF A RIVER

Flow to infiltration gallery has been analyzed for different orientation with respect to a straight reach of a river, such as, (i) a gallery perpendicular to and aligned towards the river, (ii) a gallery perpendicular to and aligned towards landside, and (iii) parallel to the river.

4.3.1 Flow to an Infiltration Gallery Aligned Perpendicular to and Towards the River

Using conformal mapping technique, Hunt (1983) has derived analytical solution to compute yield of a single collector well. The minimum travel time of a tracer from a straight river reach to the caisson could be derived making use of Hunt's derivation. In this chapter the solution has been rederived and the travel time has been found. Solution to Laplace equation pertaining to flow to a single collector is derived assuming sheet flow domain and using conformal mapping. Schwarz Christoffel mapping the steps of mapping are shown in Fig.4.7. Vertex D in z plane (Fig.4.7 (a)) only takes part in mapping of z plane onto t plane. Points A, B, C, D, A have been mapped onto $-\infty$, 0, c, 1, ∞ respectively on real axis of an auxiliary t plane.

Mapping of z (=x+iy) plane onto t(=r+is) plane

The relation between z plane to t plane is (Fig.4.7(b))

$$\frac{dz}{dt} = \frac{M}{(1-t)^{1/2}} \qquad (4.30a)$$

and

$$z = -2M(1-t)^{1/2} + N \qquad (4.30b)$$

66

Applying the condition at point B for which $t=0$, and $z=0$, $N=2M$. For point D, $t=1$ and $z=R$, hence, $M=R/2$, and

$$z = R\left\{1 - (1-t)^{1/2}\right\}$$

(4.31a)

and

$$\frac{dz}{dt} = \frac{R}{2(1-t)^{1/2}}$$

(4.31b)

For point C, $z=l$, and $t=c$. Applying this condition in (4.31a)

$$c = 1 - \left(1 - \frac{l}{R}\right)^2$$

(4.32)

Mapping of $w(=\phi + i\psi)$ onto t=(r+ is)

The complex potential $w(=\phi + i\psi)$ for half of the flow domain is shown in Fig.4.7 (c). The velocity potential ϕ is defined as (Hunt, 1983)

$$\phi = -kT\left(\frac{p}{r_w} + Y\right) + C$$

(4.33)

Assuming $C = -kTh_w$, the potential along the river is $-kT(h_r - h_w)$. The mapping of the w plane onto upper half of the t plane is given by

$$\frac{dw}{dt} = \frac{M_1}{(1-t)^{1/2}(c-t)^{1/2}(0-t)^{1/2}}$$

(4.34)

$$w = M_1 \int_{-\infty}^{t} \frac{dt}{(1-t)^{1/2}(c-t)^{1/2}(0-t)^{1/2}} - kT(h_r - h_w)$$

(4.35)

For point B, $t' = 0$ and $w=0$. Performing the integration (Byrd and Friedman, 1971), and solving for M_1

$$M_1 = \frac{kT(h_r - h_w)}{2F\left(\frac{\pi}{2}, 1 - \frac{l}{R}\right)}$$

(4.36)
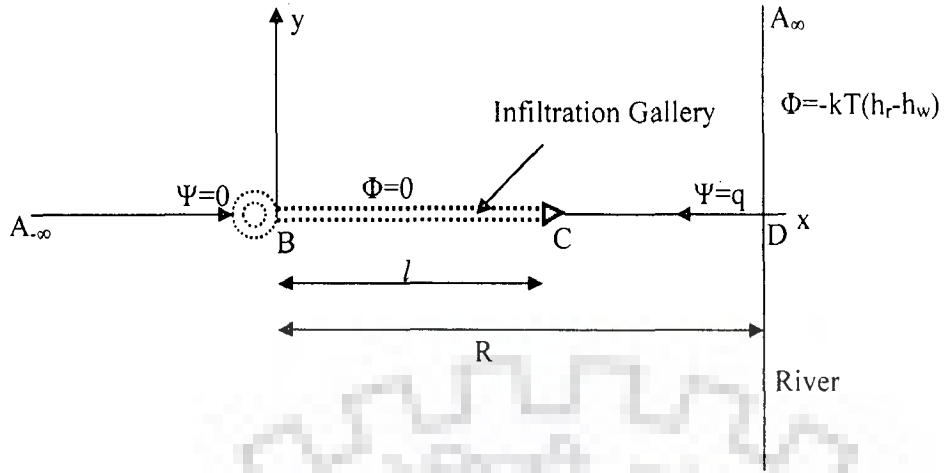
67

(a) Physical flow domain in z(=x+iy) plane
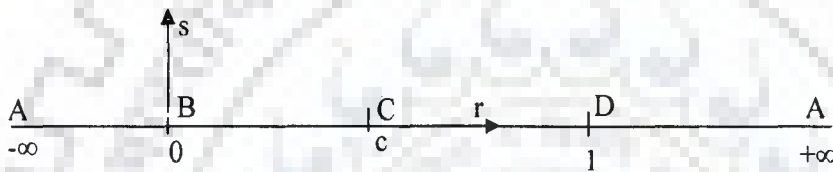
(b) Auxiliary upper half t(=r+is) plane
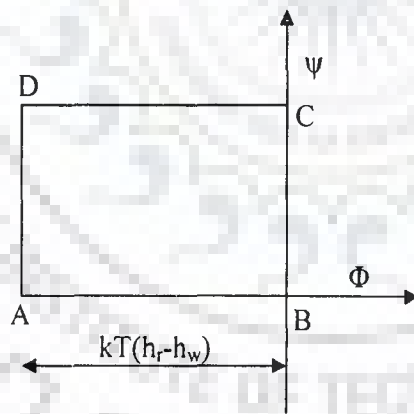
(c) Complex potential plane w=(Φ+iψ) plane

Fig. 4.7: Steps of conformal mapping for an infiltration gallery aligned perpendicular to and towards a river

68

For $0 \leq t' \leq c$

$$w = M_1 \int_0^{t'} \frac{dt}{(1-t)^{1/2}(c-t)^{1/2}(0-t)^{1/2}} = \frac{M_1}{(\pm)i} \int_0^{t'} \frac{dt}{(1-t)^{1/2}(c-t)^{1/2}t^{1/2}} \quad (4.37)$$

For point C, $t' = c$ and $w = iq$. Performing the integration, and applying the condition at point C, q is found to be

$$q = \frac{kT(h_r - h_w) \ F\left(\frac{\pi}{2}, \sqrt{1-\left(1-\frac{l}{R}\right)^2}\right)}{F\left(\frac{\pi}{2}, 1-\frac{l}{R}\right)} \quad (4.38)$$

Total flow to the infiltration gallery, $Q = 2q$.

Minimum travel time

The minimum travel time for stream water to reach the infiltration gallery would occur along the path CD. The Darcy velocity is given by

$$u - iv = \frac{1}{T}\frac{dw}{dz} = \frac{1}{T}\frac{dw}{dt}\cdot\frac{dt}{dz} \quad (4.39)$$

Incorporating $\frac{dw}{dt}$ and $\frac{dt}{dz}$ in Eq (4.39), and simplifying

$$u - iv = \frac{k(h_r - h_w)}{R \ F\left(\frac{\pi}{2}, 1-\frac{l}{R}\right)} \frac{1}{(c-t)^{1/2}(0-t)^{1/2}} \quad (4.40)$$

Along the stream line CD, the component of velocity in y direction, $v = 0$. Hence,

$$u = \frac{-k(h_r - h_w)}{R \ F\left(\frac{\pi}{2}, 1-\frac{l}{R}\right)} \frac{1}{(t-c)^{1/2}t^{1/2}} \quad (4.41)$$

Replacing t by $1-\left(1-\frac{z}{R}\right)^2 = 1-\left(1-\frac{x}{R}\right)^2$ in Eq (4.41)

$$u = \frac{-k(h_r - h_w)}{R\, F\left(\frac{\pi}{2}, 1 - \frac{l}{R}\right)} \frac{1}{\sqrt{1 - \left(1 - \frac{x}{R}\right)^2}} \frac{1}{\sqrt{1 - c - \left(1 - \frac{x}{R}\right)^2}} \qquad (4.42)$$

The negative sign indicates that the flow is in negative direction of x. The minimum

travel time τ by a conservative pollutant to travel from $x = R$ to $X = l$ is given by

$$\tau = \int_R^l \frac{dx}{(u/S)} = \int_R^l -SR\, \frac{F\left(\frac{\pi}{2}, 1 - \frac{l}{R}\right)}{k(h_r - h_w)} \sqrt{\left[1 - \left(1 - \frac{x}{R}\right)^2 \left\{1 - c - \left(1 - \frac{x}{R}\right)^2\right\}\right]}\, dx \quad (4.43)$$

Replacing $1 - c = \left(1 - \frac{l}{R}\right)^2$, $\left(1 - \frac{x}{R}\right) = X, dx = -RdX$, equation (4.43) reduces to

$$\tau = SR^2 \frac{F\left(\frac{\pi}{2}, 1 - \frac{l}{R}\right)}{k(h_r - h_w)} \int_0^{\left(1 - \frac{l}{R}\right)} \sqrt{\left(1 - X^2\right)\left(\left(1 - \frac{l}{R}\right)^2 - X^2\right)}\, dX \qquad (4.44)$$

The elliptic integral appearing in Eq.(4.44) has been tabulated by Byrd and Friedman

(1971, p60, no. 220.05; p213, no. 361.19). The elliptic integral is evaluated applying

a substitution $sn^2 v = \frac{(1 - l/R)^2 - X^2}{(1 - l/R)^2 (1 - X^2)}$. Incorporating the integral, Eq.(4.44)

reduces to

$$\tau = SR^2 \frac{F\left(\frac{\pi}{2}, 1 - \frac{l}{R}\right)}{k(h_r - h_w)} \frac{1}{3} \left[\left\{1 + \left(1 - \frac{l}{R}\right)^2\right\} E\left\{\varphi, \left(1 - \frac{l}{R}\right)\right\} - \left\{1 - \left(1 - \frac{l}{R}\right)^2\right\} F\left\{\varphi, \left(1 - \frac{l}{R}\right)\right\}\right.$$

$$\left. + \left(1 - \frac{l}{R}\right)^2 \sin\varphi \frac{\cos\varphi}{\sqrt{1 - \left(1 - \frac{l}{R}\right)^2 \sin^2\varphi}} \left\{\left(1 - \left(1 - \frac{l}{R}\right)^2\right)\left(1 - \frac{1}{1 - \left(1 - \frac{l}{R}\right)^2 \sin^2\varphi}\right) - 2\right\}\right]_{\varphi=0}^{\varphi=\pi/2}$$

70

After implementing the limits of integration

$$\tau = SR^2 \frac{F\left(\frac{\pi}{2}, 1-\frac{l}{R}\right)}{k\left(h_r - h_w\right)} \frac{1}{3} \left[\left\{1+\left(1-\frac{l}{R}\right)^2\right\} E\left\{\frac{\pi}{2},\left(1-\frac{l}{R}\right)\right\} - \left\{1-\left(1-\frac{l}{R}\right)^2\right\} F\left\{\frac{\pi}{2},\left(1-\frac{l}{R}\right)\right\}\right]$$

(4.46)

Thus, non-dimensional time factor, ς, is given by

$$\varsigma = \frac{\tau k\left(h_r - h_w\right)}{SR^2}$$

$$= \frac{1}{3} F\left(\frac{\pi}{2}, 1-\frac{l}{R}\right)\left[\left\{1+\left(1-\frac{l}{R}\right)^2\right\} E\left\{\varphi,\left(1-\frac{l}{R}\right)\right\} - \left\{1-\left(1-\frac{l}{R}\right)^2\right\} F\left\{\varphi,\left(1-\frac{l}{R}\right)\right\}\right]$$

(4.47)

Results and Discussions

Variation of dimensionless yield with l/R is presented in Fig.4.8 for an infiltration gallery near straight reach of a river and aligned perpendicularly towards the river. As seen from the figure, the yield of the collector pipe increases linearly with length of the pipe for $0.2 \le l/R \le 0.5$. For $0 \le l/R \le 0.2$, and $0.5 \le l/R \le 1$ the yield increases nonlinearly with length of pipe. Beyond $l/R \ge 0.5$, the rapid increase in yield is due to close proximity of the water body.

As noticed from Eq. (4.46), the minimum travel time is directly proportional to square of the distance of the tip of the gallery from the river, and porosity of the aquifer material. Travel time increases with increase in distance of the caisson from the river and decreases with increase in length of the gallery. The minimum travel

71

time is inversely proportional to drawdown in the caisson and hydraulic conductivity of the porous medium.
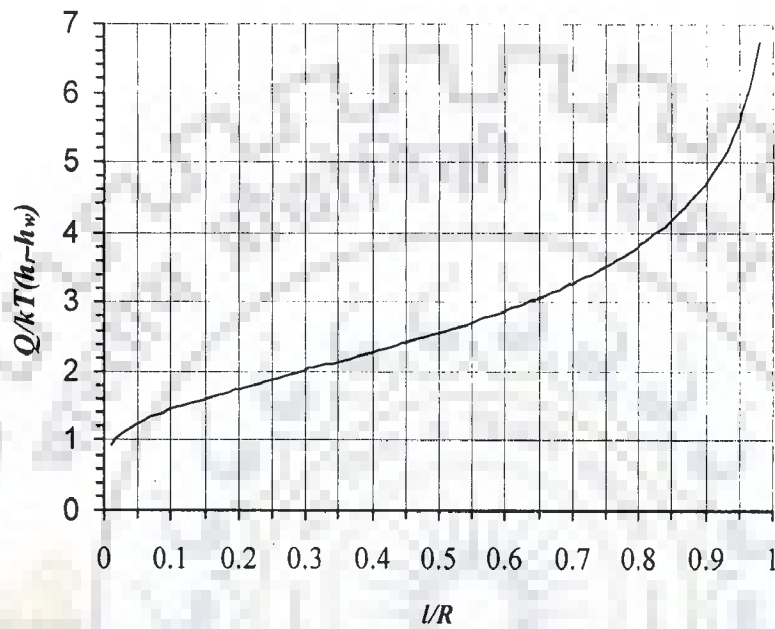
Fig.4.8: Variation of non-dimensional flow, $\dfrac{Q}{kT(h_r - h_w)}$ with l/R for an infiltration gallery aligned perpendicular to and towards a river

Fig.4.9: Variation of non-dimensional time factor, $\varsigma\left[=\dfrac{\tau\,k(h_r-h_w)}{S(R-l)^2}\right]$ with l/R

for an infiltration gallery aligned perpendicular to and towards a river

4.3.2 Flow to an Infiltration Gallery Aligned Perpendicular to the Direction of River Flow and Towards Landside

In order to provide appropriate filtration opportunity, an infiltration gallery may be laid towards the landside from the caisson. For such case, the Schwarz Christoffel mapping is similar to that where the gallery is oriented towards the stream from the caisson. The step of mapping is shown in Fig. 4.10. The physical flow domain (z=x+iy) is shown in Fig.4.10 (a).

Mapping of z plane onto t plane

The mapping function between z and t plane(Fig.4.10(b)) is

$$\frac{dz}{dt} = M\,\frac{1}{\sqrt{(1-t)}} \qquad\qquad (4.48)$$

73

$$z = -2M\sqrt{1-t} + N \qquad (4.49)$$

Applying the correspondences between t and z planes at points D, C, B, constants M, N, and parameter c are found and the following mapping functions are obtained:

$$\frac{dz}{dt} = \left(\frac{R+l}{2}\right)\frac{1}{(1-t)^{1/2}} \qquad (4.50)$$

$$z = R - \left(R+l\right)\sqrt{1-t} \qquad (4.51)$$

$$t = 1 - \left(\frac{R-z}{R+l}\right)^2 \qquad (4.52)$$

$$c = 1 - \frac{1}{(1+l/R)^2} \qquad (4.53)$$

Mapping of w plane onto t plane

The relation between $w(= \phi + i\psi)$ and t plane(Fig.4.10(c)) is

$$\frac{dw}{dt} = \frac{M_1}{(0-t)^{1/2}(c-t)^{1/2}(1-t)^{1/2}} \qquad (4.54)$$

and

$$w = M_1 \int_{-\infty}^{t} \frac{dt}{(0-t)^{1/2}(c-t)^{1/2}(1-t)^{1/2}} - kT(h_r - h_w) \qquad (4.55)$$

For point B, $t'=0$ and w=0. Applying this condition

$$M_1 = \frac{kT(h_r - h_w)}{2F\left(\dfrac{\pi}{2}, \sqrt{1-c}\right)} \qquad (4.56)$$

For $0 \leq t' \leq c$

$$w = M_1 \int_{0}^{t} \frac{dt}{(-1)^{1/2}\, t^{1/2}\, (c-t)^{1/2}\, (1-t)^{1/2}} \qquad (4.59)$$

For point c, $w=iq$. Taking $(-1)^{1/2} = -i$
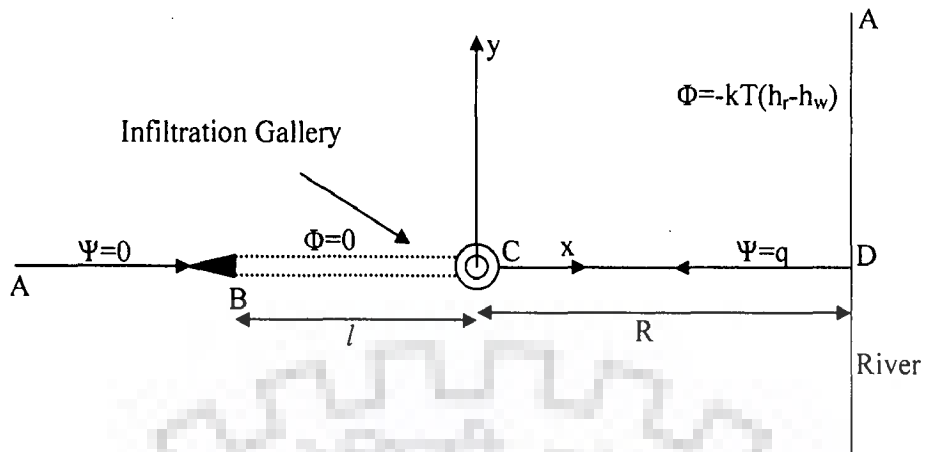
74

(a) Physical flow domain in z=x+iy plane
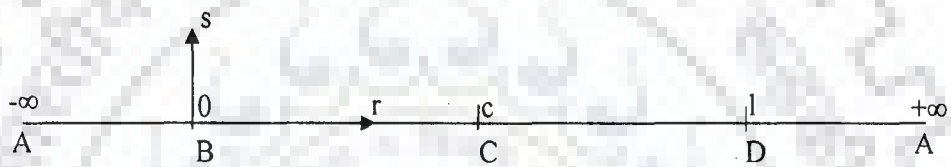
(b) Auxiliary upper half t(=r+is) plane
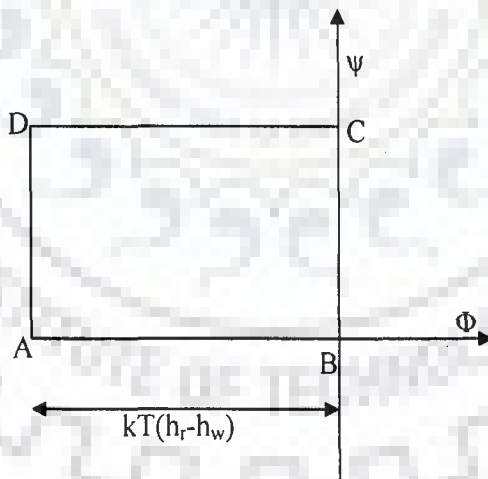
(c) Complex potential w = $(\phi + i\psi)$ plane

Fig.4.10: Steps of conformal mapping for an Infiltration Gallery Aligned Perpendicular to the Direction of River Flow and Towards Landside

75

$$q = kT(h_r - h_w) \dfrac{F\left(\dfrac{\pi}{2}, \sqrt{1 - \dfrac{1}{(1 + l/R)^2}}\right)}{F\left(\dfrac{\pi}{2}, \dfrac{1}{1 + l/R}\right)} \qquad (4.60)$$

Total flow to the infiltration gallery, Q=2q.

Minimum travel time

The travel time for river water to reach the gallery is minimum for the pathline CD.

For computation of minimum time, dimension of the caisson is neglected.

$$u - iv = \frac{1}{T}\frac{dw}{dz} = \frac{1}{T}\frac{dw}{dt} \cdot \frac{dt}{dz}$$

$$= \frac{1}{T}\frac{kT(h_r - h_w)}{2F(\pi/2, \sqrt{1-c})}\frac{1}{(0-t)^{1/2}(c-t)^{1/2}(1-t)^{1/2}}\frac{2}{R+l}(1-t)^{1/2} \qquad (4.61)$$

Along path CD, $z=x$, and $v=0$

Substituting t from Eq (4.52) in Eq(4.61) one gets

$$u = -\frac{k(h_r - h_w)}{(R+l)\,F\left(\pi/2, \dfrac{1}{1+l/R}\right)\left\{1 - \left(\dfrac{R-x}{R+l}\right)^2\right\}^{1/2}\left\{1 - \left(\dfrac{R-x}{R+l}\right)^2 - c\right\}^{1/2}} \qquad (4.62)$$

The travel time to cover distance CD is found to be

$$\tau = \int_R^0 \frac{dx}{(u/S)} = -\int \frac{S(R+l)F\left(\dfrac{\pi}{2}, \dfrac{1}{1+l/R}\right)\left\{1 - \left(\dfrac{R-x}{R+l}\right)^2\right\}^{1/2}\left\{1 - c - \left(\dfrac{R-x}{R+l}\right)^2\right\}^{1/2}}{k(h_r - h_w)}dx$$

$$\qquad (4.63)$$

let $\dfrac{R-x}{R+l} = X$

$-dx = (R+l)dX$

76

With these substitutions in equation (4.63), the travel time is found to be

$$\tau = \frac{S(R+l)^2 \, F\left(\pi/2, \frac{1}{1+l/R}\right)\frac{1}{1+l/R}}{k(h_r - h_w)} \int_0^{} \left\{(1-X^2)^{1/2}\left\{\frac{1}{(1+l/R)^2} - X^2\right\}\right\}^{1/2} dX \quad (4.64)$$

Following Byrd and Friedman (1971, p 60, 220.05) the above integral is derived. The minimum travel time is found to be

$$\tau = \frac{S(R+l)^2 \, F\left(\frac{\pi}{2}, \frac{1}{1+l/R}\right)}{3k(h_r - h_w)} \times$$

$$\left[\left\{1 + \frac{1}{(1+l/R)^2}\right\}E\left\{\frac{\pi}{2}, \frac{1}{(1+l/R)}\right\} - \left\{1 - \frac{1}{(1+l/R)^2}\right\}F\left\{\frac{\pi}{2}, \frac{1}{1+l/R}\right\}\right] \quad (4.65)$$

The dimensionless time factor is

$$\varsigma = \frac{\tau \, k(h_r - h_w)}{S(R+l)^2}$$

$$= F\left(\frac{\pi}{2}, \frac{1}{1+l/R}\right)\frac{1}{3}\left[\left(1 + \frac{1}{(1+l/R)^2}\right)E\left(\frac{\pi}{2}, \frac{1}{(1+l/R)}\right) - \left(1 - \frac{1}{(1+l/R)^2}\right)F\left(\frac{\pi}{2}, \frac{1}{1+l/R}\right)\right]$$

$$(4.66)$$

Results and Discussions

Variation of dimensionless yield of the infiltration gallery, $\dfrac{Q}{kT(h_r - h_w)}$ with

dimensionless length l/R is presented in Fig.4.11. Beyond $l/R > 0.5$ the variation of

yield with l/R is very nearly linear. The increase in flow is due to mainly increase in

flow area. The variation of dimensionless minimum travel time with l/R is presented

77

in Fig. 4.12. Though the minimum path remains same irrespective of the increase in gallery length, the minimum travel time reduces as flow from the river is increased resulting in an increase in flow velocity. The minimum travel time reduces with increase in gallery length rather sluggishly where as the travel time reduces sharply when the length of infiltration gallery is increased towards river side.
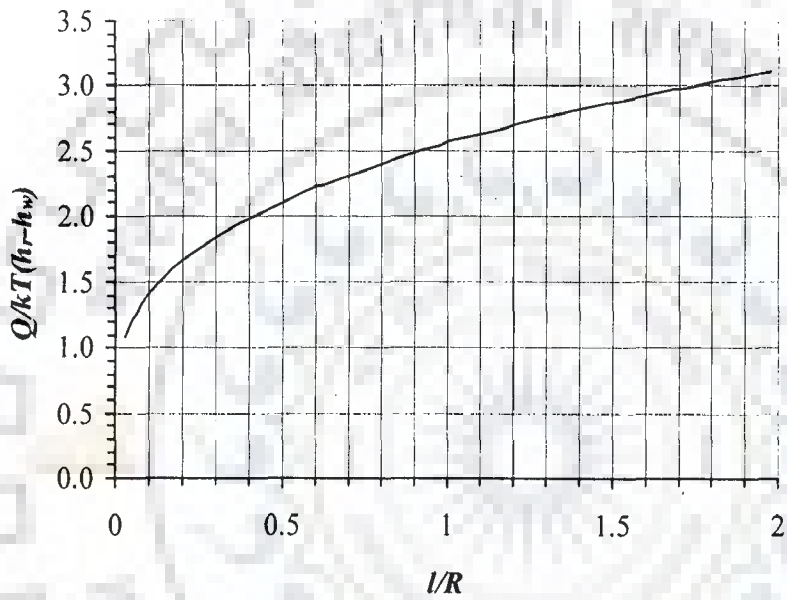
Fig.4.11: Variation of non dimensional flow, $\dfrac{Q}{kT(h_r - h_w)}$ with l/R an infiltration gallery aligned perpendicular to the direction of river flow and towards landside

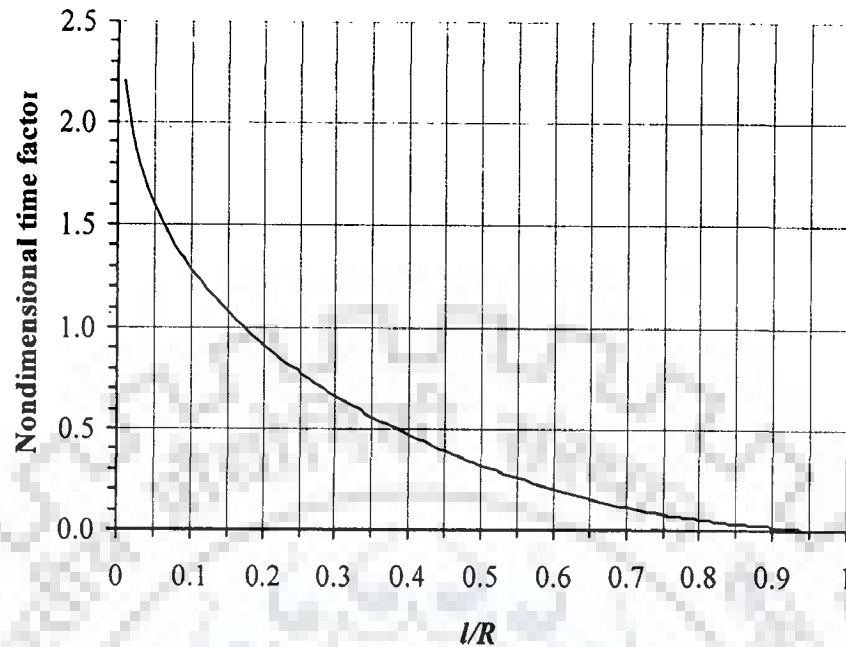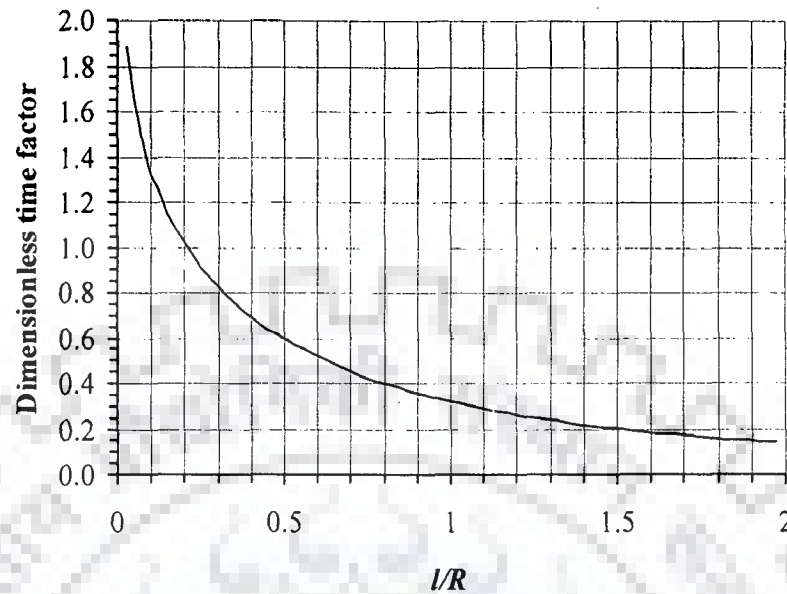Fig.4.12: Variation of non dimensional time factor, $\dfrac{\tau k(h_r - h_w)}{S(R + l)^2}$ with l/R an infiltration gallery aligned perpendicular to the direction of river flow and towards landside.

4.3.3 Flow to an Infiltration Gallery Running Parallel to a River

An infiltration gallery near a riverbank is generally constructed parallel to a straight river reach at a safe distance from the river. Assuming condition of sheet flow, and applying conformal mapping technique, yield of an infiltration gallery running parallel to a straight river reach has been quantified by Hunt (1983). Mishra (2004(b) has further simplified Hunt's solution. Using Mishra's solution the minimum travel time is derived in this chapter.

An infiltration gallery running parallel to a river is shown in Fig.4.13 (a). The thickness of the aquifer (T) is small and the flow is occurring in x-y plane. The radius of the gallery is r_w and the length of half of the gallery is l. It is required to

79

solve the Laplace equation for the flow domain in the x-y plane and derive the minimum travel time of water from the river to the caisson.

Mapping of z plane onto t plane

According to Schwarz-Christoffel transformation the conformal mapping of the flow domain, shown in Fig.4.13 (a), to the upper half of the auxiliary 't' plane, shown in Fig.4.13 (b), is given by (Harr, 1962):

$$z = M \int_0^t \frac{(t-c)}{t^{1/2}(d-t)^{1/2}(1-t)^{1/2}} dt + N$$

$$= M \int_0^t \frac{t^{1/2}}{(d-t)^{1/2}(1-t)^{1/2}} dt - Mc \int_0^t \frac{dt}{t^{1/2}(d-t)^{1/2}(1-t)^{1/2}} + N \quad (4.67)$$

M and N are constants. Since for $t = 0, z = 0$, hence, $N = 0$. Integrating (Byrd and Friedman, 1971, p72, 233.00 and 233.03, 310.02) and considering point D, for which $z=0$ and $t = d$, one finds

$$c = \frac{\int_0^d \frac{t^{1/2} dt}{(d-t)^{1/2}(1-t)^{1/2}}}{\int_0^d \frac{dt}{t^{1/2}(d-t)^{1/2}(1-t)^{1/2}}} = 1 - \frac{E(\pi/2, \sqrt{d})}{F(\pi/2, \sqrt{d})} \quad (4.68)$$

$F(\pi/2, \sqrt{d})$ and $E(\pi/2, \sqrt{d})$ are complete elliptic integrals of the first kind and the second kind with modulos $\sqrt{d}$. For an assumed value of d, the corresponding value of c can be obtained from equation (4.68). For point $C, z = il$ and $t=c$. Applying this in equation (4.67)

$$il = M \int_0^c \frac{t^{1/2} dt}{(d-t)^{1/2}(1-t)^{1/2}} - Mc \int_0^c \frac{dt}{t^{1/2}(d-t)^{1/2}(1-t)^{1/2}}$$

$$= 2(1-c)MF\{\sin^{-1}\sqrt{(c/d)}, \sqrt{d}\} - 2ME\{\sin^{-1}\sqrt{(c/d)}, \sqrt{d}\} \quad (4.69)$$

$F\{\sin^{-1}\sqrt{(c/d)},\sqrt{d}\}$, and $E\{\sin^{-1}\sqrt{(c/d)},\sqrt{d}\}$ are incomplete elliptic integrals of the first and the second kind. For $d \le t \le 1$, the relation between z and t plane is given by:

$$z = M \int_d^t \frac{t^{1/2}dt}{(d-t)^{1/2}(1-t)^{1/2}} - Mc \int_d^t \frac{dt}{t^{1/2}(d-t)^{1/2}(1-t)^{1/2}} \qquad (4.70)$$

For point E, $z = R$, and $t = 1$. Applying this condition in equation (4.70)

$$R = M \int_d^1 \frac{t^{1/2}dt}{(-1)^{1/2}(t-d)^{1/2}(1-t)^{1/2}} - Mc \int_d^1 \frac{dt}{(-1)^{1/2}t^{1/2}(t-d)^{1/2}(1-t)^{1/2}} \qquad (4.71)$$

Integrating (Byrd and Friedman,1971, p.77, 235.05,315.02;235.00)

$$(\pm)iR = 2M\ E\{\pi/2,\sqrt{(1-d)}\} - 2McF\{\pi/2,\sqrt{(1-d)}\} \qquad (4.72)$$

Dividing equation (4.69) by equation (4.72)

$$\frac{l}{R} = -\frac{(1-c)F\{\sin^{-1}\sqrt{(c/d)},\sqrt{d}\} - E\{\sin^{-1}\sqrt{(c/d)},\sqrt{d}\}}{E\{\pi/2,\sqrt{(1-d)}\} - cF\{\pi/2,\sqrt{(1-d)}\}} \qquad (4.73)$$

Thus, with an assumed 'd' and computed 'c', the corresponding l/R can be known from equation (4.73)

Mapping of w plane onto t plane

The conformal mapping of the complex potential plane (Fig 4.13 (c)) onto the 't' plane is given by:

$$w = \frac{kT(h_r - h_w)}{2F\{\pi/2,\sqrt{(1-d)}\}} \int_{-\infty}^t \frac{dt}{(0-t)^{1/2}(d-t)^{1/2}(1-t)^{1/2}} - kT(h_r - h_w) \qquad (4.74)$$

Applying the condition at point E for which $t = 0$ and $w = -kT(h_r - h_w) + iq$, q is found to be

81
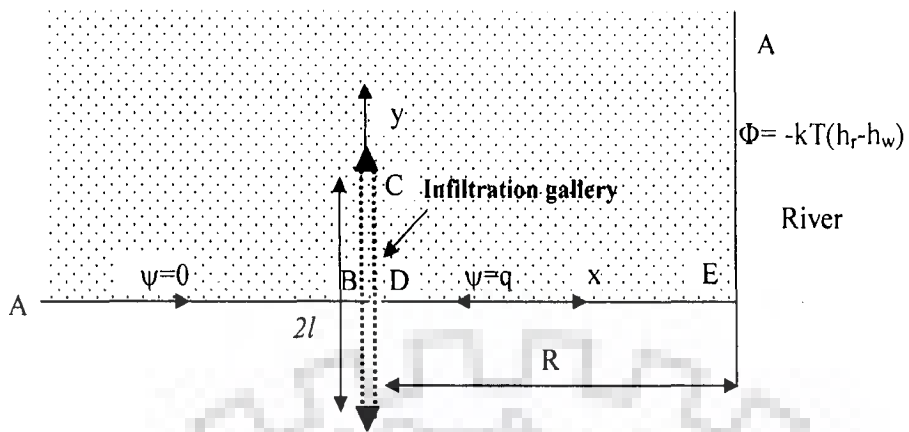
(a): Upper half of the flow domain in $z(=x+iy)$ plane (plan)
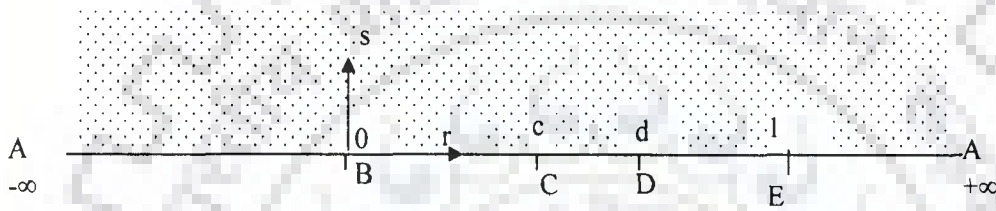
(b): Auxiliary upper half t plane ($t=r+is$)
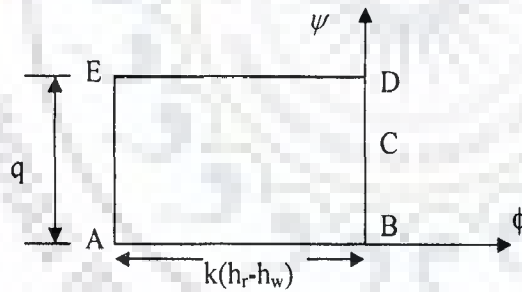
(c): Complex potential plane $(w=\phi+i\psi)$

Fig.4.13: Steps of conformal mapping for an infiltration gallery running parallel to straight reach of a river

82

$$q = kT(h_r - h_w)\frac{F(\pi/2, \sqrt{d})}{F(\pi/2, \sqrt{(1-d)})}$$ (4.75)

Total flow to gallery, Q=2q

For $0 \le t' \le d$, the relation between w and t plane is given by:

$$w = i\psi = \frac{kT(h_r - h_w)}{2F(\pi/2, \sqrt{(1-d)})}\int_0^{t'}\frac{dt}{(0-t)^{1/2}(d-t)^{1/2}(1-t)^{1/2}}$$
$$= \frac{kT(h_r - h_w)}{(\pm i)F(\pi/2, \sqrt{(1-d)})}F\left\{\sin^{-1}\sqrt{(t'/d)}, \sqrt{d}\right\}$$ (4.76)

At $t' = c$, the stream function is

$$\psi = \frac{kT(h_r - h_w)}{F(\pi/2, \sqrt{(1-d)})}F\left\{\sin^{-1}\sqrt{c/d}, \sqrt{d}\right\}$$ (4.77)

The flow to the infiltration gallery is $2q$. Incorporating the correction factor, C_I, (Appendix D) the approximate flow to the infiltration gallery is given by:

$$Q = C_I Tk(h_r - h_w)\frac{2F(\pi/2, \sqrt{d})}{F(\pi/2, \sqrt{(1-d)})}$$ (4.78)

The average entrance velocity, v_1 through the slotted- pipe of length l, and perforation P is given by:

$$v_l = \left\{C_I Tk(h_r - h_{wl})\frac{F(\pi(\pi/\sqrt{d}))}{F(\pi(\pi/\sqrt{(1-d)})}\right\}/\{Pl2\pi l_w\}$$ (4.79)

The maximum axial velocity near the caisson, v_2, is given by:

$$v_2 = \left\{ C_1 Tk \left(h_r - h_{w1} \right) \frac{F(\pi/2, \sqrt{d})}{F(\pi/2, \sqrt{(1-d)})} \right\} / \left\{ \pi r_w^2 \right\}$$ (4.80)

Travel time for the shortest distance

The travel time for river water to reach the infiltration gallery along the path *ED* is not the minimum travel time. The time will be minimum for that path line along which water enters point C, that is for the stream line defined by Eq.(4.77). This is because the velocity at point *C* is theoretically infinite. It is cumbersome to find the minimum travel time. Therefore the time for the shortest flow path is computed. The Darcy velocity is given by

$$u - iv = \frac{1}{T} \frac{dw}{dz} = \frac{1}{T} \frac{dw}{dt} \frac{dt}{dz}$$ (4.81)

From Eq.(4.74)

$$\frac{dw}{dt} = \frac{kT(h_r - h_w)}{2F\left(\pi/2, \sqrt{(1-d)}\right)} \frac{1}{(0-t)^{1/2}(d-t)^{1/2}(1-t)^{1/2}}$$ (4.82)

From Eq.(4.72)

$$M = \frac{iR}{2\left[E\{\pi/2, \sqrt{(1-d)}\} - cF\{\pi/2, \sqrt{(1-d)}\}\right]}$$ (4.83)

From Eq.(4.67)

$$\frac{dz}{dt} = \frac{iR}{2\left[E\{\pi/2, \sqrt{(1-d)}\} - cF\{\pi/2, \sqrt{(1-d)}\}\right]} \frac{(t-c) \cdot}{t^{1/2}(d-t)^{1/2}(1-t)^{1/2}}$$ (4.84)

Incorporating Eqs. (4.80), and (4.82) in Eq (4.79), and simplifying

$$u = -\frac{k(h_r - h_w)}{F\left(\pi/2, \sqrt{(1-d)}\right)} \frac{\left[E\{\pi/2, \sqrt{(1-d)}\} - cF\{\pi/2, \sqrt{(1-d)}\}\right]}{(t-c)R} \qquad (4.85)$$

The travel time, τ along shortest distance is given by

$$\tau = \int_R^0 \frac{dx}{(u/S)} = \frac{SR}{k(h_r - h_w)} \frac{F\left(\pi/2, \sqrt{(1-d)}\right)}{\left[E\{\pi/2, \sqrt{(1-d)}\} - cF\{\pi/2, \sqrt{(1-d)}\}\right]} \int_0^R (t-c)dx \qquad (4.86a)$$

or

$$\tau = \frac{SR}{k(h_r - h_w)} \frac{F\left(\pi/2, \sqrt{(1-d)}\right)}{\left[E\{\pi/2, \sqrt{(1-d)}\} - cF\{\pi/2, \sqrt{(1-d)}\}\right]} \left[\int_0^R t dx - cR\right] \qquad (4.86b)$$

or

$$\tau = \frac{SR^2}{k(h_r - h_w)} \frac{F\left(\pi/2, \sqrt{(1-d)}\right)}{\left[E\{\pi/2, \sqrt{(1-d)}\} - cF\{\pi/2, \sqrt{(1-d)}\}\right]} \left[\int_0^R t \frac{dx}{R} - c\right] \qquad (4.86c)$$

The dimensionless time factor is given by

$$\varsigma = \frac{k(h_r - h_w)\tau}{SR^2} = \frac{F\left(\pi/2, \sqrt{(1-d)}\right)}{\left[E\{\pi/2, \sqrt{(1-d)}\} - cF\{\pi/2, \sqrt{(1-d)}\}\right]} \left[\int_0^R t \frac{dx}{R} - c\right] \qquad (4.87)$$

The integral $\int_0^R t \frac{dx}{R}$ is the dimensionless area of the graph of t versus x/R, which can

be evaluated numerically. Along DE $z = x$ and t varies from d to 1.

Results and Discussions

Variation of dimensionless yield of the infiltration gallery, $\dfrac{Q}{kT(h_r - h_w)}$ with

dimensionless l/R is presented in Fig.4.14. Beyond $l/R > 0.25$ the variation of yield

with l/R is linear. The increase in flow is due to increase in length of gallery, i.e.,

increase in the flow area. The variation of dimensionless time factor with l/R is

presented in Fig.4.15. Less than $l/R < 1$ the minimum travel time decreases with increase in length of gallery. Beyond $l/R > 1$ the minimum travel time becomes constant with the further increase in the length of gallery.
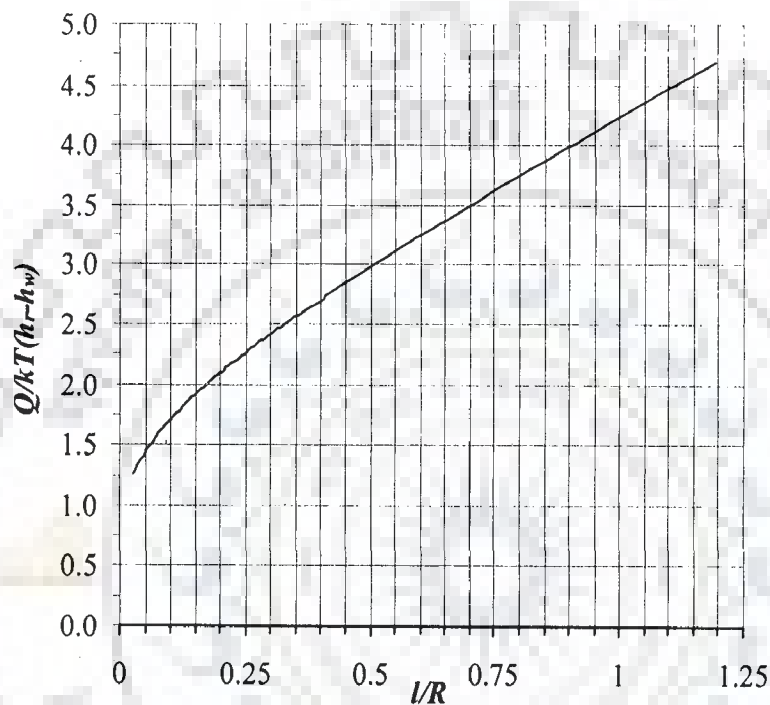
Fig.4.14. **Variation of non dimensional flow,** $\dfrac{Q}{kT(h_r - h_w)}$ **with** l/R **for an infiltration gallery running parallel to straight reach of a river**
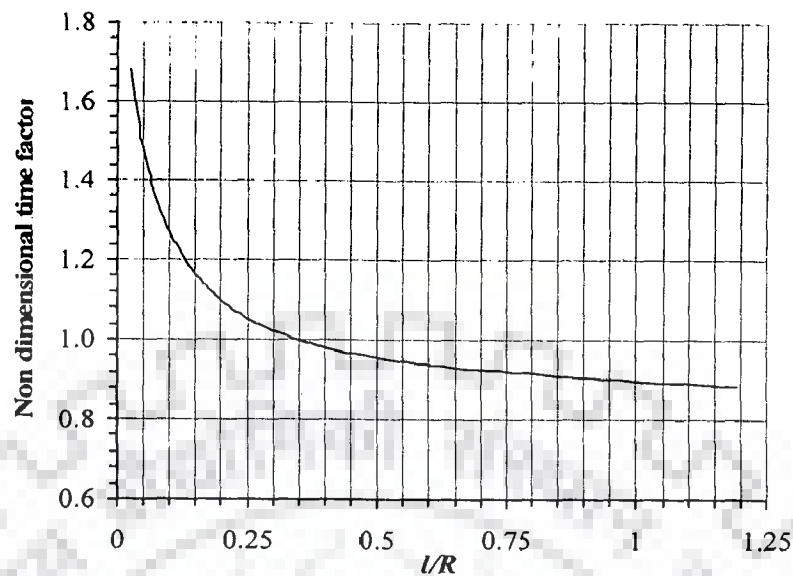
Fig.4.15. Variation of non-dimensional time factor, $\dfrac{k\left(h_r - h_w\right)\tau}{SR^2}$ with l/R for an infiltration gallery running parallel to straight reach of a river

4.4 CONCLUSIONS

In this chapter, flow to an infiltration gallery located near a meandering river reach and near a straight river reach has been analyzed. The minimum travel time has been estimated. Results are presented in non dimensional form. In case of an infiltration gallery near a meandering river reach or at the centre of an island, flow increase and travel time reduces with the increase in the length of infiltration gallery. For a given size of island, the length of the infiltration gallery has to be fixed on the basis of permissible minimum travel time. The minimum travel time should be greater than the survival life of bacteria in concern.

Infiltration gallery near a straight reach of a river may be laid in different orientation. In case of a gallery perpendicular and toward the river, the flow increases and travel time decreases sharply with the increase in the length of gallery for a given

value of R. Whereas, in case of a gallery perpendicular and towards landside, the flow increases with decreasing rate and minimum travel time reduces and become constant.

Flow to an infiltration gallery running parallel to river increase linearly with the increase in the length of gallery. The minimum travel time reduces sharply for l/R <0.25 and then decrease slowly and finally becomes constant after $l/R=1.25$

A RADIAL COLLECTOR WELL
NEAR A MEANDERING RIVER

5.1   INTRODUCTION

In an alluvial region, a river is likely to meander. In that case, it is advantageous to install a radial collector well in the concave side of the meandering reach. In such hydro-geological situation like this, it can be idealized that a constant head boundary condition prevails at a distance R around the radial collector well. Thus, a radial collector well near a meandering river reach can be conceptualised as a radial collector well at the centre of an island of radius R. Further, in practice, laterals of a radial collector well are kept partly screened. Non-perforated portion (blind) is kept near the caisson, as provision of perforated pipes near the caisson is not advantageous due to pronounced interference of laterals near the caisson. Thus, it is desirable to investigate the effect of non-perforated section on the yield of a radial collector well. In this chapter, flow to a radial collector well near a meandering river reach having partly perforated multiple laterals is analyzed and minimum travel time that would be taken by river water to reach the screens has been estimated.

5.2   STATEMENT OF THE PROBLEM

A radial collector well located near a meandering river is shown Figure 5.1. The laterals are of equal length placed at equal angular interval. Part of each lateral near the caisson is blind (non-perforated). The blind part is of length l_b and the screened (perforated) part is of length l_s. The screened part of the lateral is assumed as a

constant head boundary. It is desired to find flow to the well under steady state condition that would prevail under continuous pumping.

Let the datum be selected in the plane of the laterals; height of water level in the well above the datum is h_w, and height of water level in the river measured from the datum be h_r. Because of symmetry, half of $1/n^{th}$ part of the flow domain, shown in Fig. 5.2(a), is considered for analysis.
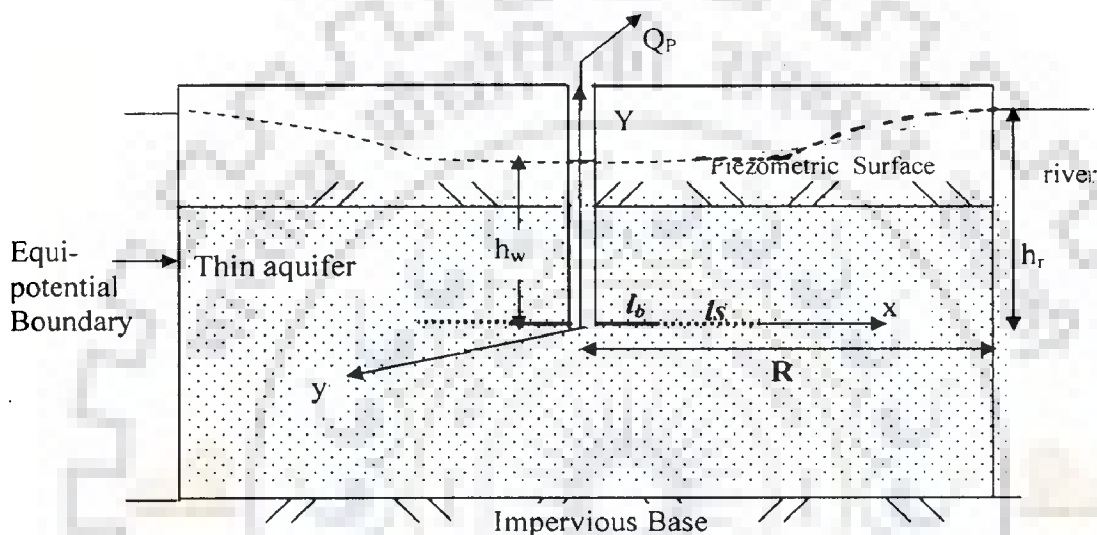
Figure 5.1: **A radial collector well with n partly screened laterals near a meandering river**

5.3 ANALYSIS: CONFORMAL MAPPING

In order to analyze, The Christoffel conformal mapping technique is applied to $1/n^{th}$ part of the flow domain

Transformation of z Plane onto Auxiliary t Plane

The conformal mapping of the flow domain ABC1C2 D shown in Fig.5.2(a) onto upper half of the auxiliary 't' plane shown in Fig.5.2(b) is given by:

$$\frac{dz}{dt} = M\ t^{1/n-1}\ (1-t)^{(n-1)/2n-1} \tag{5.1}$$

90

Integrating

$$z = M\, B_t\{1/n, (1-1/n)/2\} + N \tag{5.2}$$

$B_t\{1/n, (1-1/n)/2\}$ is an incomplete Beta function, which is defined as:

$$B_t(m,n) = \int_0^t v^{m-1}(1-v)^{n-1}\, dv \ ; \ m > 0; n > 0; t \le 1 \ ; v \text{ is a dummy variable.}$$

For point B, $t = 0$, and $z = 0$. Hence, $N = 0$. For point D, $t = 1$ and $z = R$. Hence,

$$M = \frac{R}{B\{1/n, (1-1/n)/2\}} = R\,\frac{\Gamma\{(n+1)/2n\}}{\Gamma(1/n)\,\Gamma\{(1-1/n)/2\}} \tag{5.3}$$

in which, $B(m,n)$ is complete Beta function and $\Gamma(m)$ is complete Gamma function.

For point C_1, $t = c_1$ and $z = l_b$. Hence, from equation (5.2)

$$l_b/R = \frac{\Gamma\{(n+1)/2n\}}{\Gamma(1/n)\,\Gamma\{(1-1/n)/2\}}\, B_{c_1}\{1/n, (1-1/n)/2\} \tag{5.4}$$

The parameter 'c_1' can be obtained from equation (5.4) by an iterative procedure for known l_b/R. Similarly for point $C_2, t = c_2, z = l_b + l_s$, and

$$(l_b + l_s)/R = \frac{\Gamma\{(n+1)/2n\}}{\Gamma(1/n)\,\Gamma\{(1-1/n)/2\}}\, B_{c_2}\{1/n, (1-1/n)/2\} \tag{5.5}$$

The parameter c_2 can be obtained for known $(l_b + l_s)/R$ using an iterative procedure.

Transformation of w Plane onto t Plane

The complex potential $w(= \phi + i\psi)$ plane corresponding to a unit segment flow domain ABC_1C_2D is shown in Fig.5.2(c). The velocity potential function ϕ here is defined as (Hunt, 1983):

$$\phi = -kT(p/\gamma_w + Y) + C \tag{5.6}$$

Where, k = hydraulic conductivity of the medium, p= pore water pressure; Y= elevation head measured from the horizontal plane in which the laterals have been laid. For the present

91

conceptual flow domain, $Y = 0$. Constant $C = -kTh_w$, where h_w is height of water level above the xy plane.
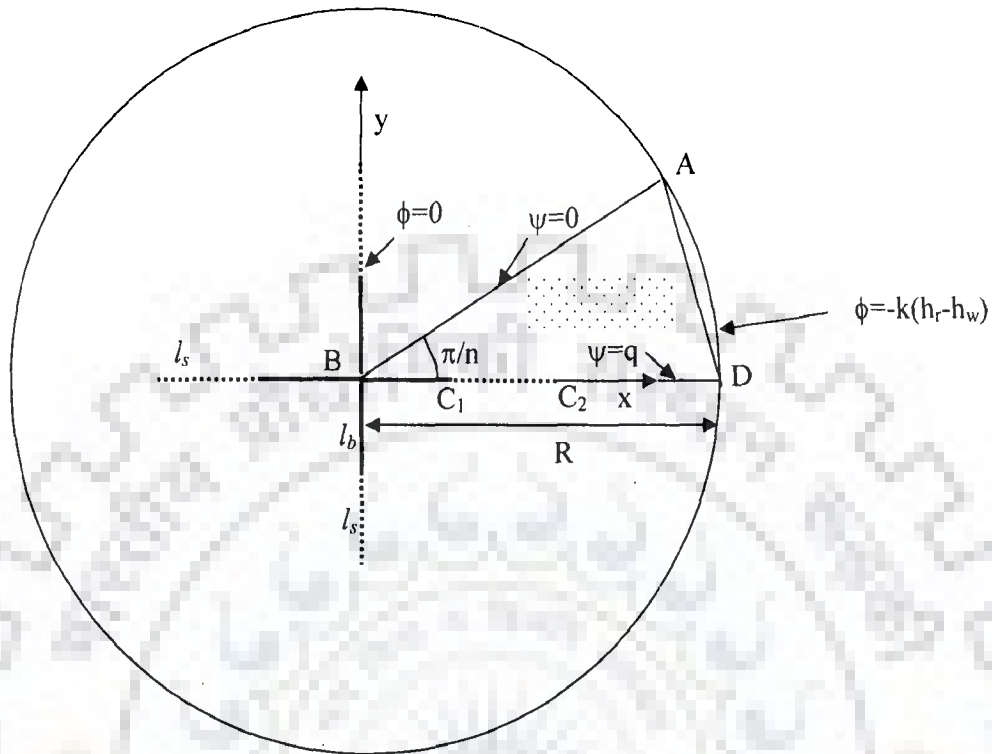
(a): Physical flow domain, z =x+iy plane
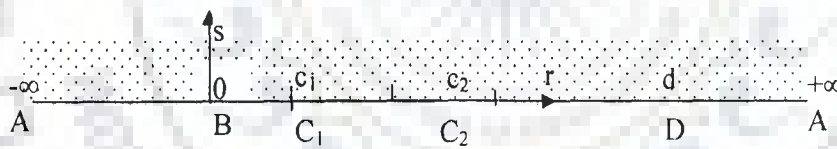
(b): Auxuliary t plane (t=r+is)
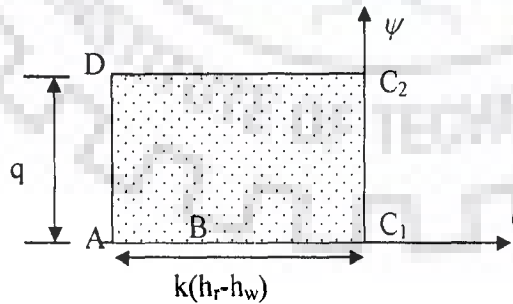
(c): Complex potential plane w (=ɸ+iψ)

Fig.5.2: Steps of conformal mapping for a radial collector well with n partly screened laterals near a meandering river

92

The mapping of the complex potential 'w' plane onto the auxiliary 't' plane is given by:

$$w = M_1 \int_{-\infty}^{t} \frac{dt}{\sqrt{(c_1 - t)(c_2 - t)(1 - t)}} - kT(h_r - h_w) \tag{5.7}$$

For point 'C_1', $t = c_1$ and $w = 0$. Performing the integration (Byrd and Friedman, 1971)

$$0 = M_1 \frac{2}{\sqrt{1 - c_1}} F(\pi/2, \sqrt{(1 - c_2)/(1 - c_1)}) - kT(h_r - h_w) \tag{5.8}$$

$F(\pi/2, \sqrt{(1 - c_2)/(1 - c_1)})$ is complete elliptic integral of the first kind with modulus $\sqrt{(1 - c_2)/(1 - c_1)}$.

The constant M_1 from equation (5.8) is found to be

$$M_1 = \frac{\sqrt{1 - c_1} \, kT(h_r - h_w)}{2F(\pi/2, \sqrt{(1 - c_2)/(1 - c_1)})} \tag{5.9}$$

For $c_1 \leq t \leq c_2$, the relation between w and t planes is given by:

$$w = M_1 \int_{c_1}^{t} \frac{dt}{\sqrt{-1}\sqrt{(t - c_1)(c_2 - t)(1 - t)}} \tag{5.10}$$

For point C_2, $t = c_2$ and $w = iq$. Performing the integration and substituting constant M_1, flow 'q' is found to be:

$$q = kT(h_r - h_w) \frac{F(\pi/2, \sqrt{(c_2 - c_1)/(1 - c_1)})}{F(\pi/2, \sqrt{(1 - c_2)/(1 - c_1)})} \tag{5.11}$$

The quantity q is half of the flow to a lateral. Therefore, the total flow 'Q' to the collector well with n laterals is $2nq$. Applying the correction factor, C_1 (Appendix D) the flow Q to the collector well can be estimated as

93

$$Q = C_1 2nkT(h_r - h_w) \frac{F(\pi/2, \sqrt{(c_2 - c_1)/(1 - c_1)}\,)}{F(\pi/2, \sqrt{(1 - c_2)/(1 - c_1)}\,)} \qquad (5.12)$$

The entrance velocity (v_1) is given by

$$v_1 = \frac{Q}{n2\pi r_w l_s P} \qquad (5.13)$$

Where, r_w is the radius of the perforated pipe, and P is the percentage of perforations of the lateral.

The maximum axial velocity (v_2) in the lateral is

$$v_2 = \frac{Q}{n\,\pi\,r_w^2} \qquad (5.14)$$

Minimum Travel Time

The travel time is minimum for the river water that follows the path line *CD*. The Darcy velocity is given by:

$$u - iv = \frac{1}{T}\frac{dw}{dz} = \frac{1}{T}\frac{dw}{dt}\cdot\frac{dt}{dz}$$

Incorporating $\dfrac{dw}{dt}$ from equation (5.7) and $\dfrac{dt}{dz}$ from equation (5.2) in above

$$= \left[\frac{\sqrt{1-c_1}\; k(h_r - h_w)}{2F(\pi/2, \sqrt{(1-c_2)/(1-c_1)}}\right]\left[\frac{\Gamma(1/n)\,\Gamma\{(1-1/n)/2\}}{R\Gamma\{(n+1)/2n\}}\right](-)\frac{t^{1-1/n}(1-t)^{1/(2n)}}{(t-c_1)^{1/2}(t-c_2)^{1/2}}$$

$$(5.15)$$

Along path *CD*, $z=x$, and $v=0$. Therefore, the minimum travel time is given by

$$\tau = \int_R^1 \frac{dx}{(u/S)} = RS\left[\frac{2F(\pi/2, \sqrt{(1-c_2)/(1-c_1)}}{\sqrt{1-c_1}\; k(h_r - h_w)}\right] \times$$

$$\left[\frac{\Gamma\{(n+1)/2n\}}{\Gamma(1/n)\,\Gamma\{(1-1/n)/2\}}\right]\int_1^R \frac{(t-c_1)^{1/2}(t-c_2)^{1/2}}{t^{1-1/n}(1-t)^{1/(2n)}}dx \qquad (5.16)$$

Let $X = x / R$; and $dx = RdX$. Incorporating these substitutions in (5.16), the dimensionless time factor is found to be

$$\varsigma = \frac{\tau k(h_r - h_w)}{R^2 S} = \left[\frac{2F(\pi/2, \sqrt{(1-c_2)/(1-c_1)})}{\sqrt{1-c_1}} \right] \times$$

$$\left[\frac{\Gamma\{(n+1)/2n\}}{\Gamma(1/n)\,\Gamma\{(1-1/n)/2\}} \right]_{1/R}^{1} \int \frac{(t-c_1)^{1/2}(t-c_2)^{1/2}}{t^{1-1/n}(1-t)^{1/(2n)}} dX \qquad (5.17)$$

The integral appearing in equation (5.16) is evaluated numerically as follows.

$z = x + iy = f(t)$;   hence,   as $y = 0$, $t = f^{-1}(x)$ and

$$\frac{(t-c_1)^{1/2}(t-c_2)^{1/2}}{t^{1-1/n}(1-t)^{1/(2n)}} = F\left[f^{-1}(x)\right] = F\left[f^{-1}(X)\right]$$. For given value of t, $F\left[f^{-1}(X)\right]$ is

evaluated and for the assumed value of t, corresponding X is obtained from equation

(5.2). A graph of $F\left[f^{-1}(X)\right]$ versus X is plotted and area under the graph gives the

value of the integrand.

5.4   RESULTS AND DISCUSSIONS

The variation of non-dimensional flow with l/R for different number of laterals for a

given value of $l_b/R=0.1$ and R=100m is presented in Fig.5.3. Flow increases

monotonically with the increase in number of laterals. The increase in flow is

significant for increased number of longer laterals. For smaller length of laterals, no

significant increase in flow is observed with the increase in number of laterals.

The variation of entrance velocity with l/R with different number of laterals is

presented in Fig.5.4. It is observed that with the increase in l/R the entrance velocity

first decreases then increases. The reason for this is that when the l/R is less, i.e., the

screen length short, hence, the entrance velocity is higher. With further increase in the

length of screen, laterals come closer to the river resulting in higher flow to the laterals consequently entrance velocity is increased.

The variation of axial velocity with l/R for different number of laterals is presented in Fig.5.5. Axial velocity increases with the increase in screen length and decreases with the increase in number of laterals.

The variation of non-dimensional time factor with l/R for different number of laterals is presented Fig.5.6. For large number and length of laterals, the travel time is less, whereas, with small number and short length of laterals the travel time is higher. The variation of nondimensional flow, entrance velocity, axial velocity and nondimensional time factor with l/R for different value of l_b/R is presented in Table 5.1. It is clear from the table that the flow increases with the increase in screen length for the same value of l/R. Flow decreases and time minimum travel time increases monotonically with the increases in blind portion. However, the entrance velocity increases sharply with the increase in blind portion.

A sample result is presented as below:

Illustrative Example:

Number of laterals, $N=8$; Length of each laterals, $l = 50m$;

Length of blind portion, $l_b=10m$; length of screen, $l_s=40m$;

Radius of island, $R = 100m$; $l_b/R=0.1$; $l/R =0.5$; Aquifer thickness, T =7.5 m;

Diameter of gallery=0.32m; Correction factor, $C_1=0.8$; Drawdown, $h_r-h_w= 6m$;

Hydraulic conductivity, k= 10m/day; ˈˈˈˈˈˈ S=0.2

For $l_b/R=0.1$, $l/R =0.5$, and N=8 the non dimensional flow (Fig.5.3), $\dfrac{Q}{kT(h_r - h_w)} =$

7.35 or $Q=7.35 \times kT(h_r - h_w)C_1 =2646 \text{ m}^3/\text{day}$.

The corresponding non dimensional time factor from Fig.(5.6) is $\dfrac{k\tau(h_r - h_w)}{SR^2} = 0.32$.

For the above set of data, the minimum travel time, τ is 10.6 days. Thus, Bacteria will take 10.6 days to reach from point D to point C_2, i.e., a distance of 50m. The average survival time of pathogenic bacteria is 30-40 days. Therefore, the length and number of laterals have to be reduced in order to increase the travel time.

For $l_b/R=0.1$, $l/R =0.30$, and N=4 the non dimensional flow (Fig.5.3), $\dfrac{Q}{kT(h_r - h_w)} = 4.2$, or $Q=4.2 \times kT(h_r - h_w)C_1 = 1512$ m^3/day.

The corresponding non-dimensional time factor from Fig. (5.6) is $\dfrac{k\tau(h_r - h_w)}{SR^2} = 0.91$.

The minimum travel time τ is 30.3 days to reach from point D to point C_2, i.e., a distance of 70m.

5.5 CONCLUSIONS

A radial collector well near a meandering river can be conceptualized to be located at the centre of an island. For a given size of an island, the major parameters of a proposed radial collector well are the number of laterals, length of screen and blind portions, and permissible drawdown in the caisson that has to be realized , keeping the minimum travel time and entrance velocity as limiting factors. Interference of laterals increases with the increase in number of laterals, in such case the increase in blind length does not affect much on the total flow to the well. However, the average entrance velocity to laterals increases sharply. The length of blind portion depends on the number of laterals.
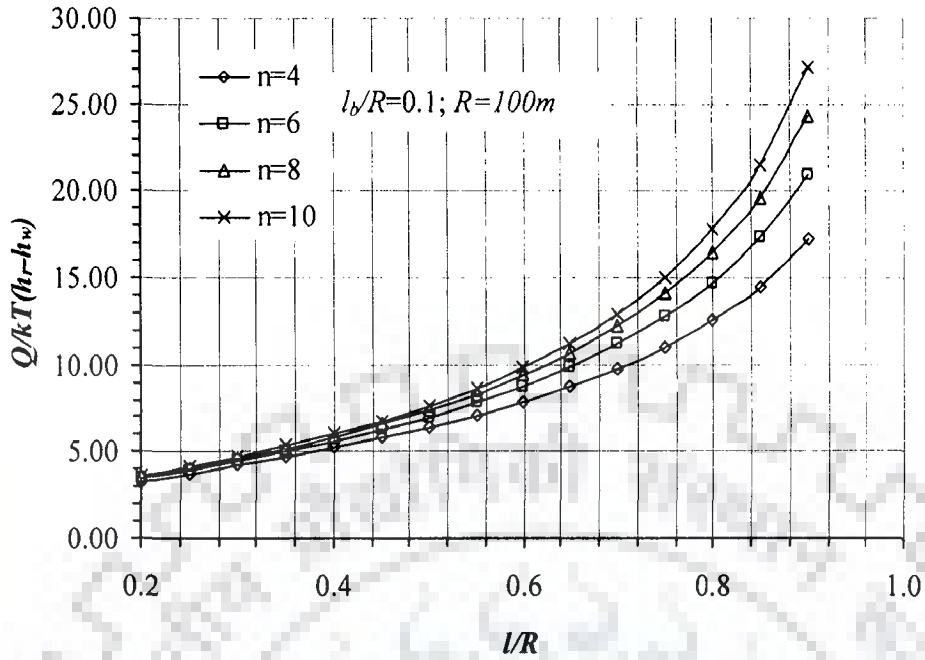
Fig.5.3: Variation of nondimensional flow with l/R for different numbers of partly screened laterals of a RCW near a meandering river
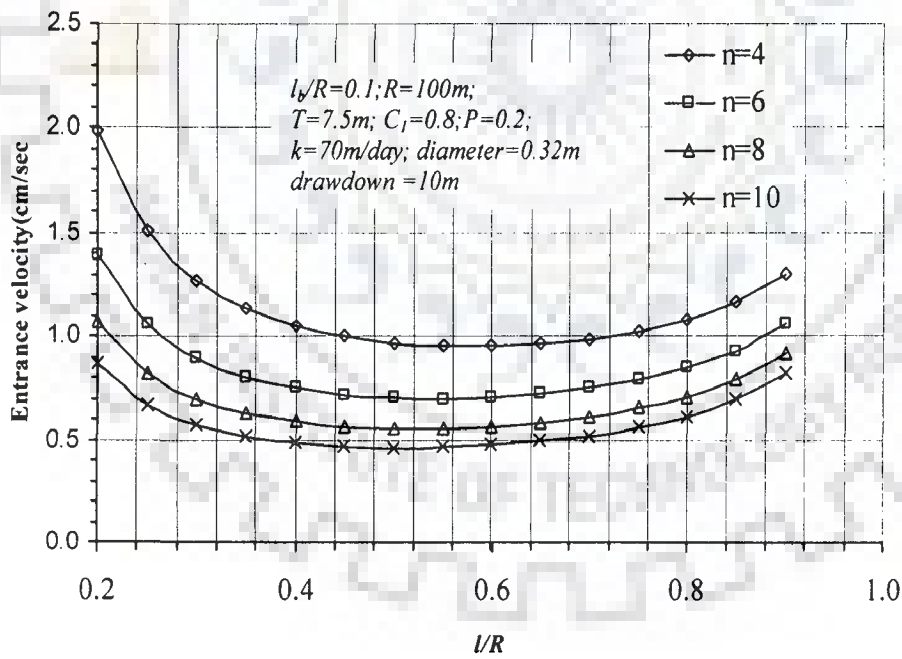
Fig.5.4: Variation of entrance velocity with l/R for different numbers of partly screened laterals of a RCW near a meandering river

98
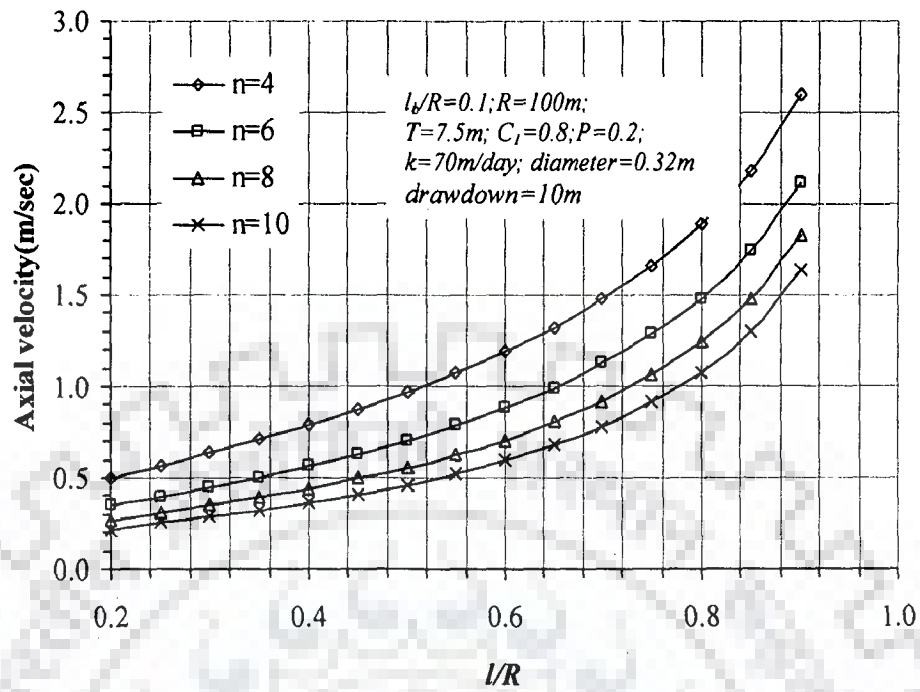
Fig.5.5: Variation of axial velocity with l/R for different numbers of partly screened laterals of a RCW near a meandering river
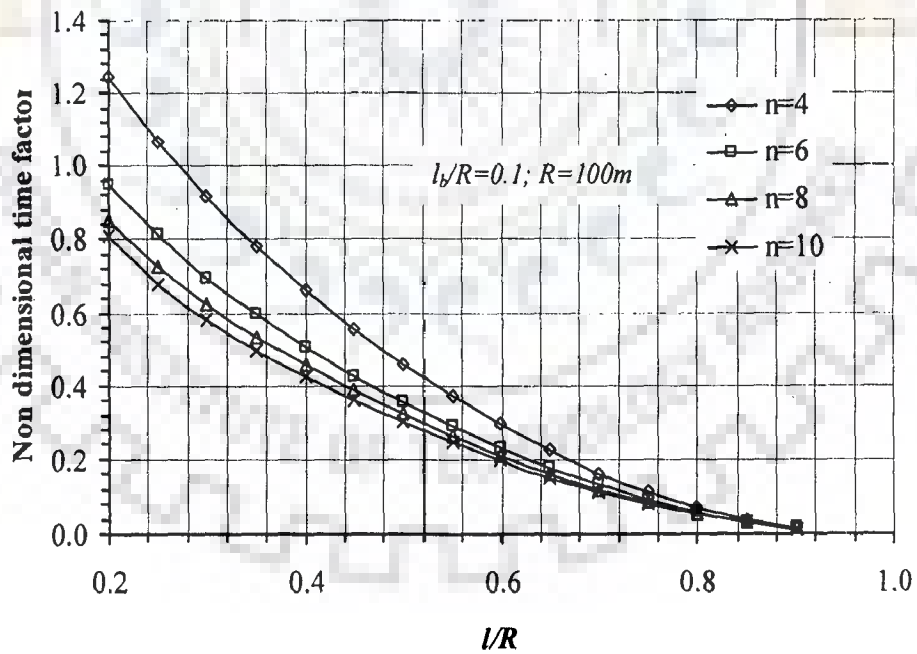
Fig.5.6: Variation of nondimensional time factor with *l/R* for different numbers of partly screened laterals of a RCW near a meandering river

Table 5.1: Variation of non-dimensional flow, entrance velocity, axial velocity, and non-dimensional time with l/R for different ratio of l_b/R.

N=8, R=100m, k=70m/day, T=7.5m, C_1=0.8, diameter of lateral=0.32m, h_r-h_w=10m, P=0.2

l_b/R	l_y/R	l/R	$Q/kT(h_r$ -$h_w)$	V_1(cm/sec)	V_2(m/s)	Time Factor
1	2	3	4	5	6	7
0.40	0.10	0.50	7.17	2.17	0.54	0.3271
0.40	0.15	0.55	8.18	1.65	0.62	0.2641
0.40	0.20	0.60	9.30	1.41	0.70	0.2095
0.40	0.25	0.65	10.59	1.28	0.80	0.1618
0.40	0.30	0.70	12.13	1.22	0.92	0.1201
0.40	0.35	0.75	14.03	1.21	1.06	0.0844
0.40	0.40	0.80	16.42	1.24	1.24	0.0545
0.40	0.45	0.85	19.62	1.32	1.48	0.0309
0.40	0.50	0.90	24.23	1.46	1.83	0.0137
0.30	0.10	0.40	5.77	1.74	0.44	0.4616
0.30	0.15	0.45	6.52	1.31	0.49	0.3873
0.30	0.20	0.50	7.35	1.11	0.56	0.3213
0.30	0.25	0.55	8.28	1.00	0.63	0.2619
0.30	0.30	0.60	9.36	0.94	0.71	0.2086
0.30	0.35	0.65	10.63	0.92	0.80	0.1614
0.30	0.40	0.70	12.16	0.92	0.92	0.1200
0.30	0.45	0.75	14.05	0.94	1.06	0.0843
0.30	0.50	0.80	16.44	0.99	1.24	0.0545
0.30	0.55	0.85	19.63	1.08	1.48	0.0309
0.30	0.60	0.90	24.24	1.22	1.83	0.0137
0.20	0.10	0.30	4.59	1.39	0.35	0.6244
0.20	0.15	0.35	5.19	1.05	0.39	0.5350
0.20	0.20	0.40	5.84	0.88	0.44	0.4568
0.20	0.25	0.45	6.56	0.79	0.50	0.3857
0.20	0.30	0.50	7.37	0.74	0.56	0.3207
0.20	0.35	0.55	8.29	0.72	0.63	0.2617
0.20	0.40	0.60	9.37	0.71	0.71	0.2085
0.20	0.45	0.65	10.64	0.71	0.80	0.1614
0.20	0.50	0.70	12.17	0.74	0.92	0.1200
0.20	0.55	0.75	14.05	0.77	1.06	0.0843
0.20	0.60	0.80	16.45	0.83	1.24	0.0545
0.20	0.65	0.85	19.63	0.91	1.48	0.0309
0.20	0.70	0.90	24.24	1.05	1.83	0.0137

l_t/R	l_s/R	l/R		V_1(cm/sec)	V_2(m/s)	Time Factor
1	*2*	*3*	*4*	*5*	*6*	*7*
0.10	0.10	0.20	3.55	1.07	0.27	0.8513
0.10	0.15	0.25	4.06	0.82	0.31	0.7251
0.10	0.20	0.30	4.61	0.70	0.35	0.6222
0.10	0.25	0.35	5.19	0.63	0.39	0.5346
0.10	0.30	0.40	5.84	0.59	0.44	0.4567
0.10	0.35	0.45	6.56	0.57	0.50	0.3857
0.10	0.40	0.50	7.37	0.56	0.56	0.3207
0.10	0.45	0.55	8.29	0.56	0.63	0.2617
0.10	0.50	0.60	9.37	0.57	0.71	0.2085
0.10	0.55	0.65	10.64	0.58	0.80	0.1614
0.10	0.60	0.70	12.17	0.61	0.92	0.1200
0.10	0.65	0.75	14.05	0.65	1.06	0.0843
0.10	0.70	0.80	16.45	0.71	1.24	0.0545
0.10	0.75	0.85	19.63	0.79	1.48	0.0309
0.10	0.80	0.90	24.24	0.92	1.83	0.0137

Fully screened laterals

l_t/R	l_s/R	l/R		V_1(cm/sec)	V_2(m/s)	Time Factor
0.0	0.10	0.10	2.59	0.78	0.20	1.2235
0.0	0.15	0.15	3.05	0.62	0.23	1.0139
0.0	0.20	0.20	3.55	0.54	0.27	0.8510
0.0	0.25	0.25	4.06	0.49	0.31	0.7251
0.0	0.30	0.30	4.61	0.46	0.35	0.6222
0.0	0.35	0.35	5.19	0.45	0.39	0.5346
0.0	0.40	0.40	5.84	0.44	0.44	0.4567
0.0	0.45	0.45	6.56	0.44	0.50	0.3857
0.0	0.50	0.50	7.37	0.45	0.56	0.3207
0.0	0.55	0.55	8.29	0.46	0.63	0.2617
0.0	0.60	0.60	9.37	0.47	0.71	0.2085
0.0	0.65	0.65	10.64	0.49	0.80	0.1614
0.0	0.70	0.70	12.17	0.53	0.92	0.1200
0.0	0.75	0.75	14.05	0.57	1.06	0.0843
0.0	0.80	0.80	16.45	0.62	1.24	0.0545
0.0	0.85	0.85	19.63	0.70	1.48	0.0309
0.0	0.90	0.90	24.24	0.81	1.83	0.0137

Chapter 6

A RADIAL COLLECTOR WELL
NEAR STRAIGHT REACH OF A STREAM

6.1 INTRODUCTION

A radial collector well constructed close to a stream induces recharge from surface water bodies. In some cases, the laterals are extended beneath the streambed to increase groundwater production. The yield of a collector well increases with increasing length and diameter of collector pipe, and proximity of the lateral screens to the river. The quality of the water gets improved as the distance of the perforated pipe from the riverbank increases. Therefore, a radial collector well should be located at an appropriate distance from the effective line of infiltration.

Analytical study of flow to radial collector well or horizontal wells in hydrological science can be dated back to Hantush and Papadopulos(1962), who investigated flow to a collector well consisting of a series of horizontal wells. Milojevic (1963) has conducted experiments using electrical analog model to analyze yield of a radial collector well near a river. Recently, Bakker et al. (2005) have applied multilayer analytic element modeling to estimate steady flow to two tier radial collector well with several laterals. Mishra and Kansal (2007) have analyzed steady flow to a radial collector well system with four fully screened laterals by applying conformal mapping and assuming laminar flow domain.

All studies on radial collector well have been done by assuming the laterals to be fully screened, whereas in practice, screened parts of the laterals start at a certain

distance from the circumference of the well. Hence, it is desirable to analyze the effect of partially screened laterals on the potential yield of a radial collector well and corresponding entrance velocity through the screen and axial velocity in the laterals.

The objective of the present chapter is to analyze the performance of a radial collector well under steady state flow conditions. Assuming condition of sheet flow, and applying Schwartz-Christoffel conformal mapping technique, yield of a radial collector well, located near a straight river reach in a thin aquifer, having four coplanar partly perforated laterals is quantified for various orientation of laterals and distance of the collector well from the river. The average entrance velocity through the collector's screen is determined. The minimum time taken by river water to reach the laterals is derived.

6.2 STATEMENT OF THE PROBLEM

A radial collector well having four co-planer partly screened laterals near straight reach of a stream is shown in Fig.6.1. The laterals are partially screened. The solid line indicates the non- perforated sections of the laterals. The total lengths of the laterals are L_1, L_2, L_3, and L_2 and the non- perforated lengths are L_{1b}, L_{2b}, L_{3b}, and L_{2b}. The caisson is located at a distance R from the river. The radius of each lateral is r_w and the thickness of the aquifer is T. The height of water level in the river above the laterals is h_r and the height in the caisson of the collector well is h_w. Points P_1 and P_2 on the on screened parts (Fig.6.1) locate the points of zero velocity (or *water divide*).

For small thickness of the aquifer, the flow domain is considered to be a horizontal plane flow domain. Thus, flow is assumed to be occurring in xy horizontal plane and is symmetrical about the x-axis.

103
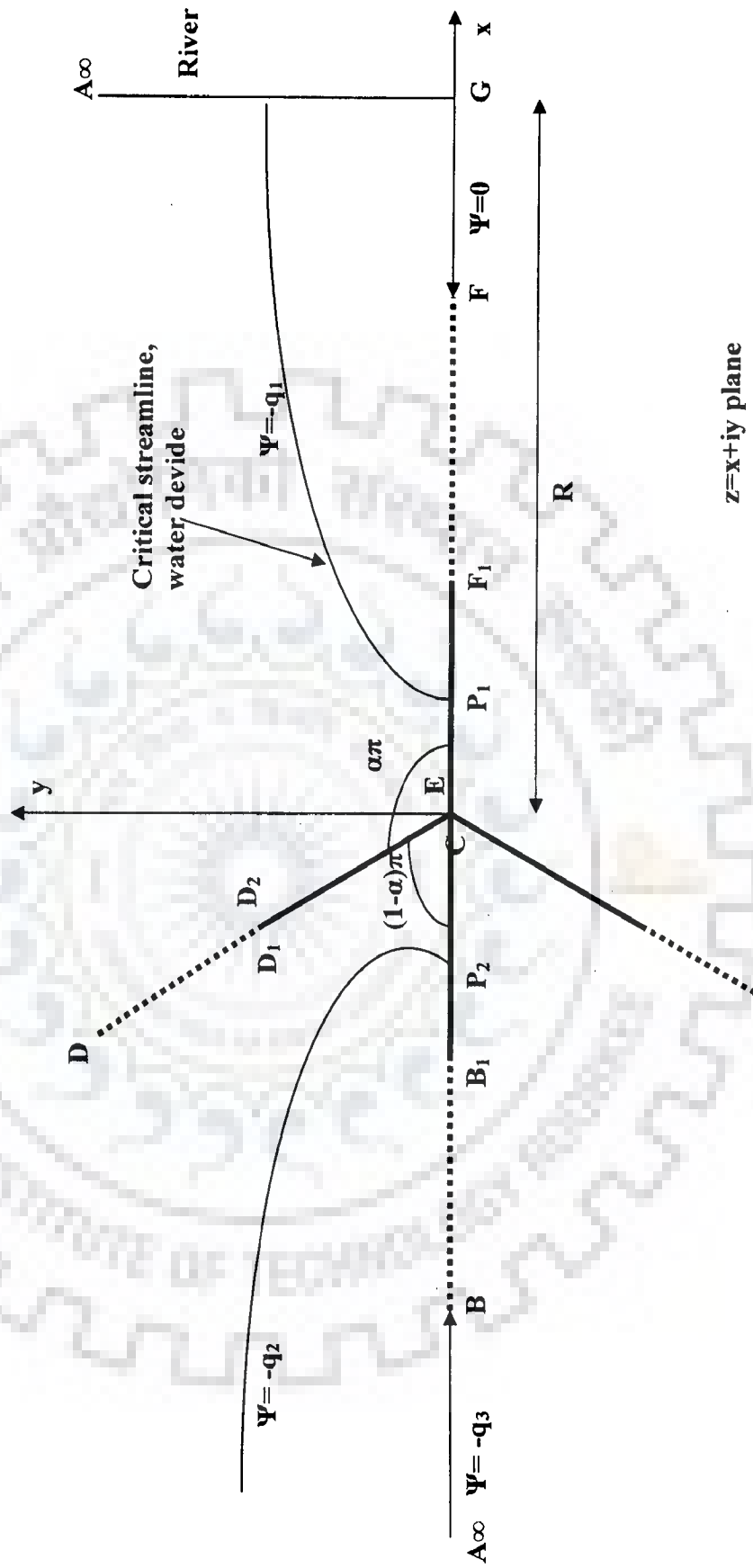
Fig. 6.1. General arrangement of laterals of a radial collector well near straight reach of a river.

104

6.3 Analytical Solution: Conformal Mapping

The Schwarz-Christoffel transformation is applicable to a simply connected polygon with straight-line boundaries having a finite number of vertices one or more of which may be at infinity. The present flow domain being symmetrical about the x-axis, half of the flow domain is considered for applying conformal mapping. Thereby, the flow domain conforms to a simple connected flow domain and gets amenable to Schwarz Christoffel conformal mapping technique. By considering symmetry in flow domain, the mapping function is considerably simplified. According to Schwarz-Christoffel-transformation, the conformal mapping of the flow domain $ABB_lCD_lDD_2EF_lFGA$ in $z(=x+iy)$ plane onto the auxiliary $t(=r+is)$ plane is given below. The auxiliary t-plane and the complex potential w-plane are shown in Fig(6.2) and Fig.(6.3), respectively.

Transformation of z(=x+iy) plane onto t(=r+is) plane

The vertices A, C, D, E, G having been mapped onto $-\infty, 0, d, 1, g$ respectively on the real axis of t plane, the mapping is given by:

$$\frac{dz}{dt} = M\frac{(d-t)}{t^\alpha(1-t)^{1-\alpha}(g-t)^{1/2}} \qquad (6.1)$$

Integrating

$$z = M\int_0^t \frac{(d-t)dt}{t^\alpha(1-t)^{1-\alpha}(g-t)^{1/2}} + N \qquad (6.2)$$

where, M and N are complex constants. For vertex C, $t=0$ and $z=0$; hence, constant $N=0$. For vertex E, $t'=1$ and $z=0$. Applying this condition one obtains

$$0 = M\int_0^1 \frac{(d-t)dt}{t^\alpha(1-t)^{1-\alpha}(g-t)^{1/2}} \qquad (6.3a)$$

105

Upper half t-plane
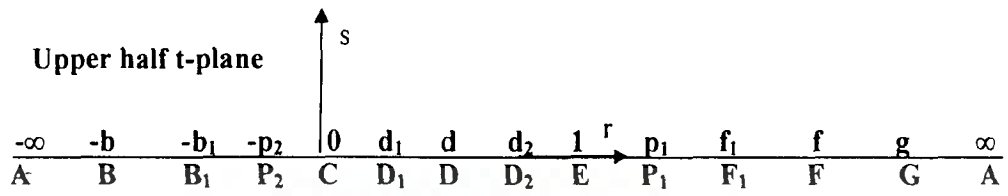
Fig.6.2 Auxiliary *t (r+is)* plane
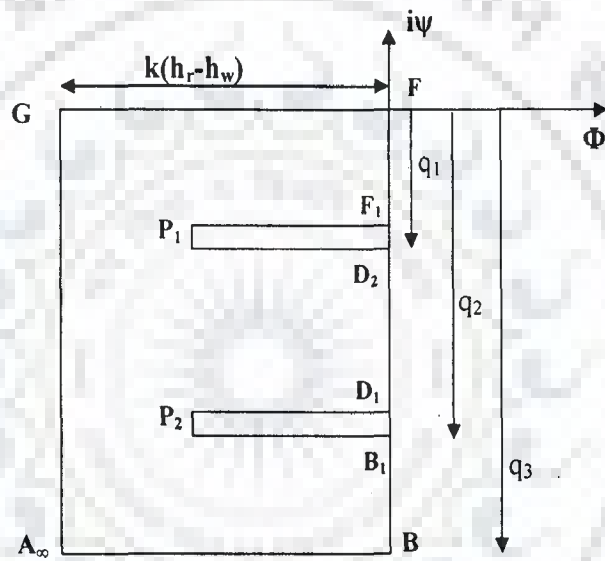
Fig. 6.3: Complex potential *(w=Φ+iψ)* plane

or

$$Md\int_0^1\frac{dt}{t^\alpha(1-t)^{1-\alpha}(g-t)^{1/2}} = M\int_0^1\frac{t\,dt}{t^\alpha(1-t)^{1-\alpha}(g-t)^{1/2}}$$ (6.3b)

Since, $M \neq 0$, therefore,

$$d = \frac{\displaystyle\int_0^1\frac{t^{1-\alpha}dt}{(1-t)^{1-\alpha}(g-t)^{1/2}}}{\displaystyle\int_0^1\frac{dt}{t^\alpha(1-t)^{1-\alpha}(g-t)^{1/2}}}$$ (6.4)

For an assumed value of parameter g, the parameter d can be computed using an iteration technique. Both integrals in the numerator and denominator of Equation (6.4) are improper integrals. The integral in the numerator is converted to a proper integral by substituting $t = 1 - v^{1/\alpha}$, where v is a dummy variable and the integral in the denominator is converted to a proper integral by splitting the integral

$\int_0^1 F(t)dt = \int_0^{1/2} F(t)dt + \int_{1/2}^1 F(t)dt$ and substituting $t = v^{1/(1-\alpha)}$ in the first and $t = 1 - v^{1/\alpha}$ in

the second integral. Thus,

$$d = \frac{\dfrac{1}{\alpha}\displaystyle\int_0^1 \frac{\left(1-v^{1/\alpha}\right)^{1-\alpha}}{\left(g-1+v^{1/\alpha}\right)^{1/2}}\,dv}{\dfrac{1}{1-\alpha}\displaystyle\int_0^{(1/2)^{1/(1-\alpha)}} \frac{dv}{\left(1-v^{1/(1-\alpha)}\right)^{1-\alpha}\left(g-v^{1/(1-\alpha)}\right)^{1/2}} + \dfrac{1}{\alpha}\displaystyle\int_0^{(1/2)^\alpha} \frac{dv}{\left(1-v^{1/\alpha}\right)^\alpha\left(g-1+v^{1/\alpha}\right)^{1/2}}}$$

(6.5)

For vertex D, $t = d$, and $z = L_2 e^{i\alpha\pi}$. Applying this condition in equation (6.2) and

incorporating a substitution $t = v^{1/(1-\alpha)}$, $dt = \dfrac{1}{1-\alpha}v^{\alpha/(1-\alpha)}$ to remove the singularity

$t = 0$, the following relation is derived.

$$_2 e^{i\alpha\pi} = M\int_0^d \frac{(d-t)dt}{t^\alpha(1-t)^{1-\alpha}(g-t)^{1/2}} = M\frac{1}{(1-\alpha)}\int_0^{d^{1-\alpha}} \frac{\left(d-v^{1/(1-\alpha)}\right)dv}{\left(1-v^{1/(1-\alpha)}\right)^{1-\alpha}\left(g-v^{1/(1-\alpha)}\right)^{1/2}}$$

(6.6)

$$1 = \frac{L_2 e^{i\pi\alpha}}{\dfrac{1}{(1-\alpha)}\displaystyle\int_0^{d^{1-\alpha}}\frac{\left(d-v^{1/(1-\alpha)}\right)dv}{\left(1-v^{1/(1-\alpha)}\right)^{1-\alpha}\left(g-v^{1/(1-\alpha)}\right)^{1/2}}}$$

(6.7)

)r point G, $t=g$ and $z = R$. Applying these in equation (6.2)

$$\zeta = M\int_1^g \frac{(d-t)dt}{t^\alpha(1-t)^{1-\alpha}(g-t)^{1/2}}$$

(6.8a)

107

Incorporating constant M from equation (6.7) in equation (6.8a)

$$R = \frac{L_2 e^{i\pi\alpha}}{\dfrac{1}{(1-\alpha)} \displaystyle\int_0^{d^{1-\alpha}} \dfrac{(d - v^{1/(1-\alpha)})dv}{(1 - v^{1/(1-\alpha)})^{1-\alpha} (g - v^{1/(1-\alpha)})^{1/2}}} \int_1^g \frac{(-1)(t-d)dt}{(-1)^{1-\alpha} t^\alpha (t-1)^{1-\alpha} (g-t)^{1/2}} \tag{6.8b}$$

Taking $-1 = e^{-i\pi}$ and simplifying equation (6.8b) reduces to

$$\frac{R}{L_2} = \frac{1}{\dfrac{1}{(1-\alpha)} \displaystyle\int_0^{d^{1-\alpha}} \dfrac{(d - v^{1/(1-\alpha)})dv}{(1 - v^{1/(1-\alpha)})^{1-\alpha} (g - v^{1/(1-\alpha)})^{1/2}}} \int_1^g \frac{(t-d)dt}{t^\alpha (t-1)^{1-\alpha} (g-t)^{1/2}} \tag{6.9}$$

The improper integral appearing in the denominator is converted to proper integral as follows:

$$\int_1^g \frac{(t-d)dt}{t^\alpha (t-1)^{1-\alpha} (g-t)^{1/2}} = \int_1^{(1+g)/2} \frac{(t-d)dt}{t^\alpha (t-1)^{1-\alpha} (g-t)^{1/2}} + \int_{(1+g)/2}^g \frac{(t-d)dt}{t^\alpha (t-1)^{1-\alpha} (g-t)^{1/2}} \tag{6.10a}$$

The singularity $t = 1$ in the first integrand is removed with a substitution $t = 1 + v^{1/\alpha}$ and the singularity $t = g$ in the second integrand is removed with a substitution $t = g - v^2$. Incorporating these, the integral (6.10a) reduces to

$$\int_1^g \frac{(t-d)dt}{t^\alpha (t-1)^{1-\alpha} (g-t)^{1/2}}$$

$$= \frac{1}{\alpha} \int_0^{\{(g-1)/2\}^\alpha} \frac{(1 + v^{1/\alpha} - d)dv}{(1 + v^{1/\alpha})^\alpha (g - 1 - v^{1/\alpha})^{1/2}} + 2 \int_0^{\{(g-1)/2\}^{1/2}} \frac{(g - d - v^2)dv}{(g - v^2)^\alpha (g - v^2 - 1)^{1-\alpha}} = I_{EG} \tag{6.10b}$$

Incorporating equation (6.10b) in equation (6.9)

$$\frac{R}{L_2} = \frac{I_{EG}}{\dfrac{1}{(1-\alpha)} \displaystyle\int_0^{d^{(1-\alpha)}} \dfrac{(d - v^{1/(1-\alpha)})dv}{(1 - v^{1/(1-\alpha)})^{1-\alpha} (g - v^{1/(1-\alpha)})^{1/2}}} \tag{6.11}$$

The parameters d and g corresponding to known R/L_2 are found using an iteration procedure. Assuming g, d is computed using equation (6.5). For this set of d and g computed R/L_2 is compared with the true value of R/L_2 and the procedure is repeated till desired accuracy is achieved. Using the iterated values of g and d, the modulus of constant M is evaluated from Eq.(6.7).

The others parameters b, b_1, d_1, d_2, f_1, and f on t-plane are computed from the geometry of the flow domain considering the correspondence between z and t planes as follows:

From equation (6.8a) the constant M is also given by

$$M = -\frac{(-1)^{(1-\alpha)} R}{\int_1^g \frac{(t-d)dt}{t^\alpha (t-1)^{1-\alpha} (g-t)^{1/2}}} = -\frac{(-1)^{(1-\alpha)} R}{I_{EG}} \tag{6.12}$$

Incorporating Eq.(6.12) in Eq.(6.2)

$$z = -\frac{(-1)^{(1-\alpha)} R}{I_{EG}} \int_0^t \frac{(d-t)dt}{t^\alpha (1-t)^{1-\alpha} (g-t)^{1/2}} \tag{6.13}$$

For point B, $z = -L_3$ and $t' = -b$. Applying this condition in above equation

$$-L_3 = -\frac{(-1)^{(1-\alpha)} R}{I_{EG}} \int_0^{-b} \frac{(d-t)dt}{t^\alpha (1-t)^{1-\alpha} (g-t)^{1/2}} = -\frac{(-1)^{(1-\alpha)} R}{I_{EG}} \int_0^{-b} \frac{(-1)^\alpha (d-t)dt}{(-t)^\alpha (1-t)^{1-\alpha} (g-t)^{1/2}}$$

$$\tag{6.14a}$$

Substituting $t = -v$, $dt = -dv$ for evaluating the integral in the numerator, and simplifying one finds $\dfrac{L_3}{R} = \dfrac{\displaystyle\int_0^b \frac{(d+v)dv}{v^\alpha (1+v)^{1-\alpha} (g+v)^{1/2}}}{I_{EG}}$ \hfill (6.14b)

The singularity $v=0$ in the integrand in the numerator is removed by

substituting $v = X^{1/(1-\alpha)}$, and $dv = \dfrac{1}{1-\alpha} X^{\frac{\alpha}{1+\alpha}}$, where X is a dummy variable.

Performing the substitution, Eq.(6.14b) is reduced to

$$\frac{L_3}{R} = \frac{\dfrac{1}{1-\alpha} \displaystyle\int_0^{b^{(1-\alpha)}} \dfrac{\left(d + X^{1/(1-\alpha)}\right)dX}{\left(1 + X^{1/(1-\alpha)}\right)^{1-\alpha}\left(g + X^{1/(1-\alpha)}\right)^{1/2}}}{I_{EG}}$$ (6.14c)

Similarly

$$\frac{L_{3b}}{R} = \frac{\displaystyle\int_0^{b_1} \dfrac{(d+v)dv}{v^\alpha (1+v)^{1-\alpha}(g+v)^{1/2}}}{I_{EG}}$$

$$= \frac{\dfrac{1}{1-\alpha} \displaystyle\int_0^{b_1^{(1-\alpha)}} \dfrac{\left(d + X^{1/(1-\alpha)}\right)dX}{\left(1 + X^{1/(1-\alpha)}\right)^{1-\alpha}\left(g + X^{1/(1-\alpha)}\right)^{1/2}}}{I_{EG}}$$ (6.15)

For point D_1, $t = d_1, z = L_{2b}e^{i\pi\alpha}$. Applying this condition in equation (6.13)

$$\frac{L_{2b}e^{i\pi\alpha}}{R} = -\frac{(-1)^{(1-\alpha)}}{I_{EG}}\int_0^{d_1} \frac{(d-t)dt}{t^\alpha (1-t)^{1-\alpha}(g-t)^{1/2}}$$ (6.16a)

Substituting $-1 = e^{-i\pi}$ in above equation and simplifying one finds

$$\frac{L_{2b}}{R} = \frac{1}{I_{EG}}\int_0^{d_1} \frac{(d-t)dt}{t^\alpha (1-t)^{1-\alpha}(g-t)^{1/2}}$$

$$= \frac{\dfrac{1}{1-\alpha} \displaystyle\int_0^{d_1^{(1-\alpha)}} \dfrac{\left(d - v^{1/(1-\alpha)}\right)dv}{\left(1 - v^{1/(1-\alpha)}\right)^{1-\alpha}\left(g - v^{1/(1-\alpha)}\right)^{1/2}}}{I_{EG}}$$ (6.16b)

For point $F_1, t = f_1, z = L_{1b}$. Applying this condition in equation (6.13)

110

$$\frac{L_{1b}}{R} = -\frac{(-1)^{(1-\alpha)}}{I_{EG}} \int_1^{f_1} \frac{(d-t)dt}{t^\alpha (1-t)^{1-\alpha}(g-t)^{1/2}}$$

(6.17a)

After simplification equation (6.17a) reduces to

$$\frac{L_{1b}}{R} = \frac{1}{I_{EG}} \int_1^{f_1} \frac{(t-d)dt}{t^\alpha (t-1)^{1-\alpha}(g-t)^{1/2}}$$

$$= \frac{\dfrac{1}{\alpha} \displaystyle\int_0^{(f_1-1)^\alpha} \frac{\left(1-d+v^{1/\alpha}\right)dv}{\left(1+v^{1/\alpha}\right)^\alpha \left(g-1-v^{1/\alpha}\right)^{1/2}}}{I_{EG}}$$

(6.17b)

For point F, $t = f; z = L_1$. Applying this condition in equation (6.13), and after simplification one gets

$$\frac{L_1}{R} = \frac{\dfrac{1}{\alpha} \displaystyle\int_0^{(f-1)^\alpha} \frac{\left(1-d+v^{1/\alpha}\right)dv}{\left(1+v^{1/\alpha}\right)^\alpha \left(g-1-v^{1/\alpha}\right)^{1/2}}}{I_{EG}}$$

(6.18)

Transformation of w- plane onto t-plane

The conformal transformation of the complex potential plane shown in Fig.(6.2) onto the auxiliary t-plane is given by:

$$\frac{dw}{dt} = M_1 \frac{(t-p_1)(t+p_2)}{\sqrt{(t+b)(t+b_1)(t-d_1)(t-d_2)(t-f)(t-f_1)(g-t)}}$$

(6.19)

Integrating

$$w = M_1 \int_f^t \frac{(t-p_1)(t+p_2)dt}{\sqrt{(t+b)(t+b_1)(t-d_1)(t-d_2)(t-f_1)(t-f)(g-t)}} + N_1$$

(6.20)

The constant N_1 is equal to the complex potential at lower limit of integration. For $t = f$ $w = 0$. Hence, in equation (6.20), $N_1 = 0$. It is different if another lower limit is chosen. Considering consecutive vertices in w plane and their corresponding

111

$$\frac{L_{1b}}{R} = -\frac{(-1)^{(1-\alpha)}}{I_{EG}} \int_{1}^{f_1} \frac{(d-t)dt}{t^{\alpha}(1-t)^{1-\alpha}(g-t)^{1/2}}$$ (6.17a)

After simplification equation (6.17a) reduces to

$$\frac{L_{1b}}{R} = \frac{1}{I_{EG}} \int_{1}^{f_1} \frac{(t-d)dt}{t^{\alpha}(t-1)^{1-\alpha}(g-t)^{1/2}}$$

$$= \frac{\frac{1}{\alpha} \int_{0}^{(f_1-1)^{\alpha}} \frac{(1-d+v^{1/\alpha})dv}{(1+v^{1/\alpha})^{\alpha}(g-1-v^{1/\alpha})^{1/2}}}{I_{EG}}$$ (6.17b)

For point F, $t = f; z = L_1$. Applying this condition in equation (6.13), and after simplification one gets

$$\frac{L_1}{R} = \frac{\frac{1}{\alpha} \int_{0}^{(f-1)^{\alpha}} \frac{(1-d+v^{1/\alpha})dv}{(1+v^{1/\alpha})^{\alpha}(g-1-v^{1/\alpha})^{1/2}}}{I_{EG}}$$ (6.18)

Transformation of w- plane onto t-plane

The conformal transformation of the complex potential plane shown in Fig.(6.2) onto the auxiliary t-plane is given by:

$$\frac{dw}{dt} = M_1 \frac{(t-p_1)(t+p_2)}{\sqrt{(t+b)(t+b_1)(t-d_1)(t-d_2)(t-f)(t-f_1)(g-t)}}$$ (6.19)

Integrating

$$w = M_1 \int_{f}^{t} \frac{(t-p_1)(t+p_2)dt}{\sqrt{(t+b)(t+b_1)(t-d_1)(t-d_2)(t-f_1)(t-f)(g-t)}} + N_1$$ (6.20)

The constant N_1 is equal to the complex potential at lower limit of integration. For $t = f$ $w = 0$. Hence, in equation (6.20), $N_1 = 0$. It is different if another lower limit is chosen. Considering consecutive vertices in w plane and their corresponding

111

locations in t plane, the following relationships are obtained. At vertex G, $t = g$ and $w = -k(h_r - h_w)$. Using this, one finds

$$M_1 = \frac{-kT(h_r - h_w)}{I_{FG}} \tag{6.21}$$

where, $I_{FG} = \int\limits_{f}^{g} \dfrac{(t-p_1)(t+p_2)dt}{\sqrt{(t+b)(t+b_1)(t-d_1)(t-d_2)(t-f_1)(t-f)(g-t)}}$

The integral I_{FG} is evaluated numerically after removing the singularities as described below. The singularities are $t = f$ and $t = g$. Splitting the integral into two parts, one can write

$$I_{FG} = \int\limits_{f}^{(f+g)/2} \frac{(t-p_1)(t+p_2)dt}{\sqrt{(t+b)(t+b_1)(t-d_1)(t-d_2)(t-f_1)(t-f)(g-t)}}$$

$$+ \int\limits_{(f+g)/2}^{g} \frac{(t-p_1)(t+p_2)dt}{\sqrt{(t+b)(t+b_1)(t-d_1)(t-d_2)(t-f_1)(t-f)(g-t)}}$$

Using substitutions $t - f = v^2; dt = 2vdv$ in the first integrand, and $g - t = v^2$; $dt = -2vdv$ in the second integrand, the singularities are removed. Thus,

$$I_{FG} =$$

$$\int\limits_{0}^{\{(g-f)/2\}^{1/2}} \frac{2(f-p_1+v^2)(f+p_2+v^2)dv}{\sqrt{(f+b+v^2)(f+b_1+v^2)(f-d_1+v^2)(f-d_2+v^2)(f-f_1+v^2)(g-f-v^2)}}$$

$$+ \int\limits_{0}^{\{(g-f)/2\}^{1/2}} \frac{2(g-p_1-v^2)(g+p_2-v^2)dv}{\sqrt{(g+b-v^2)(g+b_1-v^2)(g-d_1-v^2)(g-d_2-v^2)(g-f_1-v^2)(g-f-v^2)}}$$

Similar procedure (splitting the integration into two parts and applying suitable substitution for each part) is adopted for numerical integration of similar improper integral.

Considering the vertices F_1 and F, one finds

$$w_F = M_1 \int_{f_1}^{f} \frac{(t - p_1)(t + p_2)\,dt}{\sqrt{(t+b)(t+b_1)(t-d_1)(t-d_2)(t-f_1)(t-f)(g-t)}} + w_{F_1}$$

(6.22a)

where w_F and w_{F_1} are the complex potentials at vertices F and F_1 respectively.

After simplification, equation (6.22a) reduces to

$$\frac{q_1}{kT(h_r - h_w)} = \frac{I_{F_1 F}}{I_{FG}}$$

(6.22b)

where

$$I_{F_1 F} = \int_{f_1}^{f} \frac{(t - p_1)(t + p_2)\,dt}{\sqrt{(t+b)(t+b_1)(t-d_1)(t-d_2)(t-f_1)(f-t)(g-t)}}$$

Considering vertices D_2 and F_1

$$w_{F_1} = M_1 \int_{d_2}^{f_1} \frac{(t - p_1)(t + p_2)\,dt}{\sqrt{(t+b)(t+b_1)(t-d_1)(t-d_2)(t-f_1)(t-f)(g-t)}} + w_{D_2}$$

(6.23a)

w_{D_2} is complex potential at vertex D_2. Since, $w_{F_1} = w_{D_2}$, therefore,

$$\int_{d_2}^{f_1} \frac{(t - p_1)(t + p_2)\,dt}{\sqrt{(t+b)(t+b_1)(t-d_1)(t-d_2)(f_1-t)(f-t)(g-t)}} = 0$$

(6.24a)

or

$$\int_{d_2}^{p_1} \frac{(t - p_1)(t + p_2)\,dt}{\sqrt{(t+b)(t+b_1)(t-d_1)(t-d_2)(f_1-t)(f-t)(g-t)}}$$

$$+ \int_{p_1}^{f_1} \frac{(t - p_1)(t + p_2)\,dt}{\sqrt{(t+b)(t+b_1)(t-d_1)(t-d_2)(f_1-t)(f-t)(g-t)}} = 0$$

(6.24b)

or

113

$$\int_{d_2}^{p_1} \frac{(p_1 - t)(t + p_2)dt}{\sqrt{(t+b)(t+b_1)(t-d_1)(t-d_2)(f_1 - t)(f - t)(g - t)}}$$

$$= \int_{p_1}^{f_1} \frac{(t - p_1)(t + p_2)dt}{\sqrt{(t+b)(t+b_1)(t-d_1)(t-d_2)(f_1 - t)(f - t)(g - t)}} \tag{6.24c}$$

Considering vertices D_1 and D_2

$$w_{D_2} = M_1 \int_{d_1}^{d_2} \frac{(t - p_1)(t + p_2)dt}{\sqrt{(t+b)(t+b_1)(t-d_1)(t-d_2)(t-f_1)(t-f)(g - t)}} + w_{D_1} \tag{6.25a}$$

w_{D_1} is the complex potential at vertex D_1.

Simplifying equation (6.25a) reduces to

$$\frac{(q_2 - q_1)}{kT(h_r - h_w)} = \frac{\displaystyle\int_{d_1}^{d_2} \frac{(p_1 - t)(t + p_2)dt}{\sqrt{(t+b)(t+b_1)(t-d_1)(d_2 - t)(f_1 - t)(f - t)(g - t)}}}{I_{FG}} \tag{6.25b}$$

Considering vertices B_1 and D_1

$$w_{D_1} = M_1 \int_{-b_1}^{d_1} \frac{(t - p_1)(t + p_2)dt}{\sqrt{(t+b)(t+b_1)(t-d_1)(t-d_2)(t-f_1)(t-f)(g - t)}} + w_{B_1} \tag{6.26}$$

w_{B_1} is complex potential at vertex B_1. Since, $w_{B_1} = w_{D_1}$, therefore,

$$\int_{-b_1}^{d_1} \frac{(t - p_1)(t + p_2)dt}{\sqrt{(t+b)(t+b_1)(t-d_1)(t-d_2)(t-f_1)(t-f)(g - t)}} = 0 \tag{6.27a}$$

or

$$\int_{-b_1}^{-p_2} \frac{(t - p_1)(t + p_2)dt}{\sqrt{(t+b)(t+b_1)(t-d_1)(t-d_2)(f_1 - t)(f - t)(g - t)}}$$

$$+ \int_{-p_2}^{d_1} \frac{(t - p_1)(t + p_2)dt}{\sqrt{(t+b)(t+b_1)(t-d_1)(t-d_2)(f_1 - t)(f - t)(g - t)}} = 0 \tag{6.27b}$$

or

114

$$\int_{-b_1}^{-p_2} \frac{(p_1 - t)(t + p_2)dt}{\sqrt{(t+b)(t+b_1)(d_1-t)(d_2-t)(f_1-t)(f-t)(g-t)}}$$

$$= \int_{-p_2}^{d_1} \frac{(p_1 - t)(t + p_2)dt}{\sqrt{(t+b)(t+b_1)(d_1-t)(d_2-t)(f_1-t)(f-t)(g-t)}} = 0 \qquad (6.27c)$$

Considering vertices B and B_1

$$w_{B_1} = M_1 \int_{-b}^{-b_1} \frac{(t - p_1)(t + p_2)dt}{\sqrt{(t+b)(t+b_1)(t-d_1)(t-d_2)(t-f_1)(t-f)(g-t)}} + w_B \qquad (6.28)$$

w_B is the complex potential at vertex B. Simplifying, equation (6.28) reduces to

$$\frac{(q_3 - q_2)}{kT(h_r - h_w)} = \frac{\int_{-b}^{-b_1} \frac{(p_1 - t)(t + p_2)dt}{\sqrt{(t+b)(t+b_1)(d_1-t)(d_2-t)(f_1-t)(f-t)(g-t)}}}{I_{FG}} \qquad (6.29)$$

The parameters $b, b_1, d_1, d, d_2, f_1, f$ and g are found from the geometry of the flow domain. The parameters p_1 and p_2 are determined from equations (6.24c) and (6.27c) using Newton Raphson technique as follows.

Let functions $F_1(p_1, p_2)$ and $F_2(p_1, p_2)$ be defined as:

$$F_1(p_1, p_2) = \int_{d_2}^{p_1} \frac{(p_1 - t)(t + p_2)dt}{\sqrt{(t+b)(t+b_1)(t-d_1)(t-d_2)(f_1-t)(f-t)(g-t)}}$$

$$- \int_{p_1}^{f_1} \frac{(t - p_1)(t + p_2)dt}{\sqrt{(t+b)(t+b_1)(t-d_1)(t-d_2)(f_1-t)(f-t)(g-t)}} \qquad (6.30)$$

$$F_2(p_1, p_2) = \int_{-b_1}^{-p_2} \frac{(p_1 - t)(t + p_2)dt}{\sqrt{(t+b)(t+b_1)(d_1-t)(d_2-t)(f_1-t)(f-t)(g-t)}}$$

$$- \int_{-p_2}^{d_1} \frac{(p_1 - t)(t + p_2)dt}{\sqrt{(t+b)(t+b_1)(d_1-t)(d_2-t)(f_1-t)(f-t)(g-t)}} \qquad (6.31)$$

Let p_1^*, p_2^* be in the neighbor hood of the true solution. Then applying Taylor series expansion and neglecting higher order terms

$$F_1\left(p_1^{\bullet}, p_2^{\bullet}\right) + \frac{\partial F_1\left(p_1^{\bullet}, p_2^{\bullet}\right)}{\partial p_1}\Delta p_1 + \frac{\partial F_1\left(p_1^{\bullet}, p_2^{\bullet}\right)}{\partial p_2}\Delta p_2 = 0 \tag{6.32}$$

$$F_2\left(p_1^{\bullet}, p_2^{\bullet}\right) + \frac{\partial F_2\left(p_1^{\bullet}, p_2^{\bullet}\right)}{\partial p_1}\Delta p_1 + \frac{\partial F_2\left(p_1^{\bullet}, p_2^{\bullet}\right)}{\partial p_2}\Delta p_2 = 0 \tag{6.33}$$

In matrix notation equations (6.32) and (6.33) are written as:

$$\begin{bmatrix} \dfrac{\partial F_1}{\partial p_1} & \dfrac{\partial F_1}{\partial p_2} \\ \dfrac{\partial F_2}{\partial p_1} & \dfrac{\partial F_2}{\partial p_2} \end{bmatrix}_{p_1^*,p_2^*} \bullet \begin{bmatrix} \Delta p_1 \\ \Delta p_2 \end{bmatrix} = \begin{bmatrix} -F_1\left(p_1^*, p_2^*\right) \\ -F_2\left(p_1^*, p_2^*\right) \end{bmatrix} \tag{6.34}$$

The partial differentials appearing as elements of the Jacobian matrix are found numerically as follows:

$$\frac{\partial F_1\left(p_1^{\bullet}, p_2^{\bullet}\right)}{\partial p_1} = \left\{ \left[\int_{d_2}^{p_1^{\bullet}+\varepsilon} \frac{\left(p_1^{\bullet}+\varepsilon-t\right)\left(t+p_2^{\bullet}\right)dt}{\sqrt{(t+b)(t+b_1)(t-d_1)(t-d_2)(f_1-t)(f-t)(g-t)}} \right.\right.$$
$$\left. - \int_{p_1^{\bullet}+\varepsilon}^{f_1} \frac{\left(t-p_1^{\bullet}-\varepsilon\right)\left(t+p_2^{\bullet}\right)dt}{\sqrt{(t+b)(t+b_1)(t-d_1)(t-d_2)(f_1-t)(f-t)(g-t)}} \right] -$$
$$\left[\int_{d_2}^{p_1^{\bullet}} \frac{\left(p_1^{\bullet}-t\right)\left(t+p_2^{\bullet}\right)dt}{\sqrt{(t+b)(t+b_1)(t-d_1)(t-d_2)(f_1-t)(f-t)(g-t)}} \right.$$
$$\left.\left. - \int_{p_1^{\bullet}}^{f_1} \frac{\left(t-p_1^{\bullet}\right)\left(t+p_2^{\bullet}\right)dt}{\sqrt{(t+b)(t+b_1)(t-d_1)(t-d_2)(f_1-t)(f-t)(g-t)}} \right] \right\}/\varepsilon$$

$$\tag{6.35}$$

where ε is a very small positive number.

$$\frac{\partial F_1\left(p_1^{\bullet}, p_2^{\bullet}\right)}{\partial p_2} = \left\{ \left[\int_{d_2}^{p_1^{\bullet}} \frac{\left(p_1^{\bullet}-t\right)\left(t+p_2^{\bullet}+\varepsilon\right)dt}{\sqrt{(t+b)(t+b_1)(t-d_1)(t-d_2)(f_1-t)(f-t)(g-t)}} \right.\right.$$
$$\left. - \int_{p_1^{\bullet}}^{f_1} \frac{\left(t-p_1^{\bullet}\right)\left(t+p_2^{\bullet}+\varepsilon\right)dt}{\sqrt{(t+b)(t+b_1)(t-d_1)(t-d_2)(f_1-t)(f-t)(g-t)}} \right] -$$
$$\left[\int_{d_2}^{p_1^{\bullet}} \frac{\left(p_1^{\bullet}-t\right)\left(t+p_2^{\bullet}\right)dt}{\sqrt{(t+b)(t+b_1)(t-d_1)(t-d_2)(f_1-t)(f-t)(g-t)}} \right.$$

$$-\int_{p_1^*}^{f_1} \frac{(t-p_1^*)(t+p_2^*)dt}{\sqrt{(t+b)(t+b_1)(t-d_1)(t-d_2)(f_1-t)(f-t)(g-t)}} \ ] \ \}/\varepsilon$$

<div align="right">(6.36)</div>

$$\frac{\partial F_2(p_1^*, p_2^*)}{\partial p_1} = \{ \ [\ \int_{-b_1}^{-p_2^*} \frac{(p_1^* + \varepsilon - t)(t+p_2^*)dt}{\sqrt{(t+b)(t+b_1)(d_1-t)(d_2-t)(f_1-t)(f-t)(g-t)}}$$

$$-\int_{-p_2}^{d_1} \frac{(p_1^* + \varepsilon - t)(t+p_2)dt}{\sqrt{(t+b)(t+b_1)(d_1-t)(d_2-t)(f_1-t)(f-t)(g-t)}} \ ] \ -$$

$$[\ \int_{-b_1}^{-p_2^*} \frac{(p_1^* - t)(t+p_2^*)dt}{\sqrt{(t+b)(t+b_1)(d_1-t)(d_2-t)(f_1-t)(f-t)(g-t)}} \ -$$

$$\int_{-p_2}^{d_1} \frac{(p_1^* - t)(t+p_2)dt}{\sqrt{(t+b)(t+b_1)(d_1-t)(d_2-t)(f_1-t)(f-t)(g-t)}} \ ] \ \}/\varepsilon$$

<div align="right">(6.37)</div>

$$\frac{\partial F_2(p_1^*, p_2^*)}{\partial p_2} = \{ \ [\ \int_{-b_1}^{-p_2^* - \varepsilon} \frac{(p_1^* - t)(t+p_2^* + \varepsilon)dt}{\sqrt{(t+b)(t+b_1)(d_1-t)(d_2-t)(f_1-t)(f-t)(g-t)}}$$

$$-\int_{-p_2 - \varepsilon}^{d_1} \frac{(p_1^* - t)(t+p_2 + \varepsilon)dt}{\sqrt{(t+b)(t+b_1)(d_1-t)(d_2-t)(f_1-t)(f-t)(g-t)}} \ ] \ -$$

$$[\ \int_{-b_1}^{-p_2^*} \frac{(p_1^* - t)(t+p_2^*)dt}{\sqrt{(t+b)(t+b_1)(d_1-t)(d_2-t)(f_1-t)(f-t)(g-t)}} \ -$$

$$\int_{-p_2}^{d_1} \frac{(p_1^* - t)(t+p_2)dt}{\sqrt{(t+b)(t+b_1)(d_1-t)(d_2-t)(f_1-t)(f-t)(g-t)}} \ ] \ \}/\varepsilon$$

<div align="right">(6.38)</div>

Assuming a set of p_1^*, p_2^*, the elements of the Jocobian matrix and right hand column

matrix are computed. Using matrix inversion technique, the unknowns in equation

(6.34) are solved, which are given by:

$$\begin{bmatrix} \Delta p_1 \\ \Delta p_2 \end{bmatrix} = \begin{bmatrix} \dfrac{\partial F_1}{\partial p_1} & \dfrac{\partial F_1}{\partial p_2} \\ \dfrac{\partial F_2}{\partial p_1} & \dfrac{\partial F_2}{\partial p_2} \end{bmatrix}_{p_1^*,p_2^*}^{-1} \bullet \begin{bmatrix} -F_1\left(p_1^*, p_2^*\right) \\ -F_2\left(p_1^*, p_2^*\right) \end{bmatrix} \tag{6.39}$$

The old set p_1^* and p_2^* is replaced by a new set $p_1^* + \Delta p_1$ and $p_2^* + \Delta p_2$, and this procedure is repeated till desired accuracy is achieved. Once p_1 and p_2 are determined the flow to different collector pipes are computed using Eqs.(6.22b), (6.25b) and (6.29). Flow through lateral 1 orienting towards riverside, Q_1, is equal to $2q_1$. Flow through 2nd lateral, Q_2, is $(q_2 - q_1)$. Flow through third lateral oriented towards landside, Q_3, is $2(q_3 - q_2)$. The total flow to the collector well system, Q, is given by:

$$Q = Q_1 + 2Q_2 + Q_3 = 2q_1 + 2(q_2 - q_1) + 2(q_3 - q_2) \tag{6.40}$$

Minimum Travel Time

The travel time is minimum for the river water that follows the path line *FG*. The Darcy velocity is given by:

$$u - iv = \frac{1}{T}\frac{dw}{dz} = \frac{1}{T}\frac{dw}{dt} \cdot \frac{dt}{dz} \tag{6.41}$$

Incorporating $\dfrac{dw}{dt}$ from equation (6.19), M_1 from (6.21), $\dfrac{dt}{dz}$ from equation (6.1), and M from (6.12) in equation (6.41)

$$\frac{1}{T}\frac{dw}{dz} = u - iv = \frac{1}{T}\left[\frac{-kT(h_r - h_w)}{I_{FG}} \frac{(t - p_1)(t + p_2)}{\sqrt{(t + b)(t + b_1)(t - d_1)(t - d_2)(t - f)(t - f_1)(g - t)}} \right] \times$$

$$\left[\frac{-I_{EG}}{(-1)^{(1-\alpha)}R\dfrac{(d-t)}{t^{\alpha}(1-t)^{1-\alpha}(g-t)^{1/2}}}\right] \qquad (6.42)$$

Along path F_1G, the velocity in y direction is zero and the velocity u along x direction is given by:

$$u = \left[\frac{-k(h_r-h_w)}{I_{FG}}\right]\left[\frac{I_{EG}}{R}\right]\frac{(t-p_1)(t+p_2)t^{\alpha}(t-1)^{1-\alpha}}{(t-d)\sqrt{(t+b)(t+b_1)(t-d_1)(t-d_2)(t-f)(t-f_1)}}$$

The travel time, τ, is given by

$$\tau = \int_R^{l_1}\frac{dx}{(u/S)} = \left[\frac{-RS}{k(h_r-h_w)}\right]\left[\frac{I_{FG}}{I_{EG}}\right]\int_R^{L_1}\frac{(t-d)\sqrt{(t+b)(t+b_1)(t-d_1)(t-d_2)(t-f)(t-f_1)}}{(t-p_1)(t+p_2)t^{\alpha}(t-1)^{1-\alpha}}dx$$
$$(6.43)$$

Substituting $X = x/R$, $dx = RdX$ in equation (6.43), the dimensionless time factor, ς, is

$$\varsigma = \frac{\tau k(h_r-h_w)}{SR^2} = \left[\frac{I_{FG}}{I_{EG}}\right]\int_{(L_1/R)+\varepsilon}^{1}\frac{(t-d)\sqrt{(t+b)(t+b_1)(t-d_1)(t-d_2)(t-f)(t-f_1)}}{(t-p_1)(t+p_2)t^{\alpha}(t-1)^{1-\alpha}}dX$$

$$(6.44)$$

where, $\varepsilon = $ a very small number. Along FG, z/R $(= x/R)$ is a function of t $(= f(t))$ as depicted by equation (6.12). Alternately t is an inverse function of x/R, that is

$$t = f^{-1}(x/R) = f^{-1}(X) \qquad (6.45)$$

The integrand $\dfrac{(t-d)\sqrt{(t+b)(t+b_1)(t-d_1)(t-d_2)(t-f)(t-f_1)}}{(t-p_1)(t+p_2)t^{\alpha}(t-1)^{1-\alpha}}$ is a function t. Let it

be designated as $F(t)$, which is equal to $F\left[f^{-1}(X)\right]$. Thus, the integral

$$\int_{L_1/R}^{1} F(t)dX = \int_{L_1/R}^{1} F(f^{-1}(X))dX \tag{6.46}$$

The integral in equation (6.44) is determined as follows.

(1) In equation (6.46), at the lower limit of integration $X = L_1/R$, $t = f$ and at the

upper limit of integration $X = 1$, $t = g$.

(2) Divide $(g - f)$ into N equal parts.

(3) Select $t_i = f + \dfrac{(g-f)}{N} i$, $i = 1,2,3 \cdots N - 1$

(4) Compute $F(t_i)$, $i = 1,2,3 \cdots N - 1$

(5) Find the corresponding $X(i)$ using the relation

$$X(i) = \frac{1}{I_{EG}} \int_{1}^{t_i} \frac{(t-d)dt}{t^{\alpha}(t-1)^{1-\alpha}(g-t)^{1/2}} = \frac{1}{I_{EG}\alpha} \int_{0}^{(t_i-1)^{\alpha}} \frac{(1-d+v^{1/\alpha})dv}{(1+v^{1/\alpha})^{\alpha}(g-1-v^{1/\alpha})^{1/2}}$$

(6) Draw a graph of $F(t_i)$ versus $X(i)$ and find the area under the graph from

$X = (L_1/R) + \varepsilon$ to $X = 1$.

Entrance Velocity

The average entrance velocity through the screen section of the individual lateral is

estimated as: For example, the average entrance velocity to lateral EF is

$$V_e = \frac{Q_1 k \ (h_r - h_w) T \ C_f}{2\pi r_w \ (L_1 - L_{1b})P} \tag{6.47}$$

where, C_f is the correction factor applied due to the partial penetration of the laterals

into the aquifer of thickness, T and the percentage of perforation, P. Similarly,

entrance velocity for other laterals are estimated separately as done above for lateral

EF.

Particular Cases

From the generalized solution presented above results for the following particular cases can be obtained provided the flow domain is symmetrical about x axis.

Case 1:

The laterals are fully screened i.e., $L_{1b} = L_{2b} = L_{3b} = 0$. For such case $b_1 = 0; p_2 = 0; d_1 = 0; d_2 = 1; p_1 = 1; f_1 = 1$ as points B_1, P_2 and D_1 merge with vertex C and .points D_2, P_1 and F_1 merge with vertex E. Vertices E and C do not take part in transformation of w plane to t plane. Transformation of w plane to t plane is given by

$$\frac{dw}{dt} = M_1 \frac{1}{\sqrt{(t+b(t-f)(g-t)}}$$ (6.48)

Mishra and Kansal(2007) have given solution for this particular case. The flow to the collector well system is given by:

$$2q_3 = Q = 2kT(h_r - h_w)\frac{F(\pi/2, \sqrt{(f+b)/(g+b)})}{F(\pi/2, \sqrt{(g-f)/(g+b)})}$$ (6.49)

Case 2: The case of three laterals

Case 2.1

The lateral aligned perpendicular towards the river (EF) is absent. Such case may arise if the collector valve is closed during period of flood or for any other reason. In that case,

points F, F_1, P_1 merge with E as the $L_1 = 0$. The parameters f, f_1, p_1 merge to 1. The mapping of z plane onto t plane remains the same. The step of mapping is shown in Fig.6.4. The corresponding complex potential plane is shown in Fig 6.4(c). The mapping of w plane to t plane is modified as:

121

$$\frac{dw}{dt} = M_1 \frac{(t+p_2)}{\sqrt{(t+b)(t+b_1)(t-d_1)(t-d_2)(g-t)}} \tag{6.50}$$

$$I_{D_2 G} = \int_{d_2}^{g} \frac{(t+p_2)dt}{\sqrt{(t+b)(t+b_1)(t-d_1)(t-d_2)(g-t)}} \tag{6.51}$$

$$M_1 = \frac{-kT(h_r - h_w)}{I_{D_2 G}} \tag{6.52}$$

$$\frac{(q_2)}{kT(h_r - h_w)} = \frac{\displaystyle\int_{d_1}^{d_2} \frac{(t+p_2)dt}{\sqrt{(t+b)(t+b_1)(t-d_1)(d_2-t)(g-t)}}}{I_{D_2 G}} \tag{6.53}$$

$$\frac{(q_3 - q_2)}{kT(h_r - h_w)} = \frac{\displaystyle\int_{-b}^{-b_1} \frac{(t+p_2)dt}{\sqrt{(t+b)(t+b_1)(d_1-t)(d_2-t)(g-t)}}}{I_{D_2 G}} \tag{6.54}$$

$$F_2(p_2) = \int_{-b_1}^{-p_2} \frac{(t+p_2)dt}{\sqrt{(t+b)(t+b_1)(d_1-t)(d_2-t)(g-t)}}$$

$$- \int_{-p_2}^{d_1} \frac{(t+p_2)dt}{\sqrt{(t+b)(t+b_1)(d_1-t)(d_2-t)(g-t)}} \tag{6.55}$$

$$\frac{dF_2(p_2^{\bullet})}{dp_2} = \Big\{ \Big[\int_{-b_1}^{-p_1^{\bullet}-\varepsilon} \frac{(t+p_2^{\bullet}+\varepsilon)dt}{\sqrt{(t+b)(t+b_1)(d_1-t)(d_2-t)(g-t)}}$$

$$- \int_{-p_2-\varepsilon}^{d_1} \frac{(t+p_2+\varepsilon)dt}{\sqrt{(t+b)(t+b_1)(d_1-t)(d_2-t)(g-t)}} \Big] -$$

$$\Big[\int_{-b_1}^{-p_2^{\bullet}} \frac{(t+p_2^{\bullet})dt}{\sqrt{(t+b)(t+b_1)(d_1-t)(d_2-t)(g-t)}} -$$

$$\int_{-p_2}^{d_1} \frac{(t+p_2)dt}{\sqrt{(t+b)(t+b_1)(d_1-t)(d_2-t)(g-t)}} \Big] \Big\}/\varepsilon \tag{6.56}$$

$$F_2\left(p_2^*\right) + \frac{dF_2\left(p_2^*\right)}{dp_2} \Delta p_2 = 0 \qquad (6.57)$$

$$\Delta p_2 = -\frac{F_2\left(p_2^*\right)}{\dfrac{dF_2\left(p_2^*\right)}{dp_2}}$$

Improved $p_2 = p_2^* + \Delta p_2$

Case 2.2

The lateral aligned perpendicular towards landside (CB is absent). In that case, points B, B_1, P_2 merge with C as the $L_3 = 0$. The parameters b, b_1, p_2 merge to 0. The mapping of z plane onto t plane remains the same. The steps of mapping is shown in Fig.(6.5).The corresponding complex potential plane is shown in Fig 6.5(c). The mapping of w plane to t plane is modified as:

$$\frac{dw}{dt} = M_1 \frac{\left(t - p_1\right)}{\sqrt{\left(t - d_1\right)\left(t - d_2\right)\left(t - f\right)\left(t - f_1\right)\left(g - t\right)}} \qquad (6.58)$$

$$I_{FG} = \int_f^g \frac{\left(t - p_1\right) dt}{\sqrt{\left(t - d_1\right)\left(t - d_2\right)\left(t - f_1\right)\left(t - f\right)\left(g - t\right)}} \qquad (6.59)$$

$$M_1 = \frac{-kT\left(h_r - h_w\right)}{I_{FG}} \qquad (6.60)$$

$$\frac{\left(q_2 - q_1\right)}{kT\left(h_r - h_w\right)} = \frac{\displaystyle\int_{d_1}^{d_2} \frac{\left(p_1 - t\right) dt}{\sqrt{\left(t - d_1\right)\left(d_2 - t\right)\left(f_1 - t\right)\left(f - t\right)\left(g - t\right)}}}{I_{FG}} \qquad (6.61)$$

$$F_1\left(p_1\right) = \int_{d_2}^{p_1} \frac{\left(p_1 - t\right) dt}{\sqrt{\left(t - d_1\right)\left(t - d_2\right)\left(f_1 - t\right)\left(f - t\right)\left(g - t\right)}} - \int_{p_1}^{f_1} \frac{\left(t - p_1\right) dt}{\sqrt{\left(t - d_1\right)\left(t - d_2\right)\left(f_1 - t\right)\left(f - t\right)\left(g - t\right)}}$$

123

$$\frac{dF_1\left(p_1^{\bullet}\right)}{dp_1} = \left\{ \left[\int_{d_2}^{p_1^{\bullet}+\epsilon} \frac{\left(p_1^{\bullet}+\epsilon-t\right)dt}{\sqrt{(t-d_1)(t-d_2)(f_1-t)(f-t)(g-t)}} \right. \right.$$

$$\left. - \int_{p_1^{\bullet}+\epsilon}^{f_1} \frac{\left(t-p_1^{\bullet}-\epsilon\right)dt}{\sqrt{(t-d_1)(t-d_2)(f_1-t)(f-t)(g-t)}} \right] -$$

$$\left[\int_{d_2}^{p_1^{\bullet}} \frac{\left(p_1^{\bullet}-t\right)dt}{\sqrt{(t-d_1)(t-d_2)(f_1-t)(f-t)(g-t)}} \right.$$

$$\left. \left. - \int_{p_1^{\bullet}}^{f_1} \frac{\left(t-p_1^{\bullet}\right)dt}{\sqrt{(t-d_1)(t-d_2)(f_1-t)(f-t)(g-t)}} \right] \right\}/\epsilon \qquad (6.63)$$

$$F_1\left(p_1^{\bullet}\right) + \frac{dF_1\left(p_1^{\bullet}\right)}{dp_1}\Delta p_1 = 0 \qquad (6.64)$$

$$\Delta p_1 = -\frac{F_1\left(p_1^{\bullet}\right)}{\dfrac{dF_1\left(p_1^{\bullet}\right)}{dp_1}}$$

Improved $p_1 = p_1^{\bullet} + \Delta p_1$

Case3: Case of two collinear laterals

3.1 Two co linear laterals perpendicular to the river axis

The step of mapping is shown in Fig.6.6. In this case points C, D, and E in z plane are located at the origin, and they do not take part in transformation. Vertex G takes part in the transformation It is located at $t = 1$ in the auxiliary plane. The mapping function is given by:

$$\frac{dz}{dt} = M\frac{1}{(1-t)^{1/2}} \qquad (6.65)$$

$$z = -2M(1-t)^{1/2} + N = R\left|1-(1-t)^{1/2}\right| \qquad (6.66)$$

Parameters, f, f_1, b, and b_1 are found from Eq.(6.66) as:

$$f = 1 - \left(1 - \frac{L_I}{R}\right)^2 \qquad , \quad f_1 = 1 - \left(1 - \frac{L_{Ib}}{R}\right)^2$$

$$b = \left(1 + \frac{L_3}{R}\right)^2 - 1 \qquad , \quad b_1 = \left(1 + \frac{L_{3b}}{R}\right)^2 - 1$$

Relation between w plane and t plane

$$\frac{dw}{dt} = M_1 \frac{(t - p_I)}{\sqrt{(t + b)(t + b_I)(t - f)(t - f_I)(1 - t)}} \tag{6.67}$$

Integrating

$$w = M_1 \int_f^t \frac{(t - p_I)\, dt}{\sqrt{(t + b)(t + b_I)(t - f_I)(t - f)(1 - t)}} + N_1 \tag{6.68}$$

$$M_1 = \frac{-kT(h_r - h_w)}{I_{FG}} \tag{6.69}$$

where,

$$I_{FG} = \int_f^1 \frac{(t - p_I)\, dt}{\sqrt{(t + b)(t + b_I)(t - f_I)(t - f)(1 - t)}} \tag{6.70}$$

$$\frac{q_1}{kT(h_r - h_w)} = \frac{I_{F_I F}}{I_{FG}} \tag{6.71}$$

and

$$\frac{(q_3 - q_1)}{kT(h_r - h_w)} = \frac{I_{BB_1}}{I_{FG}} \tag{6.72}$$

where,

$$I_{BB_1} = \int_{-b}^{-b_I} \frac{(p_I - t)\, dt}{\sqrt{(t + b)(t + b_I)(f_I - t)(f - t)(1 - t)}} \tag{6.73}$$

parameter p_I is determined as follow:

125

$$F_1(p_1) = \int_{b_1}^{p_1} \frac{(p_1 - t)\, dt}{\sqrt{(t+b)(t+b_1)(f_1 - t)(f - t)(1 - t)}} - \int_{p_1}^{f_1} \frac{(t - p_1)\, dt}{\sqrt{(t+b)(t+b_1)(f_1 - t)(f - t)(1 - t)}}$$

$$(6.74)$$

$$\frac{dF_1(p_1^*)}{dp_1} = \left\{ \left[\int_{b_1}^{p_1^* + \varepsilon} \frac{(p_1^* + \varepsilon - t)\, dt}{\sqrt{(t+b)(t+b_1)(f_1 - t)(f - t)(1 - t)}} \right. \right.$$

$$\left. - \int_{p_1^* + \varepsilon}^{f_1} \frac{(t - p_1^* - \varepsilon)\, dt}{\sqrt{(t+b)(t+b_1)(f_1 - t)(f - t)(1 - t)}} \right] -$$

$$\left[\int_{b_1}^{p_1^*} \frac{(p_1^* - t)\, dt}{\sqrt{(t+b)(t+b_1)(f_1 - t)(f - t)(1 - t)}} \right.$$

$$\left. \left. - \int_{p_1^*}^{f_1} \frac{(t - p_1^*)\, dt}{\sqrt{(t+b)(t+b_1)(f_1 - t)(f - t)(1 - t)}} \right] \right\} / \varepsilon \qquad (6.75)$$

$$F_1(p_1^*) + \frac{dF_1(p_1^*)}{dp_1} \Delta p_1 = 0$$

Case 3.2 Two co linear partly non perforated laterals running parallel to the river axis

$$\frac{dz}{dt} = M \frac{(d - t)}{t^{1/2}(1 - t)^{1/2}(g - t)^{1/2}} \qquad (6.76)$$

d , g, and M can be obtained putting $\alpha = 1/2$ in Eq.(6.5), Eq(6.11), Eq(6.12) ,respectively.

For point D_1, $t = d_1, z = L_{2b} e^{i\pi\alpha}$. Applying this condition in equation (6.13)

$$\frac{L_{2b}}{R} = \frac{1}{I_{EG}} \int_0^{d_1} \frac{(d - t)\, dt}{t^{1/2}(1 - t)^{1/2}(g - t)^{1/2}} \qquad (6.78)$$

126

$$= \frac{2 \int_0^{d_1^{1/2}} \frac{(d - v^2) dv}{(1 - v^2)^{1/2} (g - v^2)^{1/2}}}{I_{EG}}$$

$$I_{EG} = 2 \int_0^{\{(g-1)/2\}^{1/2}} \frac{(1 + v^2 - d) dv}{(1 + v^2)^\alpha (g - 1 - v^2)^{1/2}} + 2 \int_0^{\{(g-1)/2\}^{1/2}} \frac{(g - d - v^2) dv}{(g - v^2)^{1/2} (g - v^2 - 1)^{1/2}} \quad (6.79)$$

transformation of w plane to t plane.

$$\frac{dw}{dt} = M_1 \frac{1}{\sqrt{(t - d_1)(t - d_2)(g - t)}} \quad (6.80)$$

Integrating

$$I_{D_2 G} = \int_{d_2}^{g} \frac{dt}{\sqrt{(t - d_1)(t - d_2)(g - t)}} \quad (6.81)$$

$$M_1 = \frac{-kT(h_r - h_w)}{I_{D_2 G}} \quad (6.82)$$

$$\frac{(q_3)}{kT(h_r - h_w)} = \frac{\int_{d_1}^{d_2} \frac{dt}{\sqrt{(t - d_1)(d_2 - t)(g - t)}}}{I_{D_2 G}} = \frac{F(\pi/2, \sqrt{(d_2 - d_1)/(g - d_1)})}{F(\pi/2, \sqrt{(g - d_2)/(g - d_1)})} \quad (6.83)$$

6.4 COMPARISON WITH EXPERIMENTAL ELECTRO DYNAMIC MODEL

Milojevic(1963) has conducted an electro dynamic model to estimated the flow to a radial collector well near a river. He has presented an equation in non- dimensional form (Eq.9, page, 144), which is rewritten below:

127

$$\frac{Q}{kT(H-h_0)} = \left(\frac{t}{L}\right)^{0.10}\left(\frac{D}{L}\right)^{0.15}\left[4.13\,m^{0.1415} - 1.22\left(\frac{T}{L}\right)\right] \times$$

$$\left(\frac{1}{Log_{10}\left(\frac{2b}{L}\right)}\right)^{\left[0.914+0.0183\,m-0.348\left(\frac{T}{L}\right)^{\frac{2}{3}}\right]} \tag{6.84}$$

Where, D= diameter of the horizontal well (drain, gallery, pipe, lateral);

t= height of drain above the impervious layer;

L= drain length; m= number of drains;

b= well distance from the riverbank;

T= water bearing layer thickness;

H-h₀= draw-down;

In the present study, symbols are as: $D=2r_w$; $t=T/2$; $b=R$; $H-h_0= h_r-h_w$

128
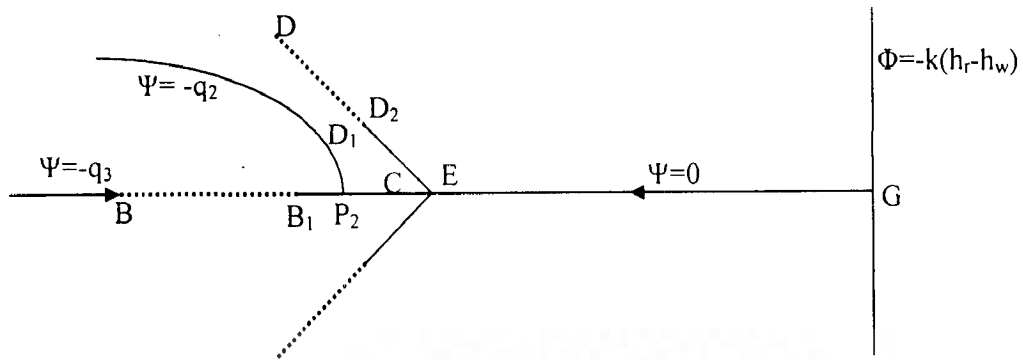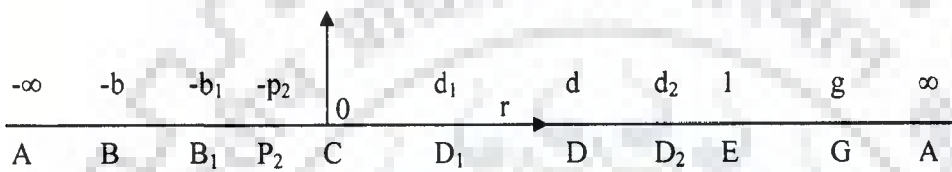
(a) z (=x+iy) plane

(b) : Auxiliary *t(=r+is)* **plane**
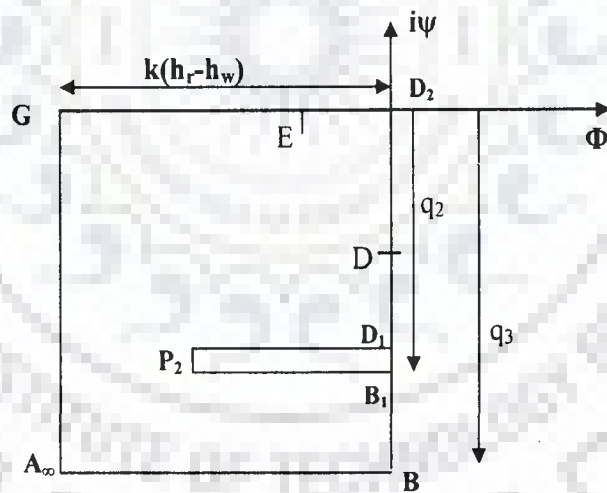
(c) : Complex potential *(w=Φ+iψ)* **plane**

Fig.6.4: Steps of conformal mapping for a radial collector well with three partly
screened laterals, case 2.1
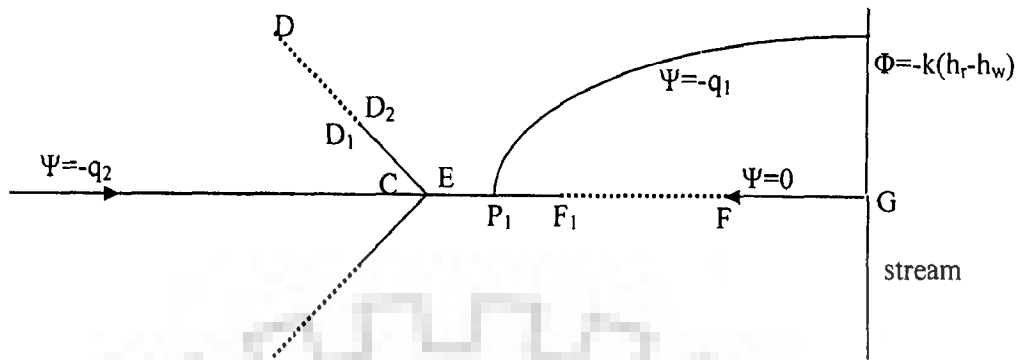
(a) z (=x+iy) plane
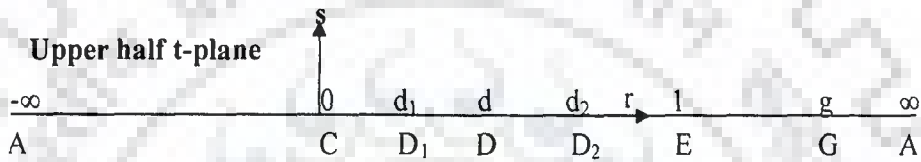
(b) : Auxiliary $t(=r+is)$ plane
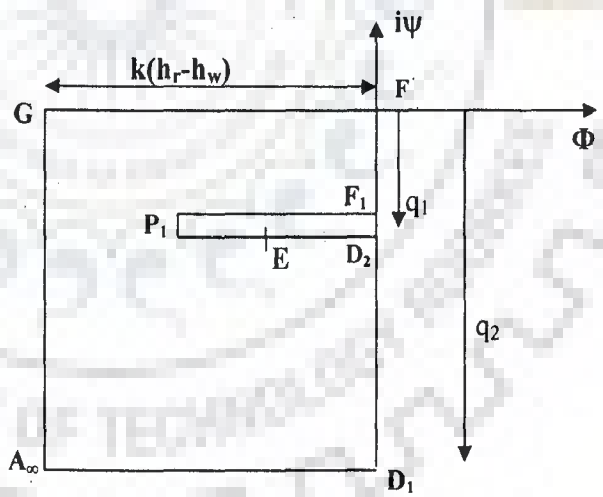
(c): Complex potential $(w=\Phi+i\psi)$ plane

Fig.6.5: Steps of mapping for a radial collector well with three partly screened laterals, case 2.2
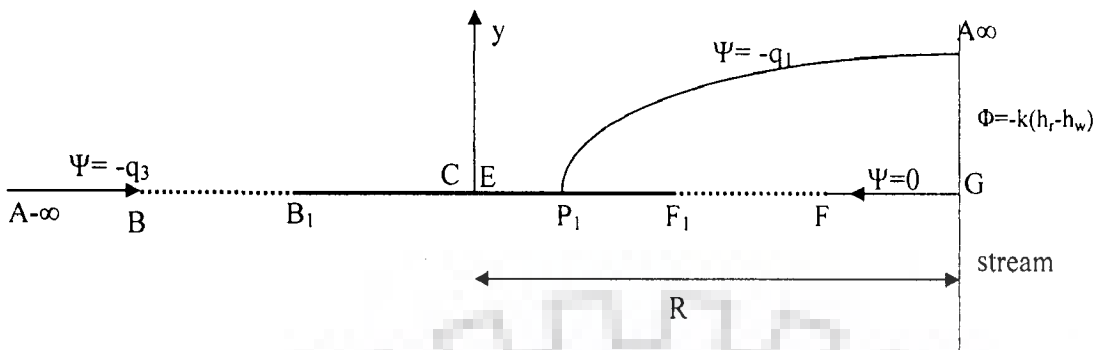
130

(a) Physical flow domain in z (x+iy) plane

Upper half t-plane
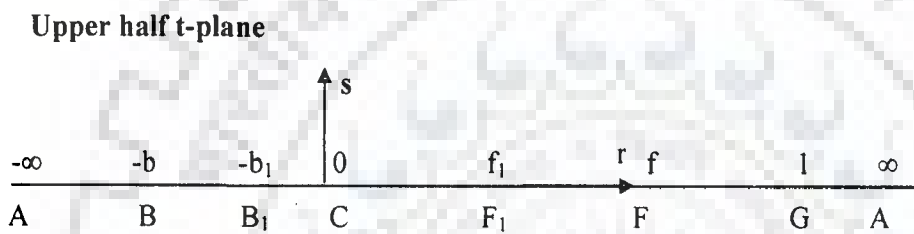
(b) Auxiliary t (r+is) plane
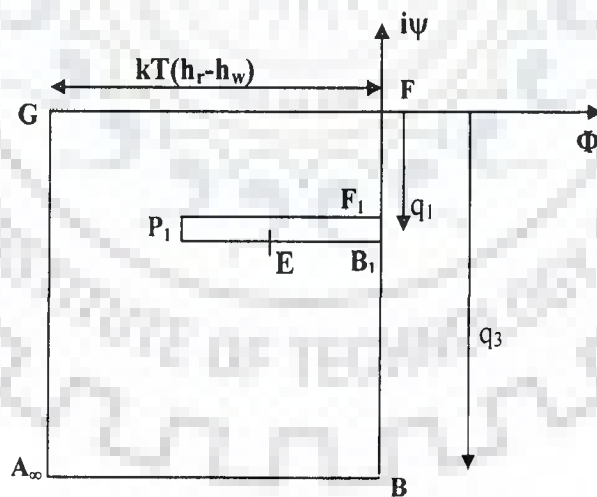
(c): Complex potential $(w=\Phi+i\psi)$ plane

Fig.6.6: Steps of mapping for two collinear partly screened laterals aligned perpendicular to the stream, case 3.1
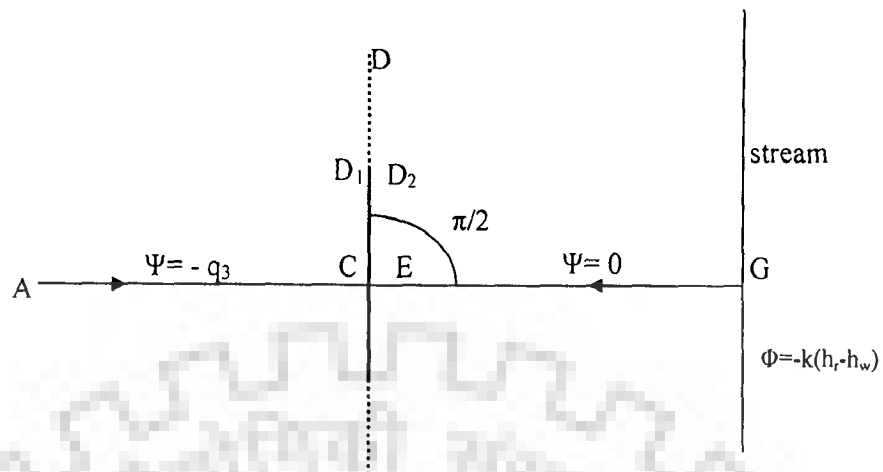
(a) Physical flow domain z= (x+iy)
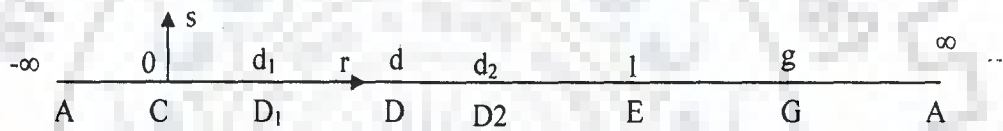
(b) Auxiliary t =(r+is) plane
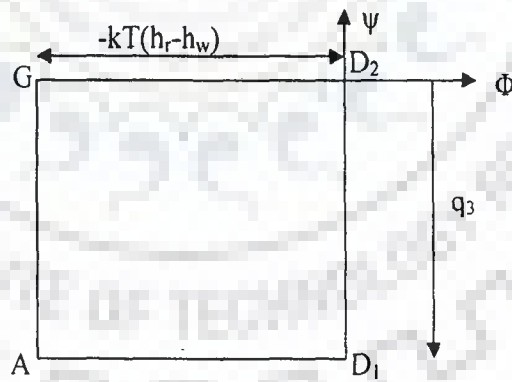
(c) Complex potential $w = (\phi + i\psi)$ plane

Fig. 6.7 Steps of mapping of two partly screened collinear laterals running parallel to a stream, case 3.2

6.5   RESULTS AND DISCUSSIONS

Total flow to the collector well and the total time taken by water to reach the laterals from the river have been presented for a given sets of hydro-geologic and system parameters. Fig (6.8) shows the flow to well for different arrangements of laterals with varying length of non-perforated length. It is found that there is no significant decrease in the flow to the well when length of non-perforated pipe is kept within 40-45% of the lateral length. However, further increase in the non-perforated length decreases the flow marginally.

Interference of well is reduces and the total flow increases when the angle between two laterals are increased as shown in Fig (6.9). Table 6.1 presents the flow to the well for different length of non- perforated section. It is found there is no significant decrease in the flow however the entrance velocity increases sharply with the decrease in the screen length. Hence, entrance velocity should be checked for individual lateral which is capturing more water or having smaller screen length. For a particular location of the well and other given parameters, the total flow to the well increases with the increase in the length of laterals Fig (6.10).

The pathogenic bacterial contamination point of view, the safe distance of the well from the river has been determined by estimating the travel time of water from point G to point F (the shortest streamline) along the x-axis. For a given hydro-geologic parameters and geometric arrangements of the laterals, the variation of S/v_x with respect to dx is shown in Fig (6.11). The total travel time is the area between the curve and the x-axis. The variations of nondimnsional flow and the travel time with L_l/R are shown in Fig (6.12a) and Fig (6.12b), respectively. Flow increases and minimum travel time decreases with the increase in length of laterals.

Non-dimensional flow for four equally spaced laterals computed in the present study is compared with the non-dimensional flow computed from the expression given by Milojovic (1963) in Table 6.2 for a given thickness of aquifer and diameter of laterals and varying L/R. The correction factor owing to the partial interception of the laterals is found to be 0.8.

In absence of lateral EF (Case 2.1), the variation of non-dimensional flow with different orientation of lateral CDE is presented Fig.(6.13). As the lateral CDE sweep towards the landside, the interference of laterals CDE on lateral BC increases and flow to lateral BC reduces whereas flow to lateral CDE increases marginally, and the total flow to the well decreases.

In absence of lateral BC (Case 2.2), the variation of non-dimensional flow with different orientation of lateral CDE is presented Fig.(6.14). As the lateral CDE sweep towards the landside, the interference of laterals CDE on lateral EF reduces and flow to lateral EF increases whereas flow to lateral CDE reduces marginally, and the total flow to the well increases.

Total yield increases with the decrease in the distance R keeping the length of laterals same, but simultaneously the retention time also decreases. Table 6.3 show that the yield remain same when ratios of R/L_1 and L_{1b}/L_1 are kept same for $L_1=L_2=L_3$ and $L_{1b}=L_{2b}=L_{3b}$. Hence, quantity and quality of flow to the collector well primarily depends on the distance of the well R and the length of each lateral (L_1, L_2, L_3) whereas the diameter, percentage of perforation and length of the screens primarily govern entrance velocity.

6.6 CONCLUSIONS

For a given hydro-geologic condition, flow to a single lateral decreases with the increase in number of laterals, due to interference of flow. However, total flow increases with the increase in number of laterals but not in same proportion, but the average entrance velocity of the flow decreases with the increase in the total length of the screen. When the screen portion of the laterals decreases flow does not decreases in the same proportion. For smaller length of laterals, the interference of flow increases, therefore, it is not beneficial to have large number of laterals of smaller length. The distance of the well from the river is the major parameter, which governs the yield and quality of water. If the length of laterals, the length of screens, and the distance of the well from the river for a particular pattern of laterals are increased or decreased by a constant factor, the yield will remain same. However, the collector well at larger distance from the river with longer laterals will produce good quality of water. The increase in the radius and the percentage of perforation increases the yield.
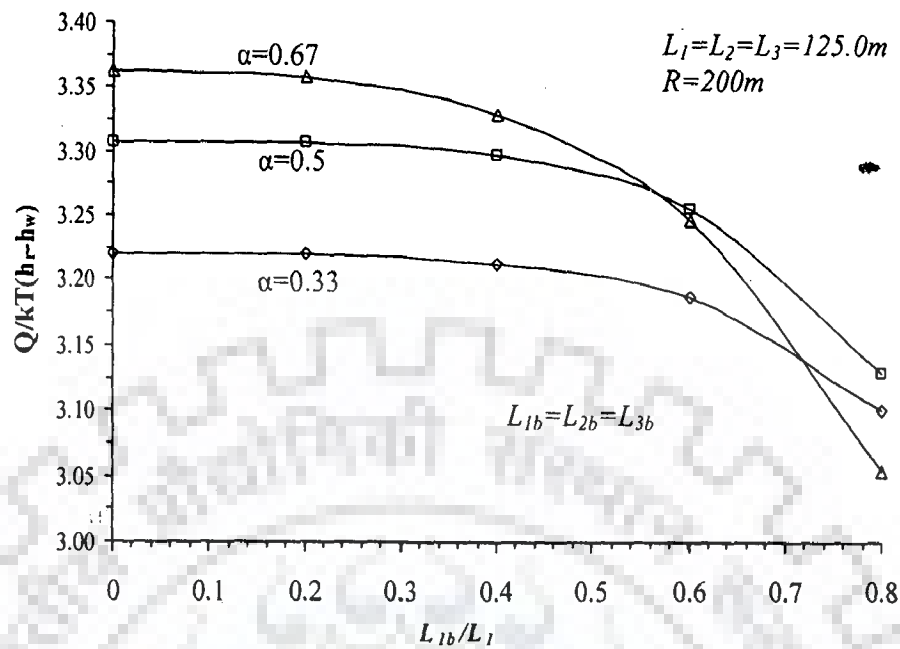
Fig.6.8: Variation of non-dimensional flow with L_{1b}/L_1 of laterals for their different arrangements
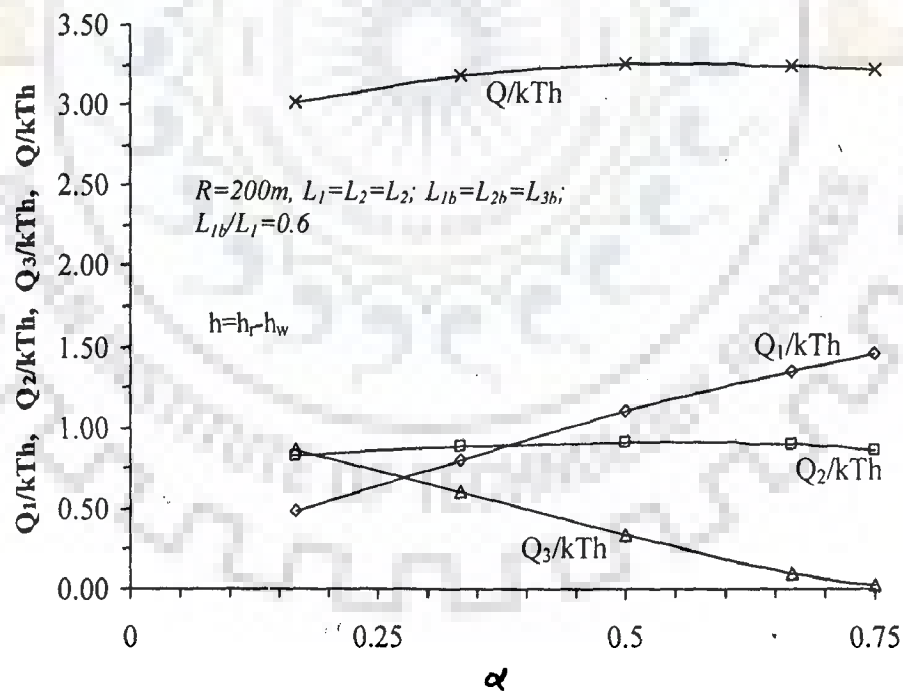
Fig.6.9: Non-dimensional flow to individual lateral for different arrangements

136

$R=200m$, $\alpha=0.5$, $L_{1b}=L_{2b}=L_{3b}=10m$,
$L_1=L_2=L_3$,
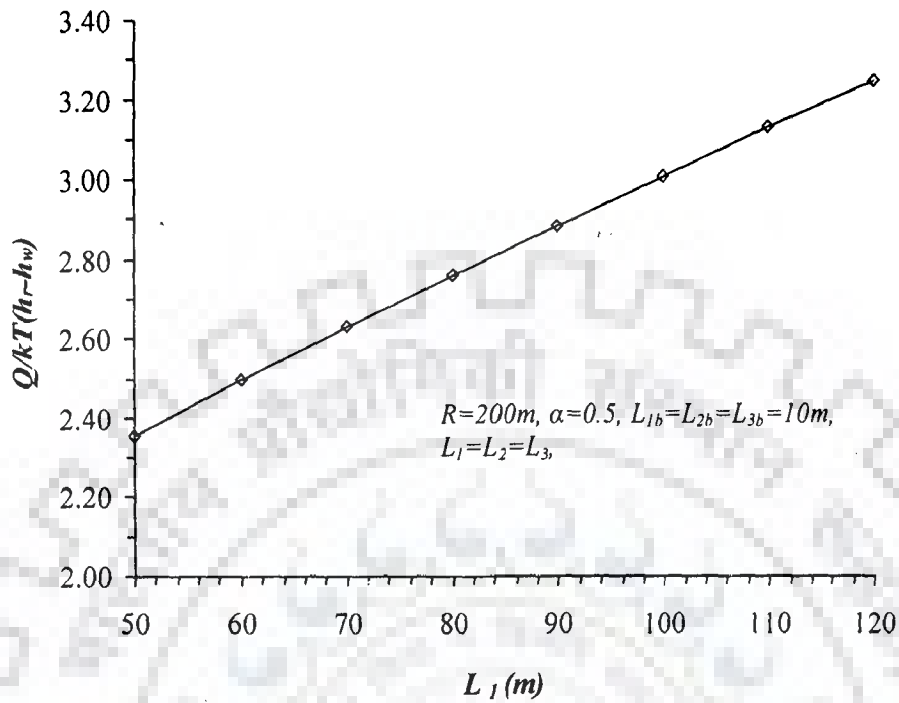
Fig.6.10: Variation of total non-dimensional flow with length of laterals

$L_1=L_2=L_3=50m$, $L_{1b}=L_{2b}=L_{3b}=10m$,
$L_{1b}/L_1=0.2$,
$R=300m$, $h=10m$, $k=70m/day$
$S=0.3$

Total minimum travel time is the
Area under the curve and the x axis
Total time =36.8 days
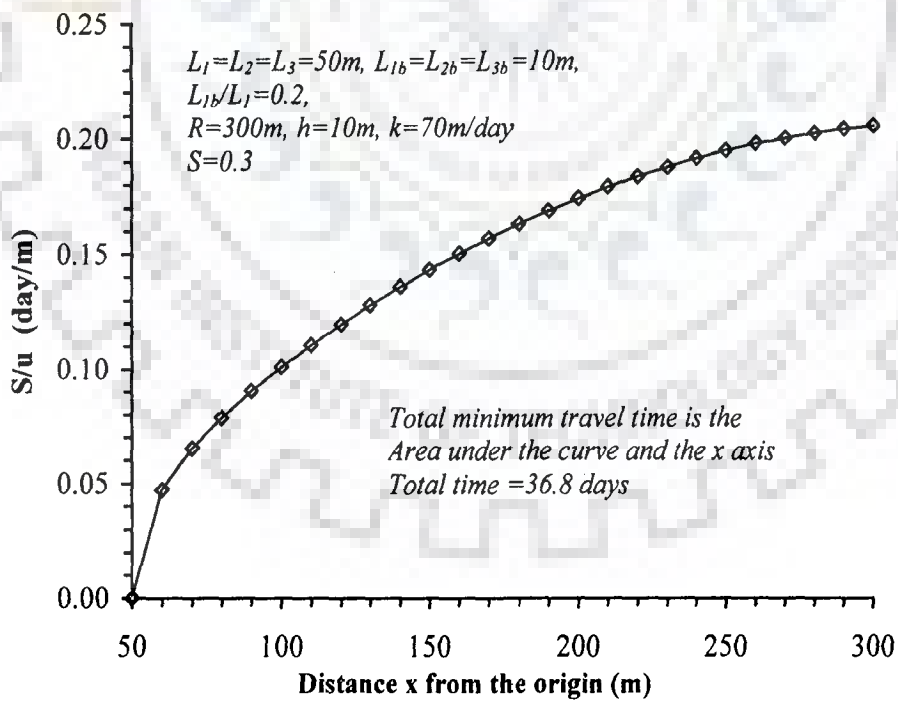
Fig.6.11: Variation of S/u with x.

137
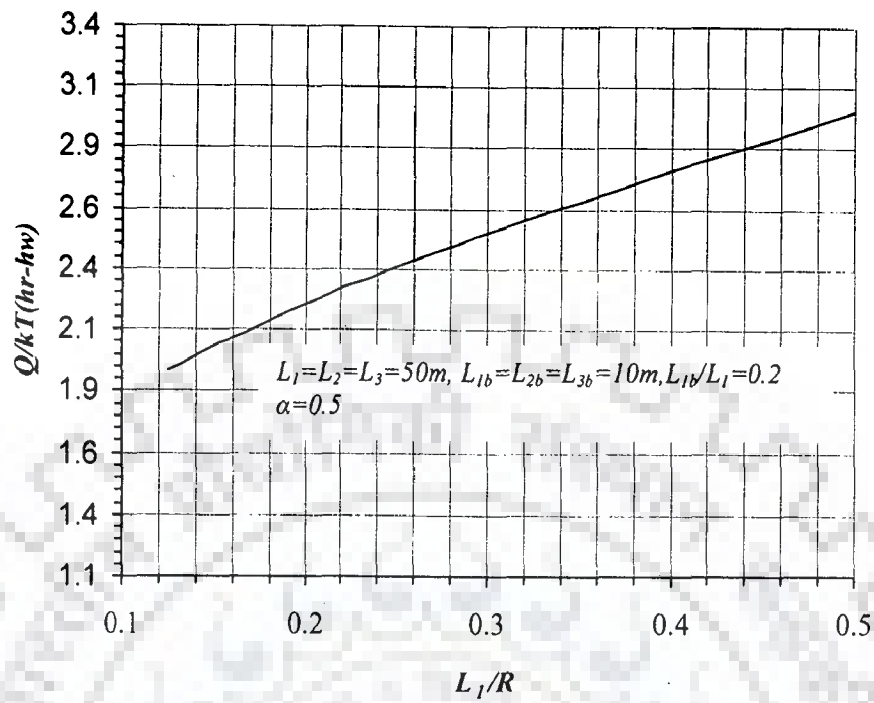
Fig.6.12(a): Variation of non-dimensional flow with L_1/R

In figure (a), the curve is labeled with:
$L_1=L_2=L_3=50m$, $L_{1b}=L_{2b}=L_{3b}=10m$, $L_{1b}/L_1=0.2$
$\alpha=0.5$

The y-axis is labeled $Q/kT(hr-hw)$ and the x-axis is labeled L_1/R.
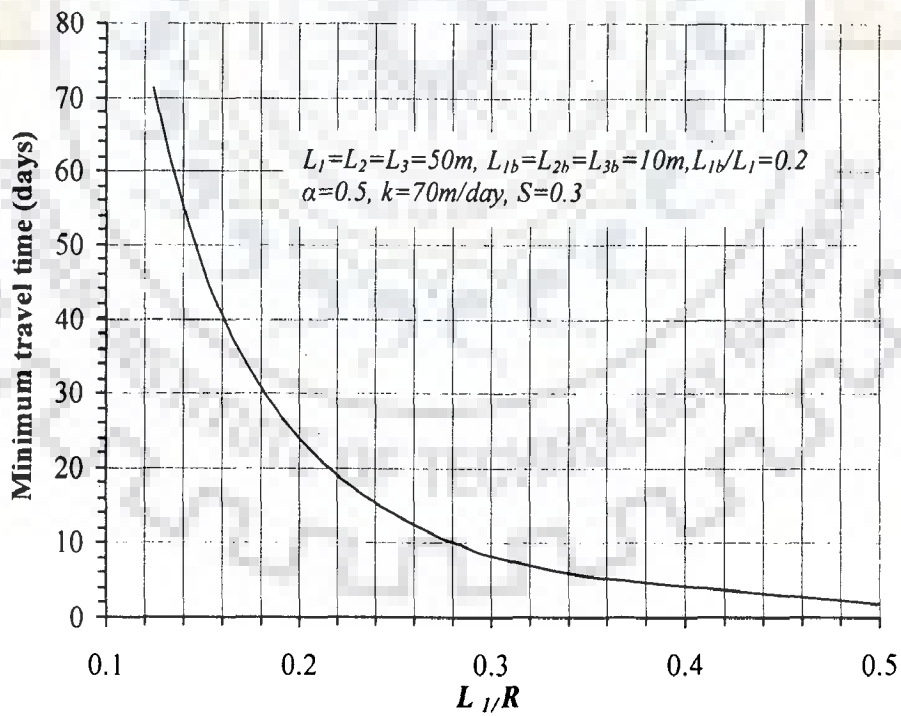
Fig.6.12(b):Variation of minimum travel time with L_1/R

In figure (b), the curve is labeled with:
$L_1=L_2=L_3=50m$, $L_{1b}=L_{2b}=L_{3b}=10m$, $L_{1b}/L_1=0.2$
$\alpha=0.5$, $k=70m/day$, $S=0.3$

The y-axis is labeled Minimum travel time (days) and the x-axis is labeled L_1/R.

138
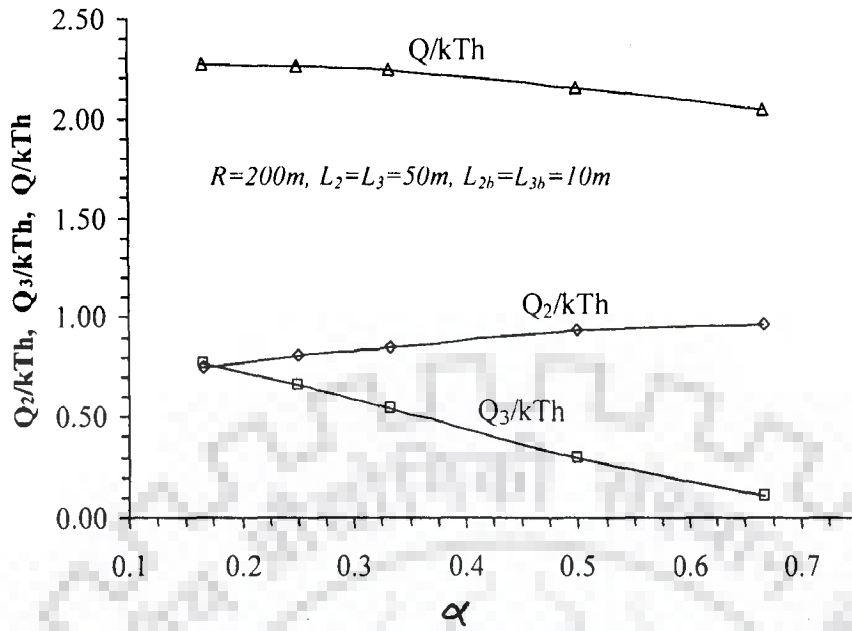
Fig.6.13: Non-dimensional flow to individual laterals for different arrangements (Case 2.1)
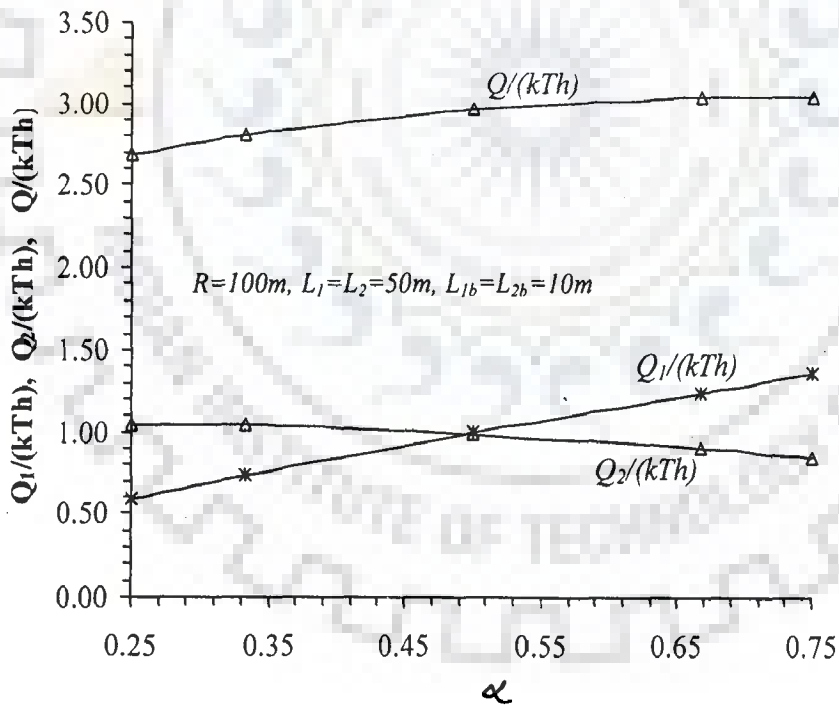
Fig.6.14: Non-dimensional flow to individual laterals for different arrangements (Case 2.2)

Table 6.1. Variation of nondimensional flow to each laterals and entrance velocity to lateral EF with L_{1b}/L_1.

$R=200m, \alpha=0.667$, $L1=L2=L3=125m$, $k=70m/day$, Aquifer thickness$=7.5m$, drawdown, $h= h_r-h_w=7m$; perforation, $P=0.2$; diameter, $d=0.32$, $L_{1b}=L_{2b}=L_{3b}$

Blind Length(m)	Q_1/kTh	Q_2/kTh	Q_3/kTh	Q/kTh	Avg. Entrance Velocity to EF cm/sec
1	2	3	4	5=2+2*3+4	6
0	1.428	0.917	0.0999	3.363	0.242
25	1.426	0.917	0.1000	3.359	0.302
50	1.406	0.912	0.1004	3.330	0.397
75	1.350	0.898	0.1010	3.247	0.571
100	1.218	0.868	0.0998	3.053	1.031

Table.6.2. Comparison of non-dimensional flow, $Q/kT(h_r-h_w)$ from Electrodynamic model and the present study.

$T=7.5m$, diameter $d=0.32m$ and number of equally spaced ($\alpha=0.5$) laterals, $m=4$

Length of each laterals	R=b (m)	L/R	Milojovic(1963)'s Electrodynamic model	Present study	Correction factor, C_f
			$Q/kT(h_r-h_w)$		
1	2	3	4	5	6=4/5
50	100	0.50	2.42	3.01	0.806
50	120	0.42	2.24	2.80	0.799
50	140	0.36	2.11	2.65	0.796
50	160	0.31	2.01	2.53	0.794

Table 6.3. Variation of minimum travel time for a given value of $L_{1,R}$ and L_{1b}/L_1 for same flow, i.e., $Q/kT(h_r-h_w)=2.58$

$S=0.2$, $k=10m/day$, drawdown, $h_r-h_w=6m$;

R (m)	$L_1=L_2=L_3$ (m)	R(m)	Shortest Distance (G to F) (m)	Non dimensional flow, $Q/kT(hr-hw)$	Minimum travel time (Days)
1	2	3	4		5
150	50	10	100	2.58	50.4
225	75	15	150	2.58	112.8
300	100	20	200	2.58	201.4
375	125	25	250	2.58	315.0

141
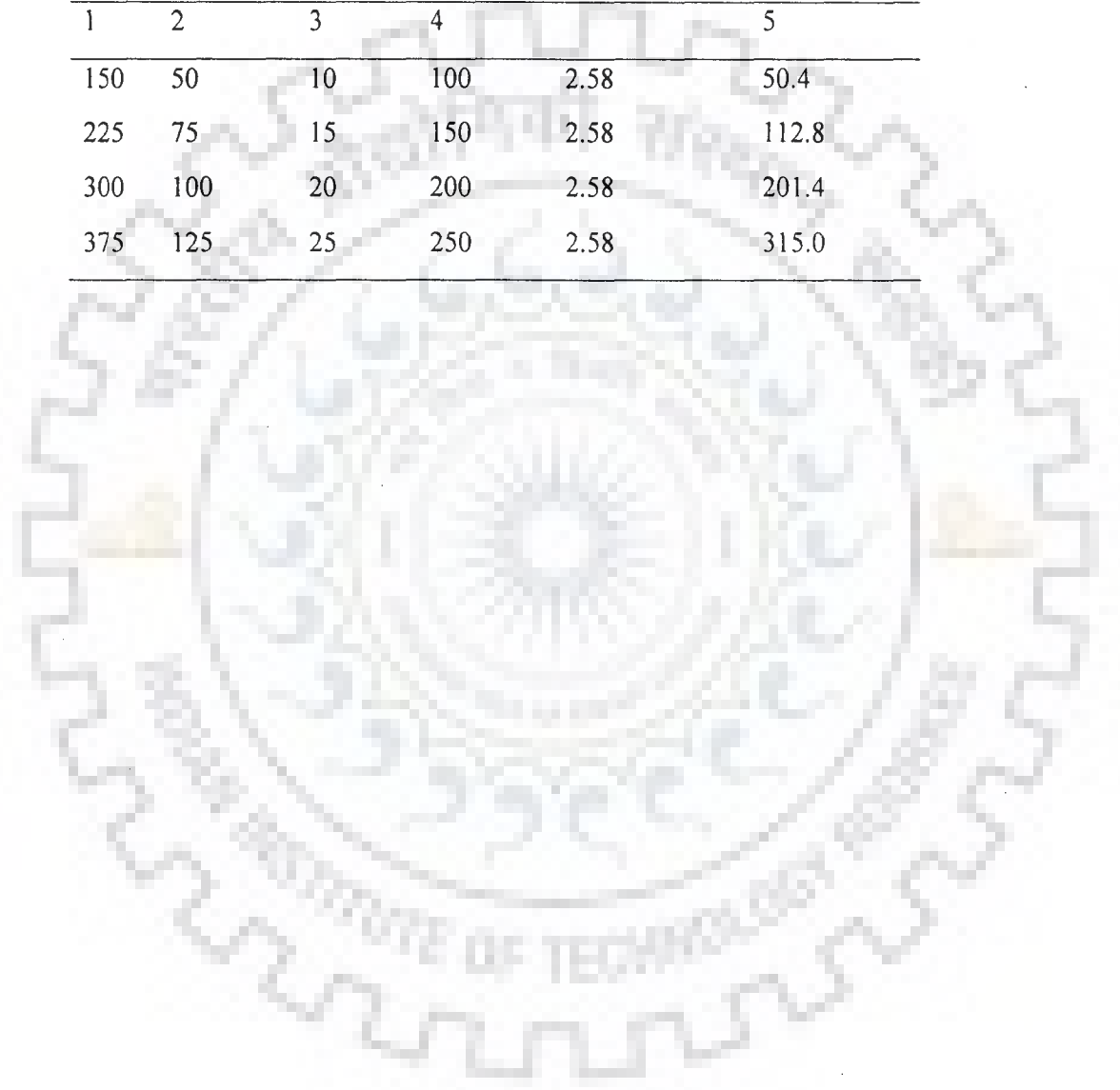
GROUNDWATER RECHARGE THROUGH A MULTI-AQUIFER SHAFT NEAR A FLOODING STREAM

7.1 INTRODUCTION

In arid and semi-arid regions, groundwater storage depletion is a common feature. Therefore, some effective measures are required to replenish the groundwater storage loss or to increase safe yield of the aquifer. A variety of methods have been developed to recharge or replenish groundwater (Oaksford, 1985). These methods include direct surface, direct subsurface and indirect recharge. In direct surface method, water moves from land surface to the phreatic aquifer by percolation through the soil such as flooding, furrow, basins, stream augmentation and over-irrigation, etc. In direct subsurface method, water is conveyed into natural openings, pits or shafts and wells, and water percolates down under gravity. Further, indirect recharge is the induced infiltration that takes place from the stream to the aquifer owing to pumping of a well near a stream-bank. A particular situation may occur when a shaft is opened to multilayer confining aquifers and is situated near a flooding stream. During flood events, the water level in the stream rises and consequently the piezometric level or water table in the upper aquifer rises, as a result, the lower aquifer gets recharged through the shaft. Further, during flood period the velocity of water in stream is sufficiently high to prevent silt deposition from sealing the streambed and stream-bank. After the recession of flood when the stream becomes a gaining stream, the presence of such multi-aquifer shafts will capture some of the ambient aquifer discharge before it reaches the stream as base flow. The acceptance rate of the aquifer

is function of aquifer parameters, radius and position of the shaft as well as peak flood rise and duration of the flood. This method could be proved effective in unconsolidated formations of permeable sand and gravel hydraulically connecting the stream and the aquifer. A vertical shaft may be considered in context of *Riverbank Filtration (RBF)* for (i) increasing the safe yield of the underlying aquifers and (ii) improving the source water quality by taking the advantage of the natural biogeochemical processes occurring in the porous medium between the stream and the shaft.

Several studies (Theis, 1941; Kazmann, 1948; Glover and Balmer, 1954; Hantush, 1965; Jenkins, 1968; Wallace et al., 1990; Wilson, 1993; Spalding and Khaleel, 1991; Hunt, 1999; Chen, 2003; Swamee, et al., 2000; Singh, 2000, 2003, etc.) have been carried out on stream-aquifer-well system in which the estimations of stream depletion and induced infiltration are the main objectives. However, all these studies have been carried out for the well tapping single aquifer, i.e., the unconfined aquifer only and no flood is passing in the stream. Recently, using discrete kernel approach, Mishra and Fahimuddin (2005) have analyzed unsteady flow through a multi-aquifer well of infinitesimally small radius situated nearby a stream during pumping, after stoppage of pumping, as well as during passage of a flood wave in the stream. The objective of this chapter is to present a solution to quantify the recharge through a multi-aquifer shaft of finite radius located near stream-bank during flood period. The increase in recharge due to various factors such as increase in diameter of the shaft, proximity of the shaft to the stream and extent of its penetration into the aquifer to be recharged, has been studied.

In nature, a single aquifer rarely exists. An aquifer is part of a system of aquifers (multi-aquifer system) separated from each other by less permeable confining layers. Several studies, mostly numerical modeling, have been carried out to analyze the groundwater flow in multiaquifer and well systems (Saleem, 1973; Fujinawa, 1977; Herrera et. al., 1980; Maddock III and Luther, 1991; Cheng and Morohunfola, 1993; Giao et. al., 1999; Baker and Strack, 2003; Neville and Tonkin, 2004, etc). Mishra, et.al. (1985), applying discrete kernel approach, have analyzed unsteady flow to a multiaquifer well tapping two aquifers separated by an aquiclude However, very few studies on multiaquifer and stream system are reported. A stream in a multiaquifer system may partially or fully penetrate the upper aquifer. It interacts directly with the top aquifer and indirectly with the lower aquifers through the well opening only if the aquifers are separated by aquicludes. Hemker(1984) and Mass(1986) address the problem of a stream in a multiaquifer system. Very few works are reported on the understanding of the interaction of a stream and multiaquifer system with or without a pumped well nearby the stream. Recently, using discrete kernel approach, Mishra and Fahimuddin (2005) have analyzed the unsteady flow through a multiaquifer well situated nearby a stream during pumping, after stoppage of pumping, as well as during passage of a flood wave in the stream.

Transient well hydraulics in a single homogeneous and isotropic nonleaky confined aquifer is the simplest case in both the practical and mathematical sense. The theory was developed by Theis (1935), known as the "Theis Equation", describing transient flow in aquifers under pumping conditions from a well in a confined non-leaky aquifer. The Theis's solution is based on the assumption that the well can be idealized as a mathematical sink (i.e. radius $r \rightarrow 0$) that has no storage capacity. Later,

Hantush (1964) given solution for drawdown around a well of finite radius assuming that the rate at which water is pumped from the well is equal to that entering the well, so that storage capacity of the well is neglected. Further, Papadopulos and Cooper (1967) given solution for drawdown in and around of a large diameter well taking the water stored into account. Some studies in which discrete kernel method has been applied to analyze unsteady flow to a large diameter well are cited here (Patel and Mishra, 1983; Mishra and Chachadi, 1985; Sen , 1986; Rushton and Singh, 1987; Barker, 1991; Chachadi and Mishra, 1992; Mishra, 2004, etc).

In this chapter, an analytical model is described to quantify groundwater recharge that would take place from the upper unconfined aquifer to lower confined aquifers through a shaft (un-pumped well of finite radius) situated near a riverbank due to the rise in stage during passage of a flood. The shaft taps first two aquifers separated by an aquiclude.

7.2 STATEMENT OF THE PROBLEM

A definition sketch of a multi-aquifer shaft for the groundwater recharge is shown in Fig.(7.1). The shaft with a radius r_w is located at a distance R from stream bank. The shaft is open to two aquifers, i.e., phreatic aquifer and lower confined aquifer of transmisivities, T_1 and T_2, and storage coefficients, S_1 and S_2, respectively. An aquiclude of thickness L separates the two aquifers and b is thickness of the lower confined aquifer. It is assumed that the stream and aquifers are in initially hydraulic equilibrium state.

The objective is to quantify the recharge to the lower aquifer through the shaft during passage of a flood wave in the nearby stream. Quantification of recharge rate is

sought for a vertical shaft penetrating fully to the lower aquifer and marginally to the lower aquifer, i.e., the shaft terminates at the base of the aquiclude layer.
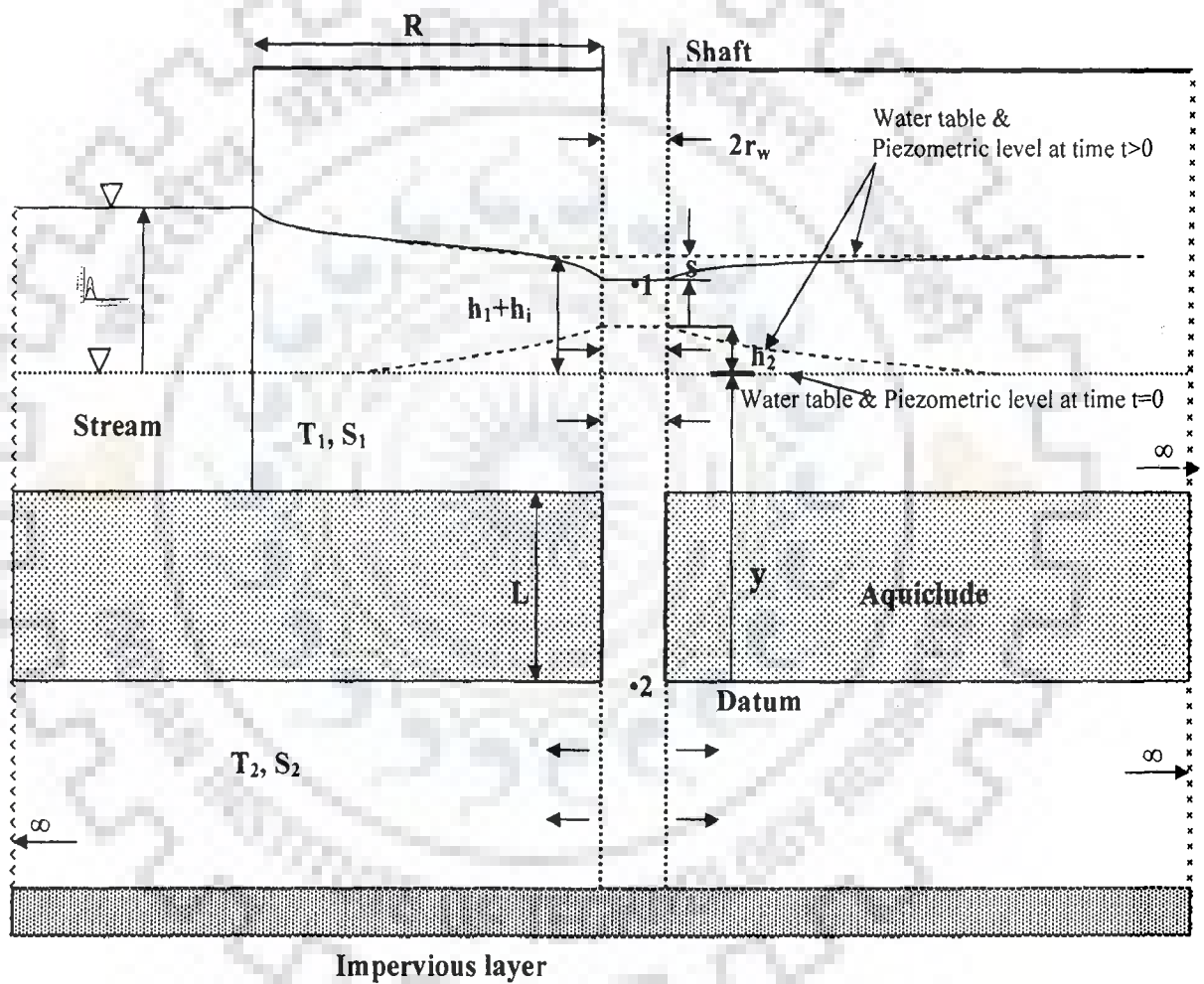
Fig.7.1: A multiaquifer shaft near a flooding stream

7.3 ASSUMPTIONS

The following assumptions have been made in the analysis:

(1) The time parameter is discrete. Within each time step, the unknown recharge rates are separate constants varying from one time step to another time step.

(2) The varying recharge is a train of pulses and an unsteady state is a succession of steady states, therefore, within a time step, Bernoulli's equation is applicable.

(3) The stream forms a straight boundary, fully penetrates the upper aquifer and is in perfect hydraulic connection with the upper aquifer. There is no clogging layer, i.e., stream resistance is neglected.

(4) Each of the aquifers is homogeneous, isotropic, and of a constant thickness in lateral extent.

7.4 ANALYSIS

To compute the recharge through a multi-aquifer shaft near stream-bank during passage of a flood wave (Fig.7.1), a mathematical expression is written applying Bernoulli's equation between points 1 and 2 with datum at the base of the aquiclude at the end of any time step n as:

$$y + h_1(n) + h_i(n) - s(n) = y + h_2(n) + \frac{v_2{}^2(n)}{2g} + \frac{fL_a v_2{}^2(n)}{4gr_w} \tag{7.1}$$

where,

y= height of initial water level from the datum;

$v_2(n) = Q(n) / \left(\left(\pi r_w{}^2 \right) \Delta t \right)$, velocity of water at point 2 during n^{th} time step; Q(n)= volume of water passing through the shaft during n^{th} time step; r_w = radius of the

147

shaft; n = an integer; Δt = time step size; f= coefficient of friction; L_a= thickness of the aquiclude; g= acceleration due to gravity;

$$h_1(n) = \sum_{\gamma=1}^{n} \left(\sigma_\gamma - \sigma_{\gamma-1} \right) \delta_h(R, n-\gamma+1, \Delta t),$$ rise in piezometric level at the shaft

face due to stream stage rise at the end of nth time step; σ_γ = rise in stream stage at

the end of γ th time step which is computed using mathematical expression for

sinusoidal flood wave proposed by Cooper and Rorabough(1963);

$\delta_h(R, n-\gamma+1, \Delta t)$ = discrete ramp kernel coefficient obtained using the unit

response function given by Carslaw and Jaeger (1959) for analogous heat conduction

problem(see the Appendix B) ; R= distance of the shaft from the stream-bank ; γ = an

integer;

$$s(n) = \sum_{\gamma=1}^{n} Q(\gamma) \, \delta_1(r_w, n-\gamma+1, \Delta t) \,,$$ drawdown in piezometric level at the shaft face

due to passing of water from the upper aquifer to the lower aquifer

; $\delta_1(r_w, n-\gamma+1, \Delta t)$= discrete pulse kernel coefficients obtained from the solution

for drawdown derived by Hantush (1964) for the fully penetrating well of finite

radius(see the Appendix C and Mishra, 2004(a));

$$h_i(n) = \sum_{\gamma=1}^{n} Q(\gamma) \, \delta_1(2R, n-\gamma+1, \Delta t),$$ rise in piezometric level at the shaft face due

to an image recharge well; and

$$h_2(n) = \sum_{\gamma=1}^{n} Q(\gamma) \, \delta_2(r_w, n-\gamma+1, \Delta t),$$ rise in piezometric level at the shaft face

in the lower aquifer owing to recharge from the upper aquifer.

Incorporating $h_1(n)$, $h_i(n)$, $s(n)$, $h_2(n)$ and $v_2(n)$ into Eq. (7.1) the following

expression is obtained:

$$\sum_{\gamma=1}^{n}\left(\sigma_\gamma - \sigma_{\gamma-1}\right)\delta_h(R,\ n-\gamma+1,\ \Delta t)\ +\ \sum_{\gamma=1}^{n}Q\ (\gamma)\ \delta_1(2R,\ n-\gamma+1,\ \Delta t)-$$

$$\sum_{\gamma=1}^{n}Q(\gamma)\ \delta_1(r_w,\ n-\gamma+1,\ \Delta t) = \sum_{\gamma=1}^{n}Q(\gamma)\ \delta_2(r_w,\ n-\gamma+1,\ \Delta t)+\left\{\frac{Q(n)}{\Delta t\,\pi r_w^2}\right\}^2\ \frac{1}{2g}$$

$$+\frac{f\,L_a}{4gr_w}\left\{\frac{Q(n)}{\Delta t\,\pi r_w^2}\right\}^2 \qquad\qquad (7.2)$$

Eq. (7.2) is rearranged and written in the form of a quadratic equation as:

$$Q^2(n)\left\{\frac{f L_a}{(\Delta t)^2\ 4g\pi^2 r_w^5} + \frac{1}{(\Delta t)^2\ 2g\,\pi^2\ r_w^4}\right\}$$

$$+ \sum_{\gamma=1}^{n}Q(\gamma)\left\{\begin{array}{l}\delta_1(r_w,\ n-\gamma+1,\ \Delta t)\ -\ \delta_1(2R,\ n-\gamma+1,\Delta t)\ +\\ \delta_2(r_w,\ n-\gamma+1,\ \Delta t)\end{array}\right\}$$

$$- \sum_{\gamma=1}^{n}\left(\sigma_\gamma - \sigma_{\gamma-1}\right)\delta_h(R,\ n-\gamma+1,\ \Delta t)\ =0 \qquad\qquad (7.3)$$

Eq. (7.3) is solved for $Q(n)$ considering positive root only as:

$$Q(n)=\frac{-b+\sqrt{b^2-4ac}}{2a} \qquad\qquad (7.4)$$

where, $a = \dfrac{f L_a}{(\Delta t)^2\,4g\pi^2 r_w^5} + \dfrac{1}{(\Delta t)^2\,2g\pi^2 r_w^4}$;

$b = \delta_1(r_w,\,1,\,\Delta t) - \delta_1(2R,\,1,\,\Delta t) + \delta_2(r_w,\,1,\,\Delta t)$;

and

$c=$

$$\sum_{\gamma=1}^{n-1}Q(\gamma)\left\{\delta_1(r_w,\ n-\gamma+1,\ \Delta t) - \delta_1(2R,\ n-\gamma+1,\ \Delta t) + \delta_2(r_w,\ n-\gamma+1,\Delta t)\right\}$$

$$- \sum_{\gamma=1}^{n}\left(\sigma_\gamma - \sigma_{\gamma-1}\right)\delta_h(R,\ n-\gamma+1,\ \Delta t)\ .$$

149

By neglecting the terms for the velocity head and the head loss due to friction

in Eq. (7.1), Eq. (7.3), which is nonlinear, becomes a simple linear equation as:

$$\sum_{\gamma=1}^{n} Q(\gamma) \begin{Bmatrix} \delta_1(r_w, n-\gamma+1, \Delta t) - \delta_1(2R, n-\gamma+1, \Delta t) + \\ \delta_2(r_w, n-\gamma+1, \Delta t) \end{Bmatrix} -$$

$$\sum_{\gamma=1}^{n} \left(\sigma_\gamma - \sigma_{\gamma-1} \right) \delta_h \left(R, n-\gamma+1, \Delta t \right) = 0 \tag{7.5}$$

The procedure for finding recharge though a shaft that penetrates marginally (i.e. zero penetration) into the lower aquifer is same as that for the fully penetrating shaft described above. In this case, the rise in piezometric level $h_2(n)$ at the shaft face owing to recharge is to be computed using discrete pulse kernel coefficients obtained from the solution for drawdown derived by Hantush (1961) for the partially penetrating well (see the appendix C and Mishra, 2004).

7.5   RESULTS AND DISCUSSIONS

Results have been obtained by solving Eq. (7.3) varying the values of different parameters of the system considering the thickness of the aquiclude, $L_a=10.00m$; the coefficient of friction, $f=0.02;$ and the time step size, $\Delta t = 1/12$ day. The proximity of the shaft to the stream, the radius and the extent of its penetration into the aquifer to be recharged are parameters that govern the volume of recharge most for a particular hydro geologic site. Distance of the shaft from the stream is a major parameter, which governs the quantity and quality of the recharge most. The recharge reduces significantly with the increase in distance of the shaft from the stream as shown in Fig. (7.2). However, a longer distance between the shaft and the stream-bank helps in removing large quantities of surface water contaminants and improves the quality of the recharge water.

The size or radius of the shaft is the second most important parameter that has to be decided to obtain maximum recharge through a shaft located at a particular distance from the stream. Fig. (7.3) shows the total volume of recharge through the shaft of different radius and placed at different distance from the stream-bank. The recharge was estimated for initial two months since onset of flood. It is found that the percentage increase in total recharge with the increase in radius is more for smaller radius as shown in Fig. (7.3). For example, total volume of water that is recharged to the lower aquifer through a shaft which is placed at $R=100m$ is increased from $3062m^3$ to $3843m^3$ when the radius is increased from $0.1m$ to $0.5m$ and it increases further to $4217m^3$ when the radius is further increased to 1.0m.

The extent of shaft's penetration into the aquifer to be recharged is another important parameter. Fig.(7.4) shows recharge through a shaft that penetrates fully and marginally into the confined aquifer. A substantial difference in the recharge is found corresponding to these two conditions, hence, the shaft should penetrate into the entire depth of the aquifer to be recharged.

Recharge decreases for greater storage coefficient of the upper aquifer as shown in Fig. (7.5a) and it increases for greater storage coefficient of the lower aquifer as shown in Fig. (7.5b). Recharge rate for different peak and duration of flood is shown in Fig. (7.6).

It is noticed from figures that some quantity of water come back from the confined aquifer to the unconfined aquifer immediately after recession of the flood. This is because that the peizometric level in the unconfined aquifer at the shaft face starts decreasing and becomes lower than the piezometric level of the confined aquifer at the well face for some time immediately after flood period.

Recharge rates computed solving Eq. (7.3) and Eq. (7.5) are compared in Table.7.1. Hydraulic heads due to the velocity and the friction loss in the aquiclude portion of the shaft would be very small even for greater depth of aquiclude (L_a), larger friction factor (f) and smaller radius (r_w). The reason for this is that water mainly flows through porous medium except in the aquiclude portion of the shaft. Hence, Eq. (7.5) can be used as a good approximation of Eq. (7.3).

7.6   CONCLUSIONS

An analytical solution, using discrete kernel approach, has been presented to quantify groundwater recharge through a multi-aquifer shaft situated near stream-bank during passage of flood in the stream. Distance of the shaft from the stream is a major parameter that governs the quantity and quality of the recharge. The recharge reduces significantly with the increase in distance of the shaft from the stream. However, a longer distance (longer travel time) between the shaft and the stream-bank helps in removing large quantities of surface water contaminants through bio-geochemical processes and improves the quality of the recharge water. The recharge increases with increase in radius of the shaft at a particular distance from the stream-bank. However, the rate of increase in recharge diminishes at larger diameter of the shaft. The shaft should penetrate fully into the aquifer that has to be recharged.

The stream–aquifer system, by an optimal management, can be used to store the runoff occurring in the stream. Multi-aquifer shafts located directly adjacent to a flooding stream can serve a means of *artificial recharge* by setting a gallery or a line of shafts parallel the bank of a stream and at a short distance from it.
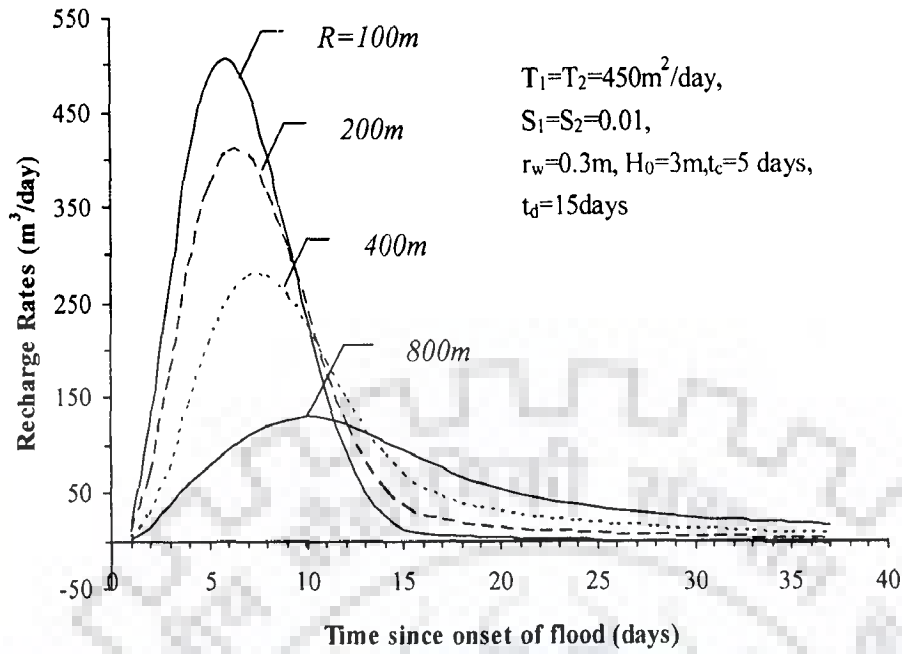
Fig.7.2: Variation of recharge rate with time for different location of the shaft from the river
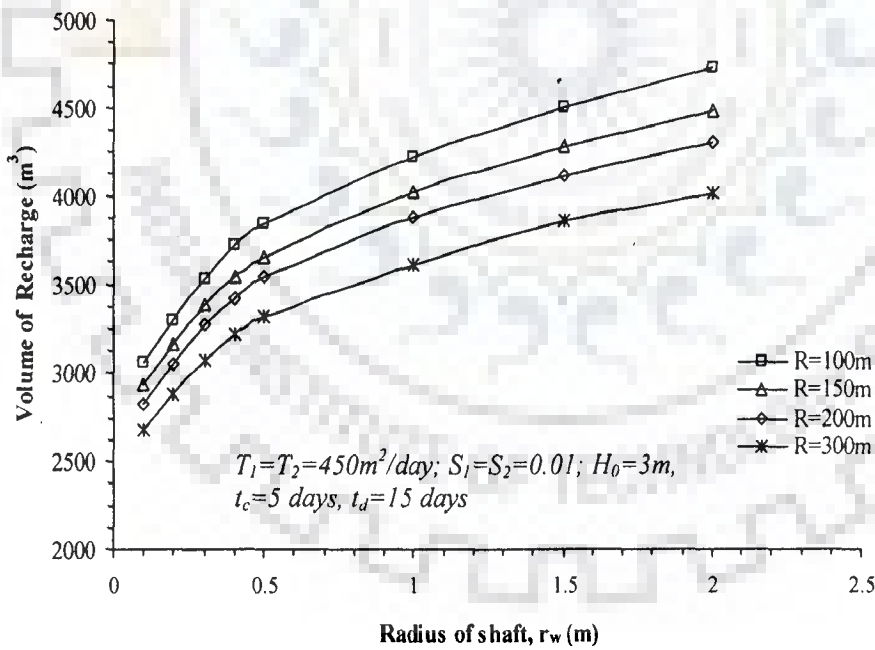
Fig. 7.3: Variation of total recharge with radius of shaft for its different location from the river

153
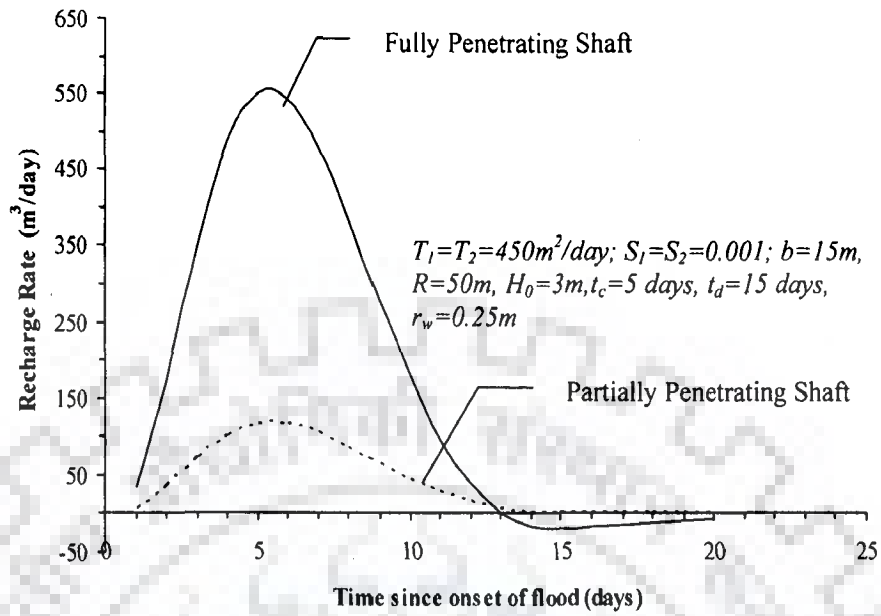
Fig.7.4: Variation of recharge rate with time for fully and partially penetrating shaft.

$T_1=T_2=450m^2/day$; $S_1=S_2=0.001$; $b=15m$, $R=50m$, $H_0=3m$, $t_c=5$ days, $t_d=15$ days, $r_w=0.25m$

$T_1=T_2=450m^2/day$; $R=100m$, $H_0=3m$, $t_c=5$ days, $t_d=15$ days, $r_w=0.3m$
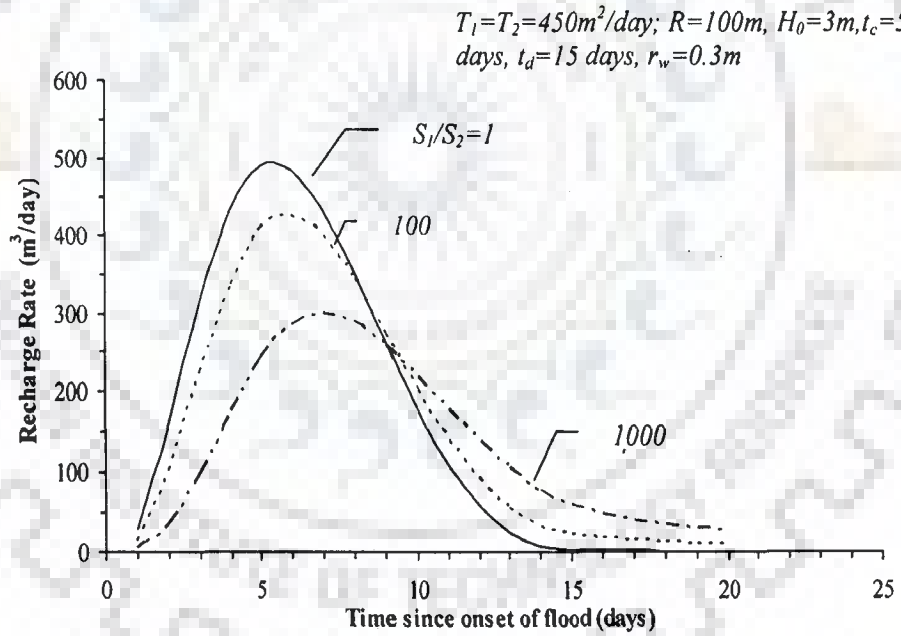
Fig.7.5a: Variation of recharge rate with time for different storage coefficients $(S_1/S_2 > 1)$

154
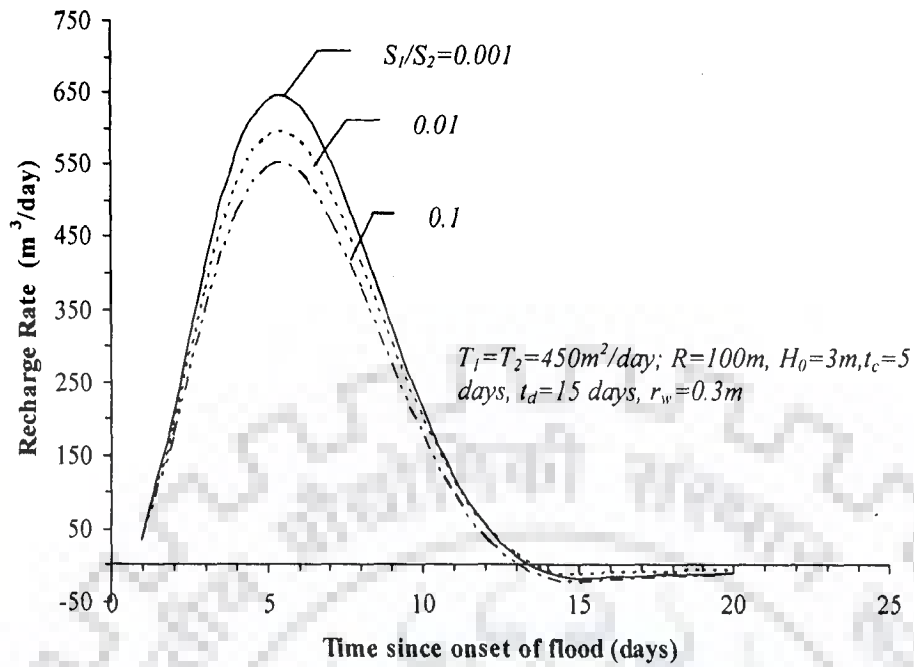
Fig.7.5b: Variation of recharge rate with time for different storage coefficients ($S_1/S_2<1$).
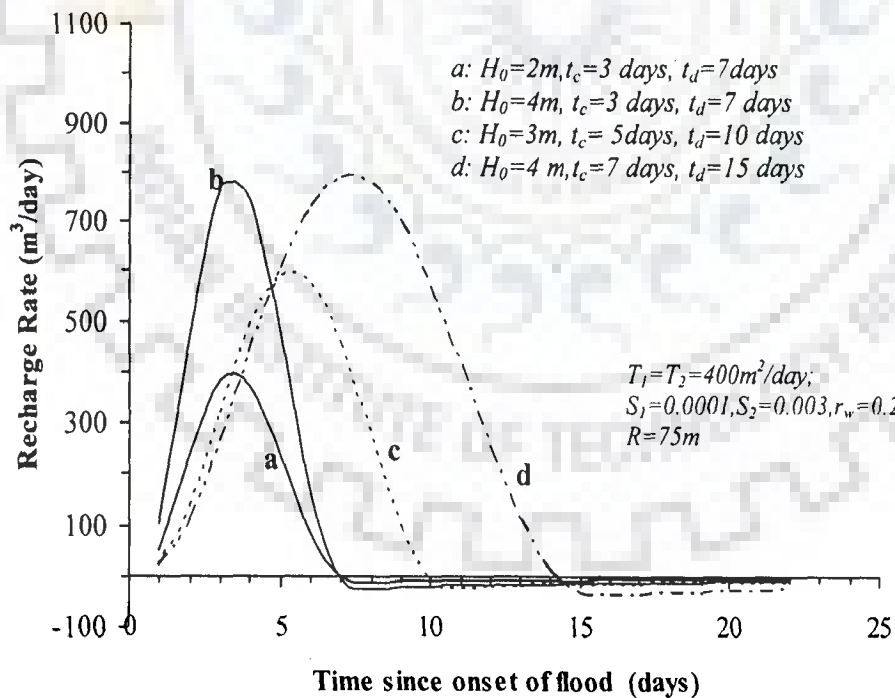
Fig.7.6: Variation of recharge rate with time for different floods.

155

Table 7.1: Recharge rate computed using Eq. (7.3) and (7.5).
$T_1=T_2=450m^2/day$; $S_1=S_2=0.001$; R $=50m$, $r_w=0.1m$,

L=10m, f=0.02, $H_0=3m$,$t_c=5days$,$t_d=15days$.

| Days | Recharge rates (m³/day) from | | |
	Eq.(7.3)	Eq.(7.5)	Difference
1	29.3318	29.3319	0.0001
2	153.1999	153.2003	0.0004
3	303.1393	303.1408	0.0015
4	418.6350	418.6380	0.0030
5	474.8673	474.8709	0.0036
6	471.3053	471.3088	0.0035
7	421.3559	421.3587	0.0028
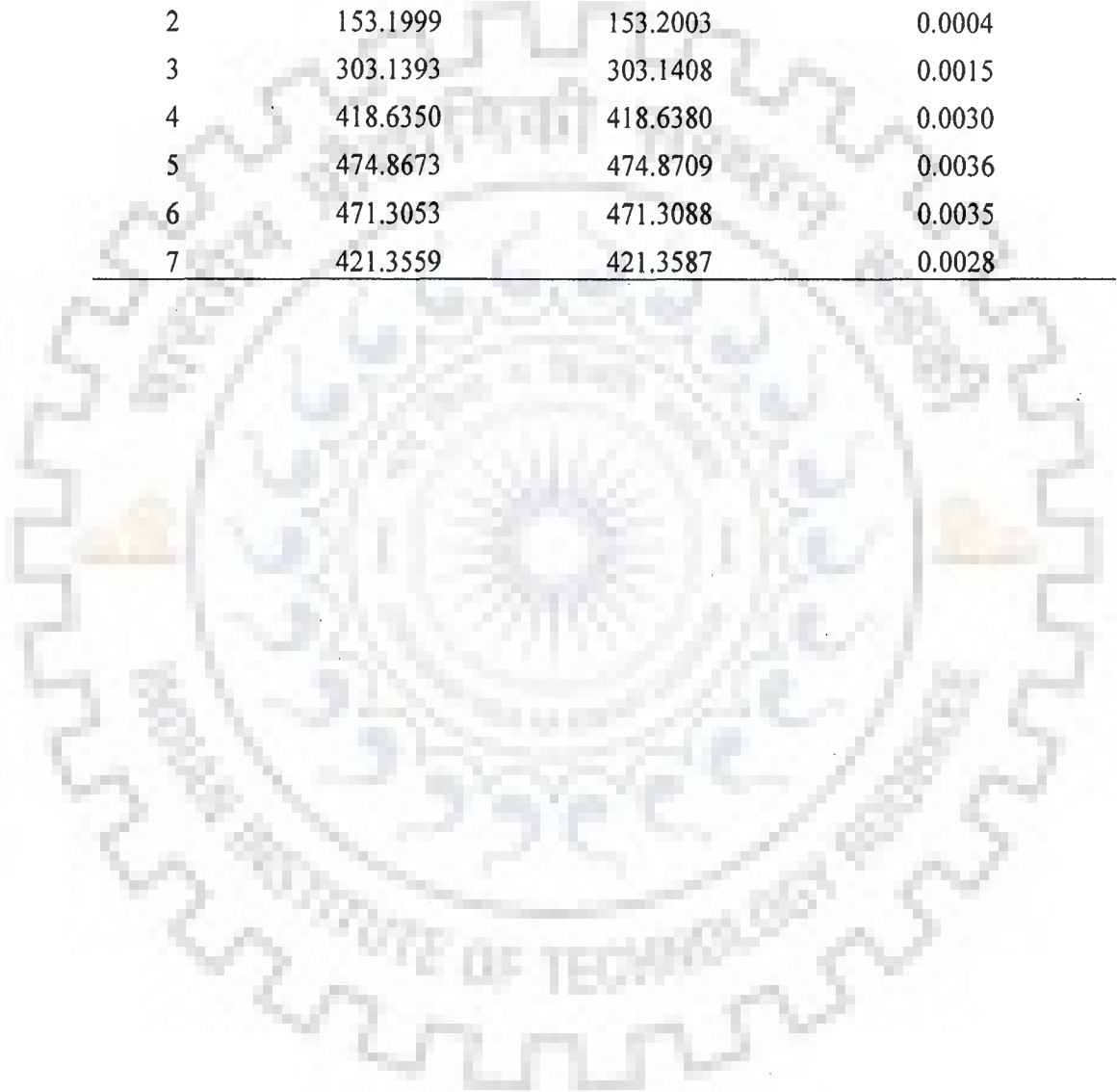
CONCLUSIONS

A radial collector well consists of a number of horizontal screened pipes (laterals) connected to a central caisson. Water enters through these horizontal laterals; therefore, analytical solutions of flow to a RCW are based on the theory of gradually varied flow in a horizontal perforated pipe (drain or gallery). An infiltration gallery can be treated as a special case of a radial collector well with only one or two collinear laterals.

If a horizontal well is pumped with a large pumping rate, different flow states such as laminar, transitional, and turbulent flows can co-exist inside the lateral and the problem must be treated as a coupled well-aquifer hydraulics problem. It is found that the laminar flow length is dependent on the radius of the collector pipe. Barring for a small length near the tip of collector pipe (free end), the flow condition inside the pipe is turbulent.

Estimation of flow to a horizontal pipe can be based on two fundamental assumptions, i.e., (i) either the total discharge through a lateral is uniformly distributed along its entire length, i.e., the uniform flux boundary condition exist along the laterals, or (ii) that the head along the lateral is uniform, i.e., Dirichelt type boundary condition exists along the laterals. Collector pipe of diameter 0.3m-0.4m is generally adopted for a radial collector well and for collector pipe with diameter 0.2m and above, the head loss is very marginal. Therefore, for steady state flow condition, either Dirichlet boundary condition or uniform flux condition can be applied without

introducing appreciable error. Dirichelt boundary condition is to be applied for solving Laplace equation for steady state flow condition. For unsteady state flow condition, the uniform flux boundary condition can be adopted conveniently.

Generally, a RCW system has many laterals ranging from 2 to 23 per well and in such case, due to interference of laterals, the flux distribution along any lateral will not be uniform. The flux per unit length will be more near the tips of the pipes than that near the caisson. The flux per unit length at any section depends on entry gradient, pipe diameter, perforation percentage, hydraulic conductivity, and the hydraulic head difference across the flow boundaries. The entry gradient, hence the flux distribution, is governed by the geometry of flow domain. Thus, in case of a collector well with several laterals, an assumption of uniform flux distribution along the laterals would misrepresent the true situation.

The flow domain of a radial collector well or an infiltration gallery in a thin aquifer near a stream can be considered as homogeneous as the radius of influence would not progress with time due to presence of the surface water body. The effective flow domain of a radial collector well or infiltration gallery will be a small part of the aquifer. The advantage of homogeneity can be taken for solving the well hydraulics problem analytically. If the objective is to estimate the production rate of a radial collector well, flow field can be considered as two-dimensional in x-y horizontal plane neglecting the resistance to vertical flow.

If the well is located near to a surface water body, the flow to the well could be treated as steady state flow during the later stage of contineous pumping. At late pumping stage, horizontal pseudo-radial flow towards a horizontal collector pipe is established which supports the assumption of sheet flow condition in a thin aquifer

158

and horizontal collector well system. Thus, the flow can be estimated by solving well-known Laplace equation for 2D flow field under steady state conditions. Thereafter, a correction factor is to be applied to take account of the partial interception of the aquifer thickness by the collectors.

Yield of a collector well is influenced by length, orientation, number and diameter of laterals, etc. and can be studied through analytical technique such as the conformal mapping technique. Conformal mapping technique is one of the methods available to solve the 2D groundwater flow problems.

The safe yield of a radial collector well or that of an infiltration gallery near a river is a function of length of gallery or laterals, location of the collector system from the surface water body (river, lake), geometry of the surface water body (straight reach or meandering reach), radius and percentage of perforation of laterals, and the hydro-geological parameters, i.e., aquifer thickness, hydraulic conductivity, and storage coefficients.

The specific capacity of an infiltration gallery located at the centre of an island increases and travel time decreases with the increase in l/R. Similar situation happens for an infiltration gallery aligned at right angle towards straight reach of a river. In case of an infiltration gallery aligned towards landside of the river, the specific capacity increases and the minimum travel time decreases monotonically with the increase in l/R. The specific capacity of an infiltration gallery running parallel to a river increases linearly with the increase in l/R, whereas, the minimum travel time increases first and then becomes almost constant.

The specific capacity of a radial collector well with multiple partly screened laterals located near meandering reach of a river increases with increase in l/R and

159

the number of laterals. However, for smaller length of laterals, the increase in the specific capacity is marginal with the increase in number of laterals. The minimum travel time decreases with increase in l/R. The entrance velocity first decreases and then increases with the increase in l/R. The reason for this is that flow increases linearly for smaller l/R and increases exponentially for l/R approaching 1. The effect of the length of non-perforated section of laterals on specific capacity and minimum travel time is not significant. However, total length of each collector remaining same, the entrance velocity increases sharply with the increase in non perforated length of the lateral.

The specific capacity of a radial collector well with four partly screened laterals located near a straight reach of a river increases with the increase in the length of screen. For a given length of laterals (nonperforated and perforated section), the specific capacity changes with the change in mutual orientation of laterals with respect to the river. For nominal blind length of laterals, the yield is maximum when three laterals are laid towards land side at an angle $\pi/3$ between them, and one is oriented towards the river side. If the blind part is more than 60% of the collector length, the maximum yield occurs when the angle between laterals is $\pi/2$ and one of laterals is oriented at right angle towards the river. The minimum travel time decreases with increase in length of laterals as screen part comes closer to the river.

The limiting entrance velocity (3 cm/sec), the limiting axial velocity (0.9 m/sec (Ray (2002), Driscoll (1987)), and the minimum travel time (average survival time of pathogenic bacteria) are the major governing parameters for the design of an infiltration gallery and a radial collector well near a river. In the design of a radial collector well, the well location, orientation of infiltration gallery or laterals with

160

respect to the river axis, radius, length of screen, percentage of perforation of collectors are determined for a given hydro-geological condition and for desired production of the well.

In sedimentary groundwater basin, and even in hard rock region, a multiaquifer system exists. In such situation, to meet the desired water supply demand, and to meet the water quality standard, it is advantageous to tap the lower aquifer. To increase the water supply capacity of the lower aquifer, the aquifer may be recharged artificially by constructing vertical shaft near a river. The quantity of water recharged during passage of a flood has been determined. The recharge increases with the increase in radius of the shaft and with close proximity of the shaft to the river. If the lower aquifer is fully intercepted by the vertical shaft, the recharge increases significantly.

Scope for further studies

The present study has been carried out with certain objectives under certain assumptions. The radial collector well-stream-aquifer interaction needs further studies focusing on:

(1) The effect of partial penetration of stream on specific yield.

(2) Comparison of performance of a vertical well and a radial collector well in a thick aquifer in respect of specific yield and energy consumptions.

(3) Performance of radial collector well during unsteady state of flow

(4) Evaluation of safe yield of a collector well system in an unconfined aquifer stream system.

(5) Safe distance of the well from a river or stream accounting for dispersion, adsorption and decay of pollutants.

A.1 CONFORMAL MAPPING

Most of the analytical methods for the solution of two dimensional groundwater problems are concerned with the determination of a function which will transform the problem from a geometrical domain within which a solution is sought into one within which the solution is easy to obtain. Let $w = \phi + i\Psi$ be an analytic function of $z = x + iy$ & suppose that a complex number $x + iy$ is located at point P_1 in z-plane. As w is a function of z, there must be some point Q_1 in w-plane corresponding to the point P_1 in z-plane. Similarly, by correspondence of a sequence of points for any curve in z-plane, there will be a corresponding curve in w plane. This is called a mapping. Conformal mapping is one of the several techniques of transformation in which the angles of intersection and the approximate shape are preserved. The usefulness of conformal mapping in two-dimensional flow problems stem in the fact that solutions of Laplace's equation remain solutions when subjected to conformal mapping. In conformal mapping technique, the crux of the problem is to find a transformation (or series of transformation) that will map conformally a complex region in z-plane into an analytic region (say) in w or t-plane of simple shape such as rectangle or circle.

A.2 SCHWARZ-CHRISTOFFEL TRANSFORMATION

In groundwater seepage problem, it is generally required to study the seepage characteristics within complicated but straight-line boundaries. Theoretically, the transformation exists which will map any pair of simply connected regions

162

conformally onto each other. The use of appropriate auxiliary mapping technique enables to transform even complicated flow regions into regular geometric shapes. Generally, these regions are polygons having a finite number of vertices, out of which one or more may be at infinity. Thus, the method of mapping a polygon from one or more planes onto upper half of another plane is of particular importance.

If a polygon is located in the z plane (z=x+iy), then transformation that maps it conformally onto the upper half of the auxiliary t plane (t=r+is) is:

$$z = M \int \frac{dt}{(t-a)^{\left(\frac{\pi-A}{\pi}\right)}(t-b)^{\left(\frac{\pi-B}{\pi}\right)}(t-c)^{\left(\frac{\pi-C}{\pi}\right)}(t-d)^{\left(\frac{\pi-D}{\pi}\right)}(t-e)^{\left(\frac{\pi-E}{\pi}\right)}} + N \qquad (A1)$$

where M and N are complex constants. A, B,C,...., are the interior angles (in radians) of the polygon in the z plane Fig (A1), and a,b,c,...., (a<b<c<..) are points on the real axis of the t-plane (Fig. A2) corresponding to the respective vertices A,B,C,...
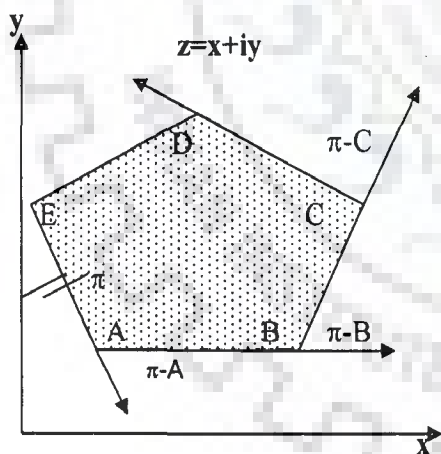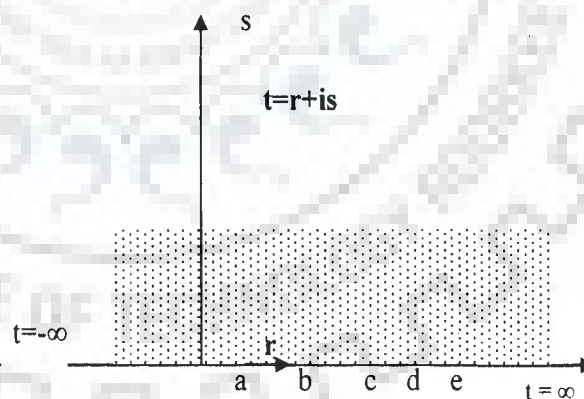

Fig.A.1   Fig.A.2

Equation A1 is called as the Schwarz-Christoffel transformation. The Schwarz-Christoffel transformation technique is applicable to a simply connected polygon with straight-line boundaries having a finite number of vertices one or more of which may

be at infinity. However, in some cases there is no physically connected flow domain. In such cases it is checked whether there is any symmetry about the real x-axis in flow domain. In case of symmetry, half of the flow domain owing to symmetry is a connected polygon and can be chosen for mapping. The mapping function gets considerably simplified and gets amenable to Schwarz Christoffel conformal mapping technique. The transformation is accomplished by opening the polygon at some convenient point (i.e. between A and E as in Fig A1) and extending one end to the t=-∞ and the other end to the t=+∞ (Fig A2). In this operation, the sides of the polygon form a straight-line which is placed along the real axis of t-plane. By choosing π as the interior angle at the opening point, it takes no part in transformation as shown in Eq.(A1). The opening point should be chosen between any two vertexes. In transformation process, any three of the values a,b,c,... , can be chosen arbitrarily to correspond to three of the vertices of the polygon A,B,C,.... The (n-3) remaining values are determined to satisfy the condition of similarity. If the opening point is kept at infinity then only two points remain to be chosen arbitrarily and (n-2) point remains to be determined.

Unless the flow domain is of very simple shape, direct analytical solution to Laplace's equation is very difficult. Conformal mapping is one of the several techniques of transformation in which a region of complex shape is transformed into a region of simpler shape by keeping the angles of intersection in magnitude and sense, and the approximate shape preserved. Through conformal mapping a complex domain is transformed into a simpler shape wherein Laplace's equation can be solved subjected to the transformed boundary conditions.

B.1 RISE OF AQUIFER WATER LEVEL LOCATED AT DISTANCE X DUE TO RISE IN STREAM STAGE AFTER TIME T.

Carslaw and Jaeger (1959) have derived solutions for heat conduction problems, which are applicable to analogous groundwater flow problems. The rise in piezometric surface corresponding to a step rise in stream stage for one dimensional transient flow of water in an initially steady state, semi-infinite, homogeneous and isotropic aquifer, bounded by a fully penetrating fairly straight stream, can be represented by the partial differential governing equation such as

$$\frac{\partial h}{\partial t} = \beta \frac{\partial^2 h}{\partial x^2} \tag{B1}$$

where, β is the hydraulic diffusivity, and h is the piezometric head.

In order to compute rise in piezometric level in the aquifer located at a distance x from the stream edge, after time t, due to the sudden rise H in stream stage, following initial and boundary conditions are to be satisfied :

Initial condition, $h(x, 0) = 0$; and

Boundary conditions

$h(0, t) = H$ and $h(\infty, t) = 0$

The solution of analogous heat conduction problem was given by Carsalaw and Jaeger (1959) which is given as

$$h(x,t) = H\left\{1 - erf\left(\frac{x}{\sqrt{4\beta t}}\right)\right\} \tag{B2}$$

where, x= distance from the bank of the stream; t= time measured since the onset of change in stream stage; T= transmissivity of the aquifer; S = storage coefficient of the aquifer; β = T/S, hydraulic diffusivity; erf (X)=error function = $\dfrac{2}{\sqrt{\pi}} \displaystyle\int_0^X e^{-u^2} du$.

B. 2   SYNTHETIC FLOOD WAVE IN A RIVER

Cooper and Rorabough (1963) have proposed synthetic generalized form of flood wave passing in a river, which can be represented as follows:

$$\sigma(t) = \begin{cases} N * H_0 (1 - \cos \omega t)\, e^{-\delta t} & \text{for } 0 \le t \le t_d \\ 0 & \text{for } 0 \rangle\, t_d \end{cases}$$
(B3)

where $\sigma(t)$ = stream stage above initial water level at any time t ;

$N = \exp(\delta t_c)/(1 - \cos \omega t_c)$; H_0= Peak height of flood stage above initial water level;

t_c = time to reach peak flood from initial stage; t_d = total duration of flood period; the

frequency of oscillation $\omega = 2\pi/t_d$, and $\delta = \omega \cot(0.5 \omega t_c)$;

The expressions for temporal and spatial distribution of piezometric head for infinite aquifers for a symmetric flood wave (δ=0, N=1/2) obtained by Cooper and Rorabough(1963) are given as

$$h(x,t) = 0.5 H_0 \left\{ \text{erfc}\left(\frac{x}{2\sqrt{\beta t}} \right) - e^{\left(-\frac{x\sqrt{\omega}}{\sqrt{2\beta}} \right)} \cos\left(\omega t - \frac{x\sqrt{\omega}}{\sqrt{2\beta}} \right) \right\} +$$

$$0.5H_0 \frac{1}{\pi} \int_0^\infty e^{(-ut)} \sin\left(\frac{x\sqrt{u}}{\sqrt{\beta}}\right) \frac{u}{u^2 + \omega^2} du \quad \text{for } t \le t_d \tag{B4}$$

$$h(x,t) = 0.5H_0 \left\{ \begin{array}{l} \mathrm{erfc}\left(\dfrac{x}{2\sqrt{\beta t}}\right) - \mathrm{erfc}\left(\dfrac{x}{2\sqrt{\beta(t-t_d)}}\right) + \\[3mm] \dfrac{1}{\pi} \int \left\{ e^{-ut} - e^{(-u(t-t_d))} \right\} \sin\left(\dfrac{x\sqrt{u}}{\sqrt{\beta}}\right) \dfrac{u}{u^2 + \omega^2} du \end{array} \right\} \quad \text{for } t > t_d \tag{B5}$$

B.3   DISCRETE KERNEL APPROACH

Many groundwater flow problems have been solved on the basis of the solutions of analogous heat conduction problems such as given by Carslaw and Jaeger (1959). These solutions for step boundary perturbation are used to generate kernels, which are basic property of a linear system. Using these discrete kernels, response of the aquifer to any type of boundary perturbations can be obtained. Discrete kernel approach, which is based on Duhamel's superposition principle for a linear system is a method to find response of variation in the input. Systems that satisfy both the homogeneous and additive rules are considered to be linear systems. These two rules, taken together, are often used as the principle of superposition and are applied to solve the problems of groundwater systems.

In addition to analytical and numerical approaches, the discrete kernel method has been successfully applied for the solution of groundwater problems for time varying perturbations in input.

To know the response of aquifer (i.e., rise in piezometic level, rate of inflow and cumulative volume) to the rise in stream stage, two types of discrete kernels, *discrete pulse kernels* and *discrete ramp kernels*, can be applied.

B.3.1 Discrete Pulse Kernels

The discrete pulse kernel is the response of the aquifer to a unit step-rise in stream stage which continues only for a period Δt. In this kernel, inputs are discretised as a train of pulses of uniform duration Δt and input is considered uniform over a time step.

Discrete pulse kernel, $\alpha\,(x, \Delta t, m)$, is thereby given as:

$$\alpha\,(x, \Delta t, m) = erf\left(\frac{x}{\sqrt{4\beta m \Delta t}}\right) - erf\left(\frac{x}{\sqrt{4\beta(m-1)\Delta t}}\right) \tag{B6}$$

and the piezometric level during m th time step applying convolution is given by

$$h(x, m\Delta t) = \sum_{\gamma=1}^{m} \frac{\sigma(\gamma-1)+\sigma(\gamma)}{2}\alpha(x, \Delta t, m-\gamma+1) \tag{B7}$$

where σ_γ = rise in stream stage at $t = \gamma\Delta t$; Δt = unit time step size; erfc= complimentary error function; and m and γ are integers.

B.3.2 Discrete Ramp Kernels

The discrete ramp kernels of the system for a particular response is defined as the response to a linearly increasing input (such as rise in stream stage) staring from zero

168

when the system is at rest and ending in an unit input (rise in stream stage) during a time span Δt. In this definition, the slope (i.e., derivative) of the time varying perturbation (stream stage rise) is constant during a time step and the input to be approximated as a series of incremental discrete ramps. Discrete ramp kernel, $\delta (x, \Delta t, m)$, is thereby given as:

$$\delta_r (x, m, \Delta t) = \frac{1}{\Delta t} \int_0^{\Delta t} erfc\left\{ \frac{x}{\sqrt{4\beta(m\Delta t - \tau)}} \right\} d\tau \qquad (B8)$$

where m = integer. Integration is performed after using a substitution $\tau = \Delta t v$, and $d\tau = \Delta t dv$, where v is a dimensional dummy variable (Mishra and Jain, 1999), and Eq. (B6) becomes

$$\delta_r (x, m, \Delta t) = 1 + \left\{ (m-1) + \frac{x^2}{(2\beta\Delta t)} \right\} erf\left[\frac{x}{\sqrt{4\beta\Delta t(m-1)}} \right] - \left\{ m + \frac{x^2}{(2\beta\Delta t)} \right\} erf\left\{ \frac{x}{\sqrt{4\beta\Delta tm}} \right\}$$

$$+ x\sqrt{\frac{(m-1)}{\beta\Delta t\pi}} \exp\left[\frac{-x^2}{4\beta\Delta t(m-1)} \right] - x\sqrt{\frac{m}{\beta\Delta t\pi}} \exp\left\{ \frac{-x^2}{4\beta\Delta tm} \right\} \qquad (B9)$$

Further, the piezometric level at distance x from the river edge at the end of mth time step, applying convolution, is given by

$$h(x, m\Delta t) = \sum_{\gamma=1}^{n} (\sigma_\gamma - \sigma_{\gamma-1}) \delta_s (x, \Delta t, m - \gamma + 1) \qquad (B10)$$

Thus, the pulse kernels are convoluted with the stream stage perturbations and the ramp kernel are convoluted with the derivatives of the perturbations in order to get

the aquifer responses to a time varying stream stage. The selection of time step size depends upon the nature of the flood wave. When there is a sharp rise in stream stage, comparatively smaller time step size should be used using discrete pulse kernels. When there is sluggish rate of rise in stream stage, coarser time step size can be used using ramp kernels. However, in both the cases, in general, ramp kernels are more efficient in estimating the aquifer response.

Selection of time step size depends on the nature of the flood wave. A sharp rise in stream stage would require comparatively smaller time step than that needed for a sluggish rate of rise in stream stage. In table B1, the rise in piezometric surface at the end of 3 day has been computed using Eq (B10) for different time step sizes for a symmetrical flood wave. The corresponding rise obtained using analytical solution given by Cooper and Rorabough (1963), i.e., Eq (B4), comes out to be 1.0541 m. As seen from the table, for a time step size of 1/10 day, the error in the prediction of the rise of piezometric level at the end of 3 days is about 0.02% only.

Table B 1. Computed rise in piezometric level

(t=3 days, x=25m, H_{max}=2.0m, t_c=2 days, σ = 4 days)	
Time step size, Δt (day)	Rise, h (m)
0.20	1.0532
0.10	1.0539
0.05	1.0541

C.1 HANTUSH'S WELL FUNCTION FOR PARTIALLY PENETRATING WELL

A vertical shaft penetrating marginally into an aquifer can be treated as a recharge well of zero penetration. Hantush (1961) has derived an analytical expression for evolution of piezometric surfaces in response to continuous uniform pumping from a well with zero penetration. The corresponding Hantush's well function can be used to compute the evolution of rise in piezometric surface due to a unit pulse recharge. The response of a linear system to a unit pulse perturbation has been designated as discrete kernel coefficient (Morel-Seytoux, 1975).

Let the unit step response function for piezometric rise at the well face of a marginally penetrating recharge well and a confined aquifer system be designated as x $U(r_w,t)$. According to Hantush(1961)

$$U(r_w,t) = \frac{1}{4\pi T} \{W(u) + 2\sum_{n=1}^{\infty} W_n(u, \frac{n\pi r_w}{b})\}$$ \hfill (C1)

b= thickness of aquifer(m); $u = \frac{r_w^2 \phi}{4Tt}$, $W(u) = \int_u^{\infty} \frac{e^{-y}}{y} dy$, and

$$W_n(u, \frac{n\pi r_w}{b}) = \int_u^{\infty} \frac{dy}{y} exp\left\{-y - \frac{1}{4y}\left(\frac{n\pi r_w}{b}\right)^2\right\}.$$

Let the time domain be discretized by time steps of uniform size Δt.

C.1.1 Discrete Pulse Kernels Coefficients, δ_p (m,Δt) :

Coefficients of discrete pulse kernels are generated using unit step repose function given by Eq (C.1) to compute the rise or drawdown at the well face of a partially penetrating well as:

$$\delta_p(m,\Delta t) = \frac{1}{\Delta t}\left[U(r_w,m\Delta t) - U(r_w,(m-1)\,\Delta t)\right]$$

$$= \frac{1}{4\pi T\Delta t}\left\{W(\frac{r_w^2 S}{4Tm\Delta t}) + 2\sum_{n=1}^{\infty}W_n(\frac{r_w^2 S}{4Tm\Delta t},\frac{n\pi r_w}{b})\right.$$
$$\left. -W(\frac{r_w^2 S}{4T(m-1))\Delta t}) - 2\sum_{n=1}^{\infty}W_n(\frac{r_w^2 S}{4T(m-1)\Delta t},\frac{n\pi r_w}{b})\right\}$$

(C2)

where, $W(u)$ and $W_n\,(u,n\pi r_w/b)$ are improper integrals as the upper limit of integration is infinite. W(u) is Theis' Well function and can be computed using the polynomial and rational approximation (Abromwitz and Stegun,1970) $W_n\,(u,n\pi r_w/b)$ is evaluated using Gaussian quadrature after converting the improper integral into proper integral and changing the limit. The procedure is as follows.

$$W_n(u,\frac{n\pi r_w}{b}) = \int_u^{\infty}\frac{1}{y}exp\left\{-y - \frac{1}{4y}\left(\frac{n\pi r_w}{b}\right)^2\right\}dy$$

$$= \int_u^{1}\frac{1}{y}exp\left\{-y - \frac{1}{4y}\left(\frac{n\pi r_w}{b}\right)^2\right\}dy + \int_1^{\infty}\frac{1}{y}exp\left\{-y - \frac{1}{4y}\left(\frac{n\pi r_w}{b}\right)^2\right\}dy$$

$$= \int_u^{1}\frac{1}{y}exp\left\{-y - \frac{1}{y}\left(\frac{n\pi r_w}{2b}\right)^2\right\}dy + \int_0^{1}\frac{1}{\zeta}exp\left\{-\frac{1}{\zeta} - \zeta\left(\frac{n\pi r_w}{2b}\right)^2\right\}d\zeta$$

172

$$=$$

$$\int_{-1}^{1} \frac{2}{(1+x)+u(1-x)} \, exp\left\{-\frac{(1+x)+u(1-x)}{2} - \frac{2}{\{(1+x)+u(1-x)\}}\left(\frac{n\pi r_w}{2b}\right)^2\right\}\frac{(1-u)}{2}\,dx$$

$$+\int_{-1}^{1} \frac{1}{(1+x)} \, exp\left\{-\frac{2}{(1+x)} - \frac{(1+x)}{2}\left(\frac{n\pi r_w}{2b}\right)^2\right\}dx$$

As x→ -1, the value of the integrand in the second integration is found as follows:

$$\frac{1}{(1+x)} \, exp\left\{-\frac{2}{(1+x)} - \frac{(1+x)}{2}\left(\frac{n\pi r_w}{2b}\right)^2\right\}$$

$$\cong\frac{1}{(1+x)} \, exp\left\{-\frac{2}{(1+x)}\right\} = \frac{1}{(1+x)(1+\dfrac{2}{(1+x)}+\dfrac{4}{2!(1+x)^2}+\cdots)} \to 0 \quad \text{as x→ -1.}$$

This integration can be performed numerically using Gauss Qudrature technique.

C.2 HANTUSH WELL FUNCTION FOR A FULLY PENETRATING WELL

Hantush(1964) has derived the well function for computation of drawdown in an artesian aquifer due to pumping from a fully penetrating well of finite radius starting from the basic solution given by Carslaw and Jaeger (1959) for an analogous heat conduction problem. The unit step response function, $U_1(r_w,t)$, for piezometric rise or drawdown at the well face of a fully penetrating well of finite radius and a confined aquifer system be is given by Hantush(1964) is:

$$U_1(r_w,t) = \frac{1}{4\pi T}\left[\frac{4}{\pi}\int_{0}^{\infty}\{1 - exp(-\tau x^2)\}\,f_1(x)dx\right] \qquad \text{(C4)}$$

in which,

$$\tau = \frac{Tt}{Sr_w^2}; \qquad f_1(x) = \frac{J_1(x)Y_0(\rho x) - J_0(\rho x)Y_1(x)}{x^2\left[J_1^2(x) + Y_1^2(x)\right]}; \qquad \rho = \frac{r}{r_w} = 1; \qquad J_0(x), \quad J_1(x)$$

=Bessel functions of first kind of zero and first order respectively; $Y_0(x)$ $Y_1(x)$=

Bessel functions of second kind of zero and first order respectively

C.2.1 Discrete Pulse Kernel, δ_1 (m,Δt):

Coefficients of discrete pulse kernels are generated using unit step repose function given by Eq (C.4) to compute the rise or drawdown at the well face of a fully penetrating well as:

$$\delta_1(m, \Delta t) = \frac{1}{\Delta t}\left[U_1(r_w, m\Delta t) - U_1(r_w, (m-1)\Delta t)\right] \qquad (C5)$$

The integral in (C4) is an improper integral as the upper limit of integration is infinite. The improper integral is reduced to a proper integral as described below.

$$I = \int_0^\infty \left[1 - exp(-\tau x^2)\right] f_1(x) dx = \int_0^1 \left[1 - exp(-\tau x^2)\right] f_1(x) dx +$$

$$\int_1^\infty \left[1 - exp(-\tau x^2)\right] f_1(x) dx = I_1 + I_2$$

$$I_1 = \int_0^1 \left[1 - exp(-\tau x^2)\right] f_1(x) dx = 0.5 \int_{-1}^1 \left[1 - exp\{\frac{-\tau(1+v)^2}{4}\}\right] f_1(\frac{1+v}{2}) dv$$

Expanding the exponential term, and applying L' Hospital's rule, it can be shown that as v tends to -1, the integrand tends to 0. The integral I_1 is a proper integral and can be evaluated numerically using Gauss qudrature.

174

$$I_2 = \int_1^\infty \left[1 - exp(-\tau x^2)\right] f_1(x)dx = \int_0^1 \left[1 - exp(-\tau / v^2)\right] f_1(1/v) \frac{dv}{v^2}$$

$$= 0.5 \int_{-1}^1 \left[1 - exp\left\{\frac{-4\tau}{(1+y)^2}\right\}\right] f_1\left(\frac{2}{1+y}\right) \frac{4dy}{(1+y)^2}$$

Limit of the integrand at the lower is found as described below.

As $y \to -1$, $\left[1 - exp\left\{\frac{-4\tau}{(1+y)^2}\right\}\right] \to 1$

$$\left[\frac{4}{(1+y)^2}\right] f_1\left(\frac{2}{1+y}\right) = \left[\frac{4}{(1+y)^2}\right] \frac{J_1(\frac{2}{1+y})Y_0(\rho\frac{2}{1+y}) - J_0(\rho\frac{2}{1+y})Y_1(\frac{2}{1+y})}{(\frac{2}{1+y})^2 \left[J_1^2(\frac{2}{1+y}) + Y_1^2(\frac{2}{1+y})\right]}$$

$$= \frac{J_1(\frac{2}{1+y})Y_0(\rho\frac{2}{1+y}) - J_0(\rho\frac{2}{1+y})Y_1(\frac{2}{1+y})}{\left[J_1^2(\frac{2}{1+y}) + Y_1^2(\frac{2}{1+y})\right]}$$

$$= \frac{J_1(\frac{2}{1+y})Y_0(\rho\frac{2}{1+y})}{\left[J_1^2(\frac{2}{1+y}) + Y_1^2(\frac{2}{1+y})\right]} - \frac{J_0(\rho\frac{2}{1+y})Y_1(\frac{2}{1+y})}{\left[J_1^2(\frac{2}{1+y}) + Y_1^2(\frac{2}{1+y})\right]}$$

As $y \to -1$, $Y_1(\frac{2}{1+y}) \to 0$; hence,

175

$$\frac{J_1(\frac{2}{1+y})Y_0(\rho\frac{2}{1+y})}{\left[J_1^2(\frac{2}{1+y})+Y_1^2(\frac{2}{1+y})\right]}$$

$$\cong\frac{J_1(\frac{2}{1+y})Y_0(\rho\frac{2}{1+y})}{J_1^2(\frac{2}{1+y})}=\frac{Y_0(\rho\frac{2}{1+y})}{J_1(\frac{2}{1+y})}\frac{\sqrt{\frac{(1+y)}{\rho\pi}}\ sin\left(\frac{2\rho}{1+y}-\frac{\pi}{4}\right)}{\sqrt{\frac{(1+y)}{\pi}}\ cos\left(\frac{2}{1+y}-\frac{3\pi}{4}\right)}$$

$=1$ (since ρ=1)

Similarly, $\dfrac{J_0(\rho\frac{2}{1+y})Y_1(\frac{2}{1+y})}{\left[J_1^2(\frac{2}{1+y})+Y_1^2(\frac{2}{1+y})\right]}\to1$

Therefore, I_2 can be evaluated using Gauss qudrature.

The peizometric level at any point at a distance r from the center of the well will be computed by substituting r in place of r_w in Eq. (C1) and Eq (C4)

C.3 APPLICATION OF IMAGE WELL THEORY

Although, many equilibrium and non-equilibrium formulae developed for the solution of groundwater problems are based on the assumption that the aquifer is of infinite areal extent, it is well known that only a few of the aquifers completely satisfy this assumption. When an aquifer is recognized as having finite dimensions, direct application of equations for computing drawdown at any point around a pumping or recharge well is precluded. However, it is possible to circumvent the analytical difficulties posed by the aquifer boundary with the application of the method of images, widely used in the theory of heat conduction in solids, for groundwater

problems as well. Ferris et. al., (1962) have discussed in detail the theory of image well for different type of aquifer boundaries such as recharge, barrier or impermeability. Imaginary wells or streams usually referred to as images at strategic locations to duplicate hydraulically the effects on flow regime caused by the known physical boundary. Use of the image, thus, is equivalent to removing a physical entity and substituting a hydraulic entity. The finite aquifer system is thereby transformed by substitution into one involving an aquifer of infinite areal extent, in which several real and imaginary wells or streams can be studied applying formulas already developed for infinite aquifer.

In a situation where a recharge or pumped well is situated nearby a perennial stream, and it is required to compute the drawdown at a point. This can be carried out using the image well theory and the mathematical expressions for draw-down at any point around the well in an infinite aquifer. For most of the field conditions, it can be assumed that the stream is fully penetrating and is equivalent to a line source at constant head. Mishra and Fahimuddin (2005) have applied the theory of image well even if stream stage is changing during passage of the flood wave because the whole system (stream, aquifer and pumped well) is considered to be a linear system.

In this study, flood wave is passing in the river, i.e., stream stage is changing. In this situation also, the theory of image can be applied as in groundwater hydrology, use of image is equivalent to removing a physical entity and substituting a hydraulic entity (Ferris et al, 1962). If the stream stage is not lowered by the flow to the real well, there shall be no drawdown (due to pumping) along the stream position (Ferris et al, 1962). A confined aquifer- stream- well system is a linear system. Therefore, the response at any point in the aquifer to the combined perturbations (pumping and flood

wave) is sum of response to each separate perturbation. In other words a rise in piezometric surface at any point in the upper aquifer is sum of rise due to flood wave alone and drawdown due to only withdrawal from the aquifer. Image well theory is very much applicable for a linear system for varying stream stage.

D.1 CORRECTION FACTOR, C_1, FOR ACCOUNTING PARTIAL INTERCEPTION OF AQUIFER THICKNESS BY COLLECTOR PIPE

Opportunity time for filtration of river water into a collector pipe all along its length is approximately same for a pipe running parallel to the axis of a straight river reach. Therefore, uniform and safe opportunity time can be maintained for a collector pipe running parallel to a river axis. The diameter of the collector pipe is generally small in comparison to the thickness of the aquifer in which the pipe is laid. A correction factor to account for partial trapping of the aquifer thickness by a collector pipe running parallel to river axis has been proposed by Mishra (2004 (b)), which is presented in this appendix.

For a long collector pipe running parallel to a river in an aquifer of considerable thickness, the flow can be assumed as two dimensional in the vertical plane perpendicular to the collector axis. The flow domain for such situation is shown in Fig.D.1. For steady flow condition, conformal mapping technique is applicable to solve the Laplace equation. To apply conformal mapping, the circular collector section is assumed as a vertical slit of length 'd' equal to diameter of the collector. The idealised flow domain is shown in Fig.D.2 (a) The flow domain is decomposed into two parts: the part towards the river consisting of an aquifer of finite width (domain ABCD), and the part away from the river consisting aquifer of semi infinite width (domain EBCF). For computing flow each part is considered separately.
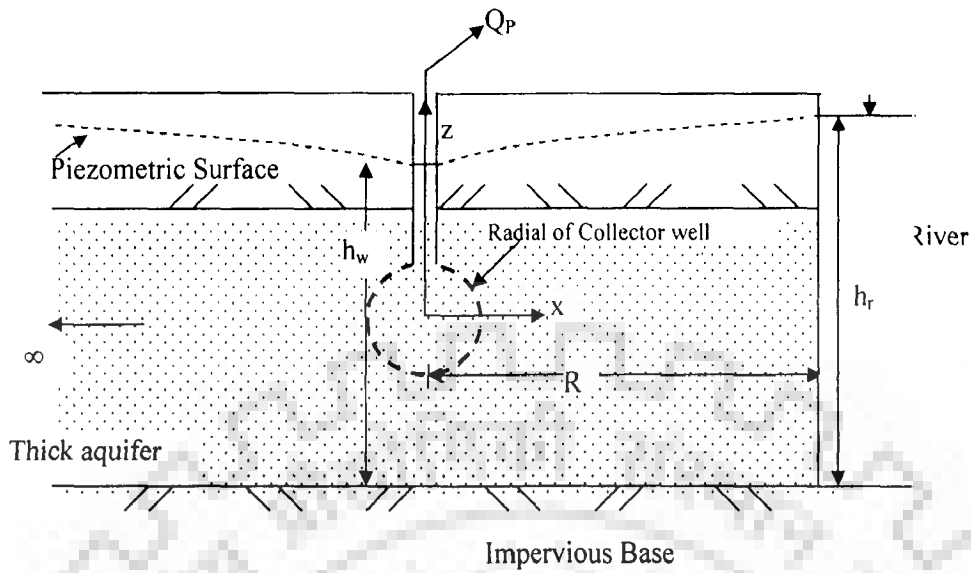
Figure D.1: A horizontal collector pipe laid parallel to a straight river reach

D.1.1 Mapping of the Flow Domain ABCD in z Plane onto t Plane

The auxiliary t $(=r+is)$ plane is shown in Fig.D.2 (b)

$$z = M \int_1^t \frac{dt}{(t^2-1)^{1/2}(t^2-b^2)^{1/2}} + R - i\frac{T}{2} \qquad (D1)$$

For $t = \infty$, $z=R$; hence,

$$R = M \int_1^\infty \frac{dt}{(t^2-1)^{1/2}(t^2-b^2)^{1/2}} + R - i\frac{T}{2} \qquad (D2)$$

Performing the integration (Byrd and Friedman, 1954) and after simplification

$$M = \frac{iT}{2F(\pi/2, b)} \qquad (D3)$$

For $b \le t \le 1$ the relation between z and t plane is given by:

$$z = M \int_b^t \frac{dt}{(-1)^{1/2}(1-t^2)^{1/2}(t^2-b^2)^{1/2}} - i\frac{T}{2} \qquad (D4)$$

For point D, t=1 and $z=R\text{-}i\ T/2$; hence,

180

$$\frac{R}{T} = \frac{F(\pi/2, \sqrt{(1-b^2)})}{2F(\pi/2, b)}$$ (D5)

For $0 \leq t \leq \alpha$, the relation between z and t plane is given by:

$$z = M \int_0^t \frac{dt}{(1-t^2)^{1/2}(b^2-t^2)^{1/2}}$$ (D6)

For point C_1, $t = \alpha$ and $z = -id/2$. Performing the integration (Byrd and Friedman, 1971) and applying this condition

$$\frac{d}{T} = \frac{F(\sin^{-1}(\frac{\alpha}{b}), b)}{F(\pi/2, b)}$$ (D7)

D.1.2 Mapping of w Plane onto t Plane

The complex potential $w \, (= \phi + i\psi)$ for the flow domain ABCD is shown in Fig.D.2(c).

The velocity potential function ϕ is defined as $\phi = -k(p/\gamma_w + y) + C_3$; k= hydraulic conductivity, p= water pressure, γ_w = unit weight of water, y=elevation head and C_3= a constant taken as kh_w. The relation between w and t plane is given by:

$$w = M_1 \int_1^t \frac{dt}{(t^2-1)^{1/2}(t^2-\alpha^2)^{1/2}} - k(h_r - h_w) + iq$$ (D8)

At $t = \infty$, w= $-k(h_r - h_w) + iq/2$.

Applying this condition

$$-k(h_r - h_w) + \frac{iq}{2} = M_1 \int_1^\infty \frac{dt}{(t^2-1)^{1/2}(t^2-\alpha^2)^{1/2}} - k(h_r - h_w) + iq$$ (D9)

From above the constant M_1 is found to be

$$M_1 = -\frac{iq}{2F(\frac{\pi}{2}, \alpha)}$$ (D10)

181

For $\alpha \leq t \leq 1$, the relation between w and t plane is given by:

$$w = \frac{-iq}{2F(\pi/2,\alpha)} \int_\alpha^t \frac{dt}{(t^2-1)^{1/2}(t^2-\alpha^2)^{1/2}} + iq \qquad (D11)$$

For point D, t =1, and w = - k(h$_r$-h$_w$) + iq. Applying this condition

$$-k(h_r - h_w) = \frac{-iq}{2F(\pi/2,\alpha)} \int_\alpha^1 \frac{dt}{(-1)^{1/2}(1-t^2)^{1/2}(t^2-\alpha^2)^{1/2}} \qquad (D12)$$

or

$$\frac{q}{k(h_r-h_w)} = \frac{2F(\pi/2,\alpha)}{F(\pi/2,\sqrt{(1-\alpha^2)})} \qquad (D13)$$

The above equation computes flow to the drain from the riverside. If the pipe intercepts the entire thickness of the aquifer, the dimensionless flow to the slit is given by:

$$q_0 /[k(h_r - h_w)] = T/R \qquad (D14)$$

The correction factor is, therefore, given by

$$C_1 = \frac{2F(\pi/2,\alpha)}{F(\pi/2,\sqrt{(1-\alpha^2)})} R/T \qquad (D15)$$

The variation of correction factor C_1 with ratio of diameter of collector pipe, d, to thickness of the aquifer T is given in Fig.D.3.

182
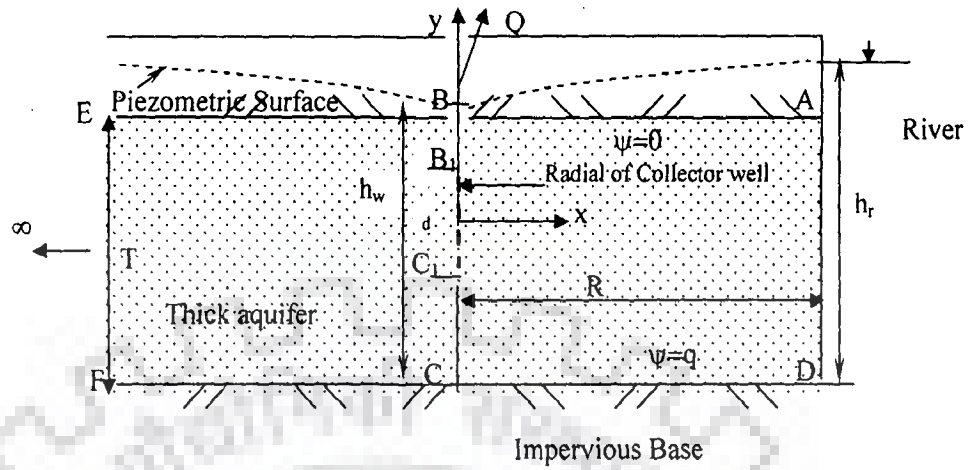
(a): Decomposition of the idealized flow domain; (i) ABCD (ii) EBCF
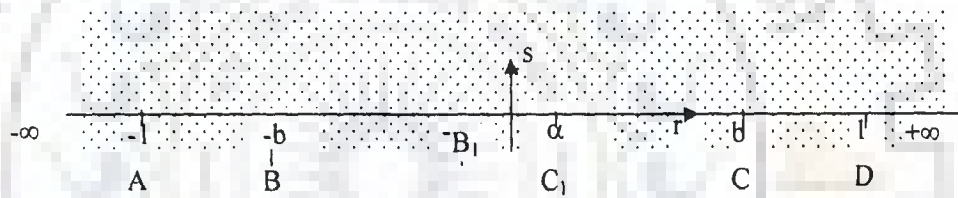
(b): Auxiliary t plane (t=r+is)
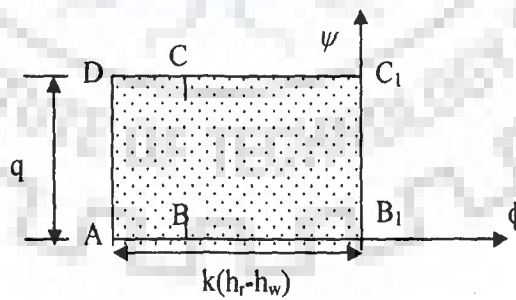
(c): Complex potential plane (w=φ+iψ)

Fig.D.2. Steps of conformal mapping for collector pipe laid parallel to a straight river reach

183

Fig.D.3: Variation of correction factor C$_1$ with *d/T*

REFERENCES

(1)   Abromowitz, M. and Stegun, I.A., 1964. Hand book of Mathematical Functions. National Bureau of Standards, Washington, D. C.

(2)   Bakker, M. and Strack, O.D.L., 2003.Analytic elements for multiaquifer flow. J. of Hydrology, 271, 119-129.

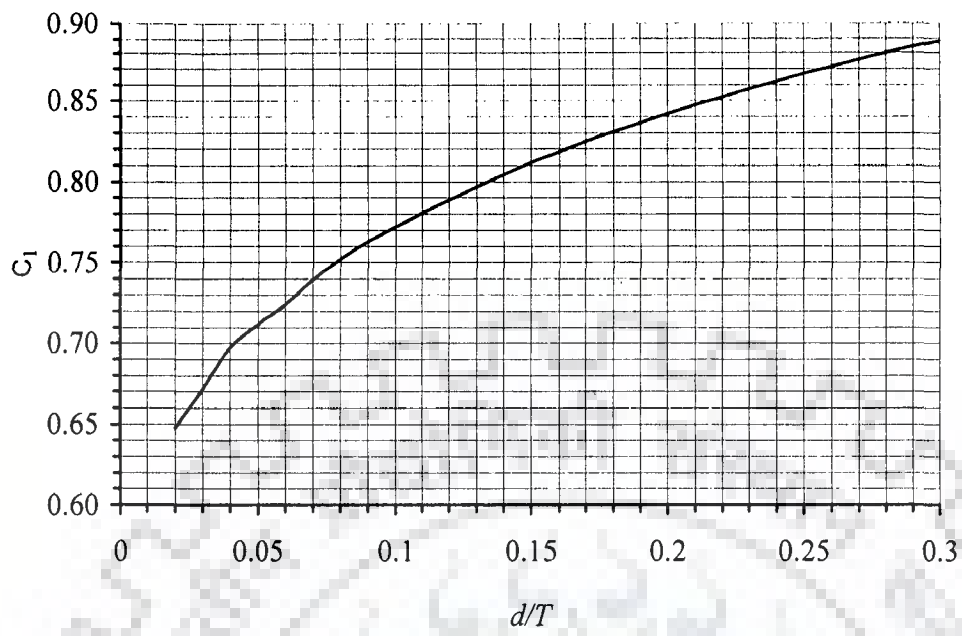(3)   Bakker, M., Kelson, V.A., and Luther, K.H.(2005).   Multilayer analytic element modeling of radial collector wells. Ground Water, 43(6), 926-934.

(4)   Barker, J.A., 1991. On the discrete kernel method for simulating pumping tests in large-diameter wells. J. of Hydrology 124, 177-183.

(5)   Bear, J. 1972. *Dynamics of fluids in porous media.* American Elsevier Publishing Company.

(6)   Berger, 2001. Removal of cryptosporidium using bank filtration. *Riverbank Filtration:Understanding Contaminant Biochemistry and Pathogen Removal.* Edited by Ray, C., NATO Science Series IV, Vol-14.

(7)   Byrd, P.F., and Friedman, M.D. (1954). *Handbook of elliptical integrals for engineers and physicists,* Springer-Verlag, Berlin.

(8)   Carslaw, H.S. and Jaeger, J.C., 1959. *Conduction of Heat in Solids.* Oxford University Press, London.

(9)   Chachadi, A.G., Mishra, G.C., 1992. Analysis of unsteady flow to a large-diameter well experiencing well loss. Ground Water, 30 (3), 369-375.

(10)   Chen, X., 2003. Analysis of pumping-induced stream-aquifer interactions for gaining streams. J. of Hydrology 275, 1-11.

(11)   Chen, X., 2001. Migration of induced-infiltrated stream water into nearby aquifer due to seasonal groundwater withdrawal. Ground Water, Sep-Oct, Vol.39 (5), 721-728

(12)   Chen, C., Wan, J. and Zhan, H., 2003. Theoretical and experimental studies of coupled seepage-pipe flow to a horizontal well. J. of Hydrology, 281, 159-171.

(13)   Cheng, A.H. and Morohunfola, O.K., 1993. Multilayered leaky aquifer systems 1. Pumping well solutions. Water Resources Research, Vol. 29(8), Aug., 2787-2800.

(14)   Cooper, H.H., Papadopulos, I.S. 1967. Drawdown in a well of large diameter. Water Resources Research, 3 (1), 241-244.

(15)   Cooper, H.H., Jr., and Rorabough, M.I., 1963. Groundwater movement and bank storage due to flood stage in surface streams. U.S. Geological Survey, Water Supply Paper 1536-J, 343-366.

(16)   Debrine, B.E., 1970. Electrolytic model study for collector wells under riverbeds. Water Resources Research, Vol. 6(3), June, 971-978.

(17)   Dillon, P.J., Miller, M., Fallowfield, H., and Hutson, J., 2002. The potential of riverbank filtration for drinking water supplies in relation to microsystin removal in brackish aquifers. 266. 209-221.

(18)   Driscoll, F. G. (1987). *Groundwater and wells*. Johnson Division, St.Paul, Minnesota, p. 769.

186

(19) Ferris, J.G., Knowles, D.B., Brown, R.H., Stallman, R.W., 1962. Theory of aquifer tests. U.S. Geological Survey. Water- Supply Paper 1536-E, 144-166.

(20) Fujinawa, K., 1977. Finite-element analysis of groundwater flow in multiaquifer- systems,I. The behavior of hydrological properties in an aquitard while being pumped. J. of Hydrology, 33, 59-72.

(21) Gerba, C.P., Wallis, C., and Melnick, J.L., 1975. Fate of wastewater bacteria and viruses in soil. J. of Irrigation and Drainage Div. ASCE, IR3, 157-174.

(22) Gidley, H.K. and Miller, J.H. 1960. Performance records of radial collector wells in Ohio River valley. J. of AWWA,Sep, 1206-1210.

(23) Gidley, H.K., 1952. Installation and performance of radial collector wells in Ohio River gravels. J. of AWWA, Dec. 1117-1126.

(24) Giao, P.H., Phien-Wej, N., and Honjo, Y., 1999. FEM quasi-3D modeling of responses to artificial recharge in the Bangkok multiaquifer system. Enviromental Modelling & Software, 14, 141-151.

(25) Glover, R.E. and Balmer, G.G. 1954. River depletion resulting from pumping a well near a river. Transactions, American Geophysical Union, Vol. 35(3), 468-470.

(26) Gollnitz, W.D., Clancy, J.L., Whitteberry, B.L., and Vogt, J.A., 2003. RBF as a microbial treatment process. J. AWWA, 95:12, 56-66.

(27) Halek, V. and Svec, J. 1979. *Groundwater hydraulics*. Elsevier scientific publishing company. New York.

(28) Hall, F.R., Moench, A.F., 1972. Application of the convolution equation to stream-aquifer relationships. Water Resources Research, 8 (2), 487-493.

(29) Hantush, M.S., 1959. Analysis of data from pumping wells near a river. J. of Geophysical Research, 64 (11), Nov., 1921-1932.

(30) Hantush, M.S., 1964. Well hydraulics. Advances in Hydroscience. V.T.Chow,ed ., Academic Press, New York, Vol. 1 , 339-340.

(31) Hantush, M.S., 1965. Wells near streams with semipervious beds. Journal of Geophysical Research ,70 (12), Jun., 2829-2838.

(32) Hantush, M.S. (1961). Drawdown around a partially penetrating well. J. Hydr. Div., ASCE, 87(HY4), 83-98.

(33) Hantush, M.S. and Papadopulos, I.S. (1962). Flow to groundwater to collector wells." J. Hydraulic Engg. ASCE, 88(5), 221-244.

(34) Harr, M.E.,1962. *Groundwater and Seepage,* McGraw-Hill, New York, 93.

(35) Hemker, C.J., 1984. Steady groundwater flow in leaky multiple-aquifer systems. J. of Hydrology. 72, 355-374.

(36) Herrera, I., Hennart, J.P. and Yates, R., 1980. A critical discussion of numerical models for multiaquifer systems. Advances in Water Resources, Vol. 3, Dec, 159-163.

(37) Hornberger, G.M., Ebert, J., Remson, I., 1970. Numerical solution of the Boussinesq equation for aquifer-stream interaction. Water Resources Research 6 (2), 601-608.

(38)   Huisman, L. and Olsthoorn , T. N.,1983. *Artificial groundwater recharge,* Pitman Advanced Publishing Program, Boston, 53.

(39)   Hunt, B., 1999. Unsteady stream depletion from ground water pumping. Ground Water 37 (1), 98-102.

(40)   Hunt, H., 2002. American experience in installing horizontal collector wells. *Riverbank filtration, improving source-water quality,* edited by C.Ray, G.Melin, and R.B. Linsky. Kluwer Academic Publishers, The Netherlands, 29-34.

(41)   Hunt, B. 2005. Flow to vertical and non vertical wells in leaky aquifers. J. of Hydrologic engineering, ASCE, Vol. 10(6), Nov-Dec, 477-484

(42)   Hunt, B., 1983. *Mathematical Analysis of Groundwater* Resources, Butterworths, Boston, 184-191.

(43)   Joshi, S.D.(1991). *Horizontal Well Technology,* Tulsa, Oklahoma, PennWell Publishing Co.

(44)   Kaplani-Zare, M., Zhan, H., and Samani, N. 2005. Water flow from a horizontal tunnel in an unsaturated zone. J. of Hydrology, 303, 125-135.

(45)   Kaplani-Zare, M., Zhan, H., and Samani, N. 2005. Analytical study of capture zone of a horizontal well in a confined aquifer. . J. of Hydrology, 307, 48-59.

(46)   Kawecki, M.W.,2000. Transient flow to a horizontal well. Ground Water, 38(6), 842-850.

(47)   Kazmann, R.G., 1947. River infiltration as source of groundwater supply. Transactions, paper no 2339, J. ASCE, June, 404-424

(48)   Kazmann, R.G., 1948. The induced infiltration of river water to wells. Transaction, American Geophysical Union, 29 (1), Feb, 85-92.

(49)   Kazmann, R.G. 1949. The utilization of induced stream infiltration and natural aquifer storage at Canton, Ohio. J. of Economic geology, Vol. 44, Sep. 514-524.

(50)   Lin, C.L., 1972. Digital simulation of the Boussinesq equation for a water table aquifer. Water Resources Research, 8 (3), 691-697.

(51)   Maddock III, T. and Lacher, L. 1991. Drawdown, velocity, storage, and capture response functions for multiaquifer sustems. Water Resources Research, Vol. 27(11), Nov, 2885-2898.

(52)   Mass, C., 1986. The use of matrix differential calculus in problems of multiaquifer flow. J. of Hydrology 99, 43-67

(53)   Mikels, F.C., and F.H.Klaer, Jr.(1956). "Application of groundwater hydraulics to the development of water supplies by induced infiltration." International Association, Sci. Hydrology, symp, Darcy, Dijon, Publ, 41.

(54)   Milojevic, M. (1963). "Radial collector wells adjacent to the river bank. J. Hydr. Div.,89 (6),133-151.

(55)   Mishra, G.C. and Kansal, M.L , 2007. Flow to radial collector well near a river. J. of Hydrology (communicated)

(56)   Mishra, G.C. and Chachadi, A.G., 1985. Analysis of flow to a large-diameter well during recovery period. Ground Water, 23 (5), Sep- Oct, 646-651.

(57)   Mishra, G.C., Nautiyal, M.D., Chandra, S., 1985. Unsteady flow to well tapping two aquifers separated by an aquiclude. J. of Hydrology 82, 357-369.

(58) Mishra, G.C. and Jain, S.K., 1999. Estimation of Hydraulic diffusivity in Stream- Aquifer system, Journal of Irrigation and Drainage Engg. ASCE, Mar-Apr, 74-81.

(59) Mishra, G.C., 2004(a). Quantification of artificial groundwater recharge. Water resources of   arid areas. Ed. Stephenson, D., Shemang, E.M., Chaoka, T.R., A.A. Balkema   publishers, London. 105-113.

(60) Mishra, G.C. and Fahimuddin, M., 2005. Stream multiaquifer well interactions. J. of Irrigation and Drainage Engg. ASCE, 131(5), 433-439.

(61) Mishra, G.C., 2004(b). Specific Capacity of a Radial Collector Well near a River.A Two-Day Workshop on Riverbank Filtration. March1-2. Dept.Civil Engg.Roorkee.

(62) Mishra, G.C., Palaniappan, A.B., Kumar, S., Goyal, V., Jain,C.K., and Singh,V.(1999) Final report on exploration of construction of infiltration gallery inside the bed of river Yamuna at Agra. National Institute of Hydrology, Roorkee, India.

(63) Mishra, G.C., and Kansal, M.L., 2005. Radial collector well as an alternate source of water supply – a case study. J. Indian Building Congress, 12(1), 3-12.

(64) Mohammed, A., and Rushton, K., 2006. Horizontal wells in shallow aquifers: Field experiment and numerical model. J. of Hydrology, 329, 98-109.

(65) Moench, A.F., Kisiel, C.C., 1970. Application of the convolution relation to estimating recharge from an ephemeral stream. Water Resources Research 6 (4), 1087-1094.

(66) Moore, J.E. and Jenkins, C.T., 1966. An evaluation of the effect of groundwater pumpage on the infiltration rate of a semipervious streambed. Water Resources Research 2 (4), 691-696.

(67) Morel-Seytoux, H.J. and Daly, C.J., 1975. A discrete kernel generator for stream-aquifer studies. Water Resources Research 11 (2), 253-260.

(68) Murdoch, L.C., 1994. Transient analysis of an interceptor trench. Water Resources Research, Vol. 30(11), Nov. 3023-3031.

(69) Neville, C.J. and Tonkin, M.J., 2004. Modelling multiaquifer wells with Modflow. Ground Water, Vol. 42(6), Nov-Dec, 910-919.

(70) Newsom, J.M. and Wilson, J.L., 1988. Flow of ground water to a well near a stream-effect of ambient ground-water flow direction. Ground Water 26 (6), 703-711.

(71) Oaksford, E.T. (1985). "Artificial Recharge: Methods, Hydraulics, and Monitoring". Artificial Recharge of Groundwater. Edited by Takashi A. (1985),. Butterworth Publisher.69-127.

(72) Papadopulos, I.S. and Cooper, H.H., 1967. Drawdown in a well of large diameter. Water Resources Research, 3(1), 241-244.

(73) Park, E. and Zhan, H. 2002. Hydraulics of a finite-diameter horizontal well with wellbore storage and skin effect. J. of Hydrology, 25, 389-400.

(74) Park, E. and Zhan, H. 2003. Hydraulics of horizontal wells in fractured shallow aquifers systems. J. of Hydrology, 281, 147-158.

(75) Patel, S.C. and Mishra, G.C., 1983. Analysis of flow to a large diameter well by a discrete kernel approach. Ground Water 21 (5), 573-576.

(76)   Pinder, G.F., Bredehoeft, J.D., Cooper Jr, H.H., 1969. Determination of aquifer diffusivity from aquifer response to fluctuations in river stage. Water Resources Research 5 (4), 850-855.

(77)   Polubarinova-kochina, P.Y. 1962. *Theory of groundwater movement.* Princeton University press, Princeton, New Jersey.

(78)   Rowe, P.P., 1960. An equation for estimating transmissibility and coefficient of storage from river-level fluctuations. Journal of Geophysical Research 65 (10), 3419-3424.

(79)   Rushton, K.R. and Singh, V.S., 1987. Pumping test analysis in large diameter wells with a seepage face by kernel function technique. Ground Water 25 (1), 81-90.

(80)   Ray, C., Melin,G, and Linsky, R. B., 2002. *Riverbank filtration: improving source-water quality.* Dordrecht, The Netherlands: Kluwer Academic Publishers,3.

(81)   Ray, C., Grischek, T, Schubert, J., Wang, J.Z., and Speth, T.F., 2002. A perspective of Riverbank Filtration. J. of AWWA, April, 149-160.

(82)   Saleem, Z.A., 1973. Method for numerical simulation of flow in multiaquifer systems. American Geophysical Union, 1465-1469.

(83)   Schubert, J., 2002. Hydraulic aspects of riverbank filtration-field studies. J. of Hydrology, 266, 145-161.

(84)   Sen, Z. 1986. Discharge calculation from early drawdown data in large-diameter wells. J. of Hydrology, 83, 45-48.

(85)   Sontheimer, H., 1980. Experience with riverbank filtration along the Rhine River. J. of AWWA, July, 386-390.

(86) Singh, S.K., 2000. Rate and volume of stream depletion due to pumping. Journal of Irrigation and Drainage Engg. ASCE, 336-338.

(87) Singh, S.K., Mishra, G.C., Swamee, P.K., Ojha, C.S.P., 2002. Aquifer diffusivity and stream resistance from varying stream stage. Journal of Irrigation and Drainage Engg. ASCE, 57-61.

(88) Singh, S.K., 2003. Flow depletion of semipervious streams due to pumping. Journal of Irrigation and Drainage Engg. ASCE, 449-453.

(89) Singh, S.K., 2004. Ramp kernels for aquifer responses to arbitrary stream stage. J of Irrigation and Drainage Engg. ASCE, 460-467.

(90) Sophocleous, M., Townsend, M.A., Vogler, L.D., McClain, T.J., Marks, E.T., Coble, G.R., 1988. Experimental studies in stream-aquifer interaction along the Arkansas river in central Kanas- Field testing and analysis. J. of Hydrology, 98 , 249- 273.

(91) Spalding, C.P. and Khaleel, R., 1991. An evaluation of analytical solutions to estimate drawdowns and stream depletions by wells. Water Resources Research, 27 (4), 597-609.

(92) Spirdonoff, S.V.(1964)." Design and use of radial collector wells." J. of AWWA, Jun, 689-698.

(93) Stone, R. 1954. Infiltration galleries. Proceedings, ASCE, Sanitary Engineering Div., Separate No. 472, Vol 80, Aug, 472/1-472/12

(94) Steward, D.R. and Jin, W., 2001. Gaining and losing sections of horizontal wells. Water Resources Research, Vol. 37(11), Nov., 2677-2685.

(95) Sun, D. and Zhan, H., 2006. Flow to a horizontal well in an aquitard-aquifer system. J. of Hydrology, 321, 364-376

(96) Swamee, P.K., Mishra, G.C., Chahar, B.R., 2000. Solution for a stream depletion problem. Journal of Irrigation and Drainage Engg. ASCE, 125-126.

(97) Theis, C.V., 1935. The relation between the lowering of the piezometric surface and the rate and duration of discharge of well using groundwater storage. Transactions, American Geophysical Union. 16, 519-524.

(98) Theis, C.V., 1941. The effect of a well on the flow of a nearby stream. Transaction, American Geophysical Union. 734-737.

(99) Todd, D.K., 1955. Ground-water flow in relation to a flooding stream. Proc., ASCE, Separate No. 628, 1-20.

(100) Tufenkji, N., Ryan, J.N., and Elimelech, M., 2002. The promise of bank filtration, Enviromental science & technology, Nov., 423A428A.

(101) U.S. dept of Interior, 1981, *Groundwater manual*, Water resources and power services, Chapter XII, 341-349

(102) Wallace, R.B., Darama, Y., Annable, M.D., 1990. Stream depletion by cyclic pumping to wells. Water Resources Research, 26 (6), 1236-1270.

(103) Weiss, W.J., Bouwer, E.J., Ball, W.P., O'Melia, C.R., Lechevallier, M.W., Arora, H., and Speth, T.F., 2003. Riverbank filtration- fate of DBP precursors and selected microorganism. J. of AWWA, 95:10, October. 68-81.

(104) Weiss, W.J., Bouwer, E., Aboytes, R., LeChevallier, M.W., O' Melia, C.R., Le, B.T., Schwab, K.J., 2005. Riverbank filtration for control of microorganisms: Results from field monitoring. Water Research, 39, 1990-2001.

(105) Wilson, J.L., 1993. Induced infiltration in aquifers with ambient flow. Water Resources Research, 29 (10), 3503-3512.

(106) Yale, R.A., 1958, Use of radial collector well in Skagit County, wash. J of AWWA, June, 125-128.

(107) Zhan, H. and Park, E.,2003. Horizontal well hydraulics in leaky aquifers. J. of Hydrology, 281, 129-146.

(108) Zhan, H. and Cao, J., 2000. Analytical and semi analytical solutions of horizontal well capture times under no-flow and constant-head boundaries. Advances in Water Resources, 23, 835-848.

(109) Zhan, H., Zlotnik, V.A., 2002. Groundwater flow to horizontal and slanted wells in water table aquifers. Water Resources Research, 38(7), 101029/R000401.

(110) Zhan, H., 1999. Analytical study of capture time to a horizontal well. J. of Hydrology, 217, 46-54.

(111) Zhan, H., Wang, L.V., and Park, E., 2001. On the horizontal-well pumping tests in anistropic confined aquifers. J. of Hydrology, 252, 37-50.